Draft version 1.1

ATLAS NOTE

October 13, 2014

Search for ttH in the multilepton final state: results

S. Biondi[f], D. Boumediene[a], D. Calvet[a], D. DeMarco[h], S. Gentile[g], D. Hohn[m], Y. Ilchenko[c], M. Kuna[g], C. Lester[b], F. Manghi[f], J. Mcfayden[l], S. Monzani[g], F. Nuti[k], P. Onyisi[c], R. Ospanov[b], D. Paredes[a], M. Pitt[i], G. Salamanna[e], J. Schaarschmidt[i], F. Seifert[d], R. Shang[j], A. Sidoti[f], A. Sopczak[d], S. Valentinetti[f], D. Zanzi[k]

[a]*LPC Clermont*
[b]*Univ. Pennsylvania*
[c]*Univ. of Texas at Austin*
[d]*IEAP CTU in Prague*
[e]*Univ. Roma Tre*
[f]*Univ. Bologna*
[g]*Univ. Roma I*
[h]*Univ. Toronto*
[i]*Weizmann Inst. of Sc.*
[j]*Univ. Illinois at Urbana Champaign*
[k]*Univ. Melbourne*
[l]*Univ. College London*
[m]*University of Bonn*

Abstract

Contents

1 Introduction

This note describes analysis channels and procedures used to obtain final statistical results for measuring top quark Yukawa coupling in ttH production channel [1].

2 Analysis overview

2.1 Description of signal

2.2 Overview of analysis channels

2.3 Overlap removal between channels

The channels are primarily classified by the number of light leptons. These are counted with a single identification choice common to all channels (described in Note 1), a common p_{T} threshold (10 GeV), and overlap removal definition. Each analysis may further tighten the cuts relative to this baseline (e.g. by raising the p_{T} cut or tightening isolation or $|\eta|$ cuts), but in no case are the cuts loosened, which ensures that all channels are orthogonal by construction. The $2\ell + 0\tau$ and $2\ell + \tau$ channels are separated by the number of tau candidates (0 or == 1); this again ensures these channels have no candidates in common.

Overlaps between the multilepton channels and other $t\bar{t}H$ channels have been investigated, using the $t\bar{t}H$ samples with inclusive Higgs decays. A minor overlap is seen between the dilepton bb analysis and the 3ℓ channel, due to a bug in the implementation of the third lepton veto in dilepton bb. However these events all lie in signal-poor regions of the dilepton analysis (mostly in 4 jet, 2 b-tag) and so the statistical impact is expected to be negligible. A more serious concern is the overlap between the $\ell+2\tau$ analysis and the $\ell+\tau$, $H \to bb$ channel, but again here the multilepton events lie in background-dominated regions of the bb analysis. Strategies to reduce this overlap are being studied.

The acceptance of the multilepton analyses for other Higgs production modes (gluon-gluon fusion, vector boson fusion, and vector boson associated production) is studied with ggF, VBF, and VH samples produced with inclusive Higgs decays. These samples correspond to a few times the expected SM yield for the 2012 dataset. No events are accepted by any of the multilepton analyses from non-$t\bar{t}H$ production mechanisms. Fake lepton rates are low enough that we expect the only potential real backgrounds to arise from VH+jets production, which is suppressed by requiring b-tags in the final state. Since the VH production cross section is only $\sim 8\times$ the $t\bar{t}H$ rate, we expect the additional object requirements to largely eliminate the contribution. **Cross checks to confirm this will be done.**

2.4 MC-estimated backgrounds

All background contributions not involving non-prompt or charge-flipped leptons are estimated from Monte Carlo simulations. The dominant backgrounds in all channels are $t\bar{t}V$, tZ, and VV. The events are generated using multileg LO generators (Madgraph for $t\bar{t}V$ and tZ, Sherpa for VV). NLO generators are not used because the signal regions frequently require emission of two or more extra color-charged partons relative to the base process, which is simulated at less than matched LO accuracy by our current NLO generators. Data-MC discrepancies in the spectra of the number of jets in WZ-rich regions are seen with Powheg+Pythia but not with Sherpa, strongly suggesting that we should use the latter.

We also use MC simulations of $t\bar{t}$ and single top production for data-MC comparisons in regions without dedicated data-driven background estimates (basically, everything that is not a signal region). We use Powheg+Pythia as the event generator for these processes. Although technically Powheg+Pythia is subject to the less-than-LO accuracy mentioned above, it has been shown to reproduce njet spectra and the heavy flavor fraction extremely well in the $t\bar{t}H(bb)$ analyses (especially after a mild reweighting in $t\bar{t}$ p_{T} and top quark p_{T}, motivated by the 7 TeV differential cross section measurement, is applied).

2.5 Data-driven backgrounds

2.6 Sources of experimental systematic uncertainties

The list of systematics to be considered and included in the final analysis is given in Tables 1-3, along with their type, source, description, workspace name and status of inclusion in our current framework.

The experimental systematic treatments are evaluated by ATLAS performance groups and are evaluated in the multi-lepton analysis either as an overall event re-weighting or as a rescaling of the object energy and momentum. The JVF systematic requires a variation of the cut. The effect of the systematics are evaluated for both up(high) and down(low) variations, which correspond to a 1 σ fluctation of the relevant weight or scale. The event yields are rerun for each fluctuation and 1-σ errors on those yields are obtained. These are incorporated into the fit as unit gaussians, scaled by the overall 1-σ effect. The variation in event yields for ttH, ttW and ttZ due to experimental uncertainties are classified respectively in Tables 30-35, Tables 36-41 and Tables 42-47 (Appendix A). For simplicity, the most important systematics per channel are also summarized in Table 4-6 and the sum of the squares of all the experimental uncertainties is reported in Table 7. Shapes of the impact of the experimental systematics variations on kinematic distributions are provided for each analysis in Figures 1 and 2. They are illustrated by distributions of the scalar sum of p_{T} of selected objects HT, the invariant mass of the two leading leptons M_{ll}^{01} and the tau p_{T}.

2.6.1 Trigger

Events must contain an identified lepton, with above 25 GeV/c, that matches to one of the primary electron and photon triggers for 2012, EF_e24vhi_medium1 || EF_e60_medium || EF_mu24i_tight || EF_mu35_tight. The per-object trigger efficiencies and errors are provided by the electron and muon performance groups and are calculated with respect to the appropriate offline identification working point using Z tag-and-probe samples. The procedure for obtaining the electron and muon trigger efficiency scale-factors and efficiencies are detailed in [2] and [3], respectively. The efficiency measurements are the most up-to-date versions using the full 2012 dataset found on the electron [4] and muon [5] trigger twikis. The electron trigger efficiencies are $\sim$ 90%, while the muon are a bit lower due to muon trigger coverage, $\sim$70%. The per-object-efficiences are then combined using the latest version of the standard package to assess the event-level efficiency. The overall effect of the trigger efficiency errors on the analysis is small compared to object identification and isolation uncertainties.

2.6.2 Electrons

The electron energy smearing and scale systematic uncertainties have been calculated by the E-gamma Analysis group for ATLAS-GEO-20-00-01 using the Z sample. Since these corrections result in a very small effect on the analysis, all scale corrections are taken at once (ELEC_SCALE). A single set of electron resolution variations is also considered (ELEC_RES). The electron reconstruction, identification and isolation efficiency systematics are incorporated as event weight flucations and are discussed in more depth in Note 1.

2.6.3 Muons

The muon smearing and scale systematic uncertainties likewise have been calculated by the Muon Combined Performance group by studying the Z and J/Ψ sample. There is a single set of scale (MUON_SCALE) systematics for the momentum scale variations and two sets for the muon-spectrometer and inner detector momentum resolution variations (MUON_RES_ID, MUON_RES_MS). The reconstruction/indentification and isolation efficiency systematics are incorporated as event weight fluctuations and are discussed

2.6.4 Jets

The Jet Energy Scale and Resolution Uncertainties are calculated by varying various components by 1 σ using a prescription from the Jet-Tau-EtMiss group for 2012 data and LC Jets. The components fall in to a number of categories: in-situ jet energy correction, η-intercalibration, high p_{T} jets, non-closure, close-by jets, flavour composition and response for b and non-b jets, and event pile-up. In total this corresponds to 23 separate variations detailed in Table 2. Each variation causes a rescaling of the jet-momentum. Additionally, a single JER systematic is evaluated as well as systematic on the JVF cut.

The procedure for deteriminted the JES/JER and associated systematic errors is discussed in depth elsewhere.

2.6.5 B-Tagged Jets

The b-tagging efficiency and mis-tag rate systematic uncertainties are calculated as event weights for a number of eigenvector variations for 4 categories of truth jets: b-jets,charm jets, light flavor jets and taus. The efficiencies and uncertainties are calculated using the latest tag and prescription, recommended by the Jet-Tau-Etmiss group for LC jets at the 70% efficiency operating point of the MV1 Tagging algorithm. There are 6 b, 4 charm, 4 tau, and 12 light flavor variation eigenvectors to consider. The combined effect of the 6 btag eigenvecter variations on ttH, ttZ and ttW event can be seen in Fig. 3.

2.6.6 Hadronic Taus

Three sources of systematic uncertainties related to hadronically decaying taus enter in the analysis: The tau identification scale factor (TauIDSF), the electron-veto scale factor (TauEVSF) and the energy scaling (TauScale). The latter one is included in form of a variation of p_{T} of the taus, as summarized in Table 1. The scale factors and systematic uncertainties are evaluated by the Atlas Tau Working Group and implemented with the provided package TauCorrUncert-00-00-13. The systematic variations are calculated depending on the ID working point, p_{T}, eta and number of tracks of the tau, as well as the electron identification working point in case of the TauEVSF. They include the total up and down variations by 1 σ for TauScale and TauEVSF and the statistical and systematic uncertainties for TauIDSF. Here, the systematic contributions of the TauIDSF are treated as correlated over all p_{T} and eta bins while the statistical contributions are uncorrelated with each other and with the systematic part. At this point the TauScale variations are already propagated to the TauSF uncertainties in the process of evaluating them and are hence treated as uncorrelated to the SF systematics.

The 1 σ up and down variations are applied to the offline analysis to evaluate the effect on the resulting yields. Therefore, the nominal tau p_{T} is replaced by the up and down variations for TauScale while the Tau SF weights are varied by the up and down variations of TauIDSF and TauEVSF in case a truth match to a true tau, respectively true electron is found, according to the recommendations of the Atlas Tau Working Group. The largest resulting variations for the different analysis subchannels are summarized in Tables 4-6.

2.6.7 Pile-Up

Simulated events are re-weighted in order to reproduce the pile-up condition observed in data. Simulations match well the number of minimum bias vertices when the average number of interactions per bunch crossing, $< \mu >$, is scaled by 1.11 ± 0.03. To assess an uncertainty due to pile-up, the yields in the signal regions have been evaluated for several $< \mu >$ scale factors (see Appendix B). For values compatible within the uncertainty with 1.11, the variation in yields is at most 2% in any region. Due to

212 the smallness of the variations, we have considered the pile-up systematics negligible for the purposes of
213 this analysis.

Type	Description	Name	Application	Ntuple	Analysis
		Trigger			
Scale Factors	Trigger Efficiency	LepTrigSFEventWeight	Event Weight	✓	✓
		Muons			
Scale Factors	Reconstruction and Identification	MuonReco	Event Weight	✓	✓
	Isolation	MuonIso	Event Weight	✓	✓
p_{T} Scale	p_{T} Scale	SCALE	p_{T} Weight	✓	✓
Resolution	Inner Detector Energy Resolution	ID	p_{T} Weight	✓	✓
	Muon Spectrometer Energy Resolution	MS	p_{T} Weight	✓	✓
		Electrons			
Scale Factors	Reconstruction and Identification	ElecId	Event Weight	✓	✓
	Isolation	ElecIso	Event Weight	✓	✓
p_{T} Scale	p_{T} Scale	ElecScale	p_{T} Weight	✓	✓
Resolution	Energy Resolution	ElecResolution	p_{T} Weight	✓	✓
		Hadronic Taus			
Scale Factors	Identification BDT	TauIDSF	Event Weight	✓	✓
	Electron Veto BDT	TauEVSF	Event Weight	✓	✓
p_{T} Scale	p_{T} Scale	TauScale	p_{T} Weight	✓	✓

Table 1: Summary of experimental systematics to be included in the analysis for muons, electrons and hadronic tau objects, with the systematics type, description, name, application, availability in the common ntuple production and status of inclusion in the analysis results.

Type	Origin	Name	Ntuple	Analysis
		Jets		
Resolution		JER	✓	✓
Jet Vertex Fraction		JVF	✓	✓
Energy Scale	In-Situ	NP_Statistical1,2,3JES	✓	✓
		NP_Modelling1,2,3,4JES	✓	✓
		NP_Detector1,2,3JES	✓	✓
		NP_Mixed1,2JES	✓	✓
	η intercalibration	Eta_ModellingJES	✓	✓
		Eta_StatAndMethodJES	✓	✓
	High p_{T}	HighPtJES	✓	✓
	Pile-Up	NPVJES	✓	✓
		MuJES	✓	✓
		PilePtJES	✓	✓
		PileRhoJES	✓	✓
	Non Closure	NonClosure_AFIIJES	✓	✓
	Flavour	FlavRespJES	✓	✓
		bJES	✓	✓
		FlavCompJES	✓	✓

Table 2: Summary of experimental systematics to be included in the analysis for jets, with their systematics type, origin, name, availability in the common ntuple production and status of inclusion in the analysis results.

Type	Origin	Name	Ntuple	Analysis
		b-tags		
Scale Factors	MV1 b-tagger efficiency on b originated jets in bins of η	JetTagWeightB0-5	✓	✓
	MV1 b-tagger efficiency on c originated jets in bins of η	JetTagWeightC0-3	✓	✓
	MV1 b-tagger efficiency on tau originated jets in bins of η	JetTagWeightT0-3	✓	✓
	MV1 b-tagger efficiency on light flavoured originated jets in bins of η and p_{T}	JetTagWeightLight0-11	✓	✓

Table 3: Summary of experimental systematics to be included in the analysis for b-tagged jets, with their systematics type, origin, name, availability in the common ntuple production and status of inclusion in the analysis results.

Syst. Variation Selection	1^{st} Unc. Down-Up(%)	2^{nd} Unc. Down-Up(%)	3^{rd} Unc. Down-Up(%)
1l_2tau	TauIDSF -6.58 6.82	TauScale -3.57 4.09	lepTrigSFEventWeight -1.28 1.28
2ee4jets	ElecIso -4.00 4.08	ElecId -1.59 1.60	JetTagWeightB5 -1.22 1.16
2ee≥5jets	ElecIso -4.06 4.15	FlavCompJES -3.77 2.40	NP_Modelling1JES -3.76 2.34
2em4jets	ElecIso -2.04 2.04	MuonIso -1.97 1.97	FlavCompJES 1.30 -2.44
2em≥5jets	FlavCompJES -2.85 3.15	NP_Modelling1JES -2.47 3.08	ElecIso -2.04 2.04
2mm4jets	MuonIso -3.88 3.95	FlavCompJES 3.85 -2.20	FlavRespJES 3.30 -0.99
2mm≥5jets	MuonIso -3.93 4.00	FlavCompJES -3.36 2.74	NP_Modelling1JES -3.09 3.13
2l_tau	TauScale -3.15 3.17	TauIDSF -2.74 2.74	FlavCompJES -2.25 0.89
3l	MuonIso -3.44 3.52	ElecIso -2.61 2.66	NP_Modelling1JES -1.88 1.48
4l	MuonIso -4.68 4.85	ElecIso -3.52 3.61	ElecId -1.79 1.81

Table 4: Most relevant systematics variation on the *ttH* expected events for all the analysis channels.

Syst. Variation Selection	1^{st} Unc. Down-Up(%)	2^{nd} Unc. Down-Up(%)	3^{rd} Unc. Down-Up(%)
1l_2tau	TauScale -5.04 8.60	TauIDSF -4.10 4.18	FlavCompJES -3.96 0.05
2ee4jets	ElecIso -4.29 4.38	FlavCompJES -2.53 -1.46	JetTagWeightB5 -1.82 1.80
2ee≥5jets	ElecIso -4.44 4.54	FlavCompJES -3.26 4.83	NP_Modelling1JES -4.00 4.57
2em4jets	ElecIso -2.16 2.16	MuonIso -2.03 2.03	NP_Modelling1JES 0.20 2.68
2em≥5jets	FlavCompJES -5.21 3.53	NP_Modelling1JES -4.94 3.85	PileRhoJES -2.85 2.68
2mm4jets	MuonIso -4.04 4.12	JetTagWeightB5 -1.34 1.28	FlavCompJES 0.38 1.52
2mm≥5jets	MuonIso -4.07 4.16	FlavCompJES -3.74 2.22	NP_Modelling1JES -3.51 2.38
2l_tau	TauScale -6.35 1.95	MuonIso -2.26 2.28	NPVJES 0.19 3.24
3l	MuonIso -3.44 -3.52	JetTagWeightB5 -2.93 2.96	ElecIso -2.88 2.94

Table 5: Most relevant systematics variation on the *ttW* expected events for all the analysis channels.

Syst. Variation Selection	1^{st} Unc. Down-Up(%)	2^{nd} Unc. Down-Up(%)	3^{rd} Unc. Down-Up(%)
1l_2tau	TauIDSF -6.52 6.73	TauScale -3.49 4.93	NP_Modelling1JES -1.36 1.65
2ee4jets	ElecIso -4.16 4.25	NPVJES -2.57 -2.27	NP Modelling1JES -1.73 -3.40
2ee≥5jets	ElecIso -4.46 4.56	FlavCompJES -1.52 5.27	NP_Modelling1JES -1.47 4.65
2em4jets	JER — 3.55	ElecIso -2.19 2.19	MuonIso 2.04 -2.04
2em≥5jets	NP_Modelling1JES -4.32 2.39	FlavCompJES -3.00 1.96	ElecIso -2.25 2.25
2mm4jets	MuonIso -4.01 4.09	FlavCompJES 2.89 3.94	JER — 3,26
2mm≥5jets	FlavCompJES -5.45 4.20	MuonIso -4.09 4.18	NP_Modelling1JES -4.48 3.29
2l_tau	MuonIso -2.32 2.34	FlavCompJES -2.99 1.97	NP_Modelling1JES -2.67 1.91
3l	MuonIso -3.61 3.71	ElecIso -2.70 2.77	NP_Modelling1JES -1.76 2.51
4l	JER — -5.16	MuonIso -4.81 5.00	ElecIso -3.78 3.90

Table 6: Most relevant systematics variation on the *ttZ* expected events for all the analysis channels.

Total Systematic Uncertainty	2ee4j Down	2ee4j Up	2ee5jincl Down	2ee5jincl Up	2em4j Down	2em4j Up	2em5jincl Down	2em5jincl Up	2mm4j Down	2mm4j Up
ttH	-4.68	5.84	-8.24	6.14	-5.10	3.50	-5.52	6.40	-5.20	7.51
ttW	-7.20	5.45	-8.72	11.30	-3.63	6.22	-9.72	7.95	-4.54	5.23
ttZ	-9.68	5.07	-5.87	10.98	-4.07	6.16	-8.37	4.99	-5.24	8.69
Total Systematic Uncertainty	2mm5jincl Down	2mm5jincl Up	1l2t Down	1l2t Up	2lt Down	2lt Up	3l Down	3l Up	4l Down	4l Up
ttH	-7.28	6.75	-7.91	8.39	-6.40	5.92	-5.84	5.59	-6.54	6.54
ttW	-8.63	6.88	-9.26	10.04	-7.48	7.79	6.36	8.16	—	—
ttZ	-9.73	8.18	-8.12	9.18	-7.52	7.21	-6.14	6.66	-9.58	6.94

Table 7: Sum in quadrature of all the systematic uncertainties on the number of event yields per channel.

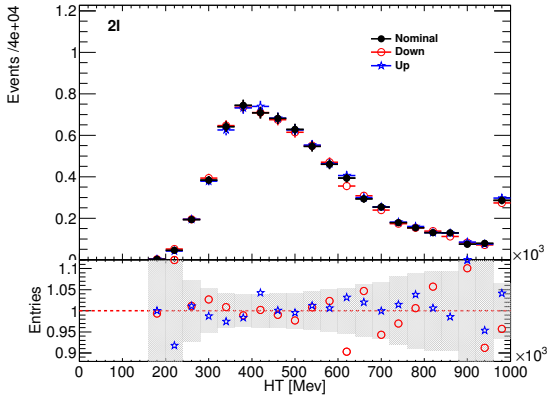

(a) Eta ModellingJES

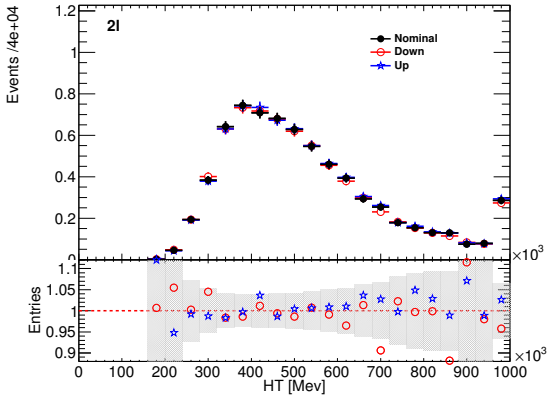

(b) FlavRespJES

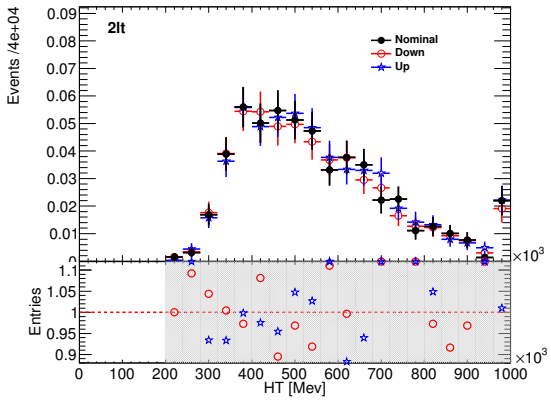

(c) FlavCompJES

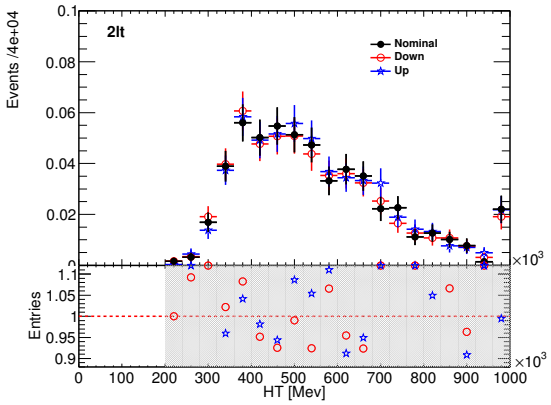

(d) NP_Modelling1JES

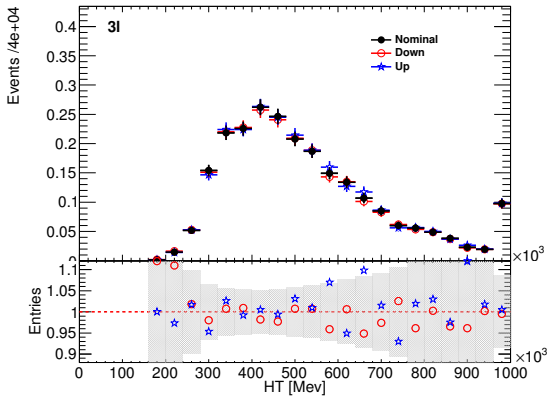

(e) PileRhoJES

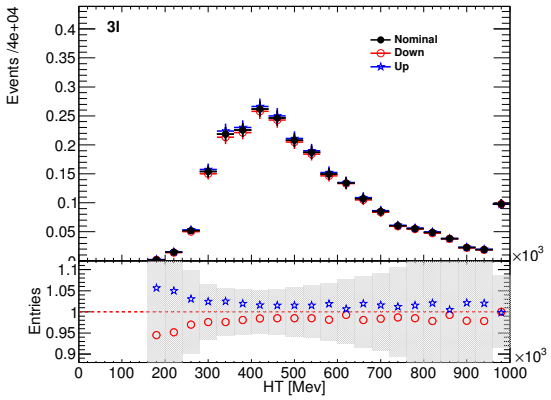

(f) JetTagWeightB5

Figure 1: (a), (b) Expected HT distribution for ttH events in the 2lep (anyjet and any flavour) channel (black) compared with the HT distributions obtained by the up and down variation of the most important Jet systematics (blue and red). (c), (d) Expected HT distribution for ttH events in the 2lep+tau channel (black) compared with the HT distributions obtained by the up and down variation of the most important Jet systematics (blue and red). (e), (f) Expected HT distribution for ttH events in the 3lep channel (black) compared with the HT distributions obtained by the up and down variation of the most important Jet systematics (blue and red).

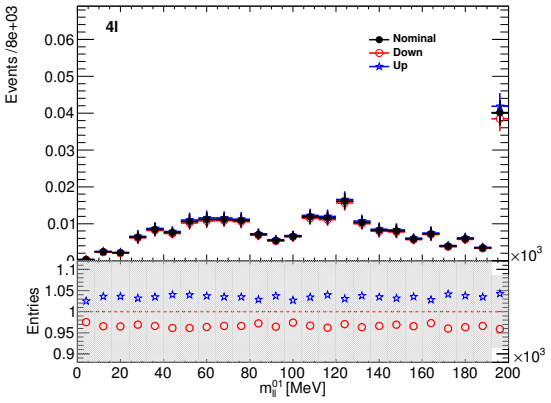

(a) ElecIso

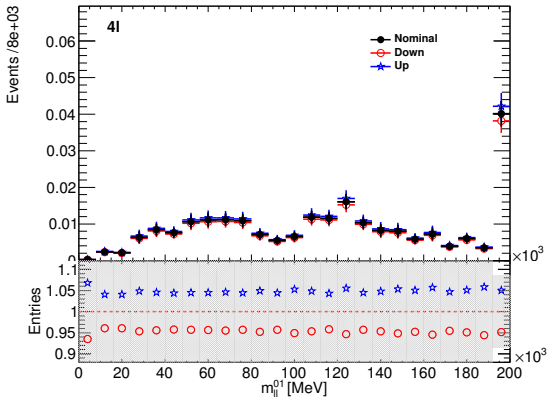

(b) MuonIso

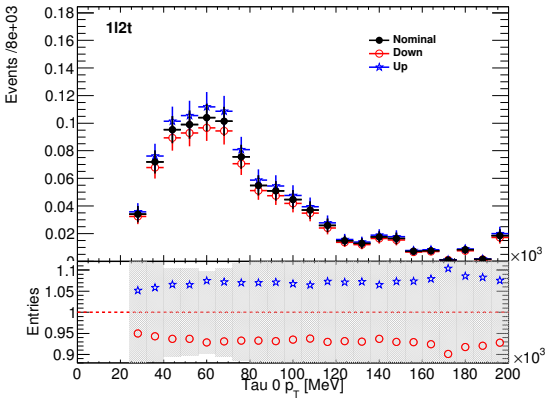

(c) TauIDSF

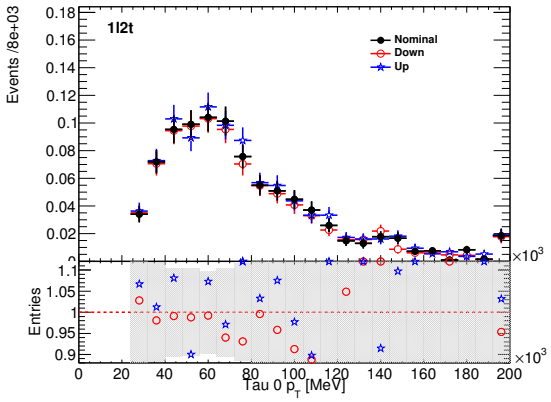

(d) TauScale

Figure 2: (a), (b) Expected Mll01 distributions for ttH events in the 4lep channel (black) compared with the Mll01 distributions obtained by the up and down variation of the most important lepton systematics (blue and red). (c), (d) Expected Tau pT distributions for ttH events in the 1lep+2tau channel (black) compared with the Tau pT distributions obtained by the up and down variation of the most important hadronic tau systematics (blue and red).

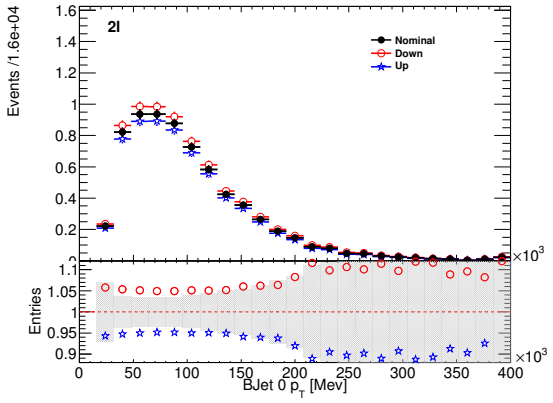

(a) ttH

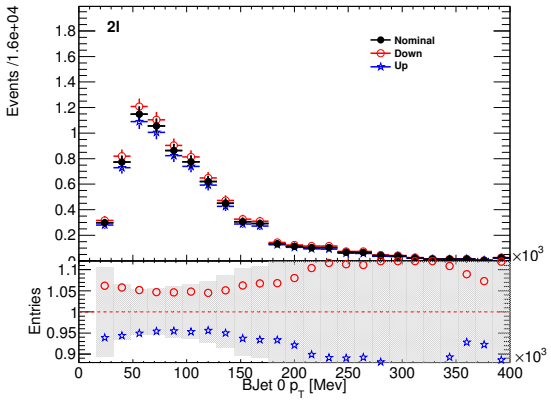

(b) ttZ

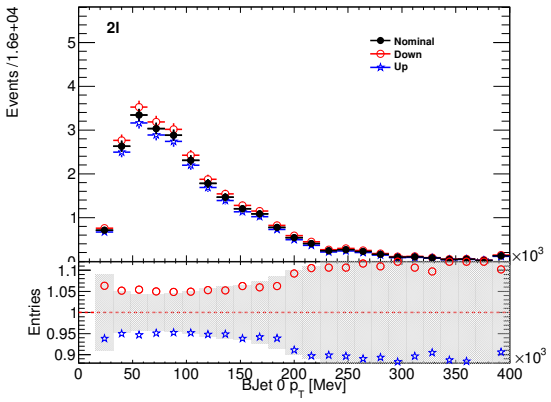

(c) ttW

Figure 3: (a), (b), (c) Expected leading BJet Pt distributions for ttH, ttZ and ttW events in the 2lep channel. The systematic effect shown is the combined effect of the 6 btag eigenvector variations.

3 $t\bar{t}H$ and $t\bar{t}V$ Production Cross Sections and Theoretical Uncertainties

This section describes the simulation of the $t\bar{t}H$ and $t\bar{t}V$ productions. Uncertainties from the choice of the factorisation (μ_F) and renormalisation μ_R scales as well as from the PDF sets are considered evaluating their impacts on both the production cross sections and on the event selection efficiencies.

3.1 $t\bar{t}H$ Production

The $t\bar{t}H$ production is modelled using matrix elements obtained from the HELAC-Oneloop package [6] that corresponds to the NLO QCD accuracy. POWHEG BOX [7, 8, 9] serves as an interface to the shower Monte Carlo programs. The samples created using this approach are referred to as PowHel samples. CT10NLO PDF sets are used and the factorisation (μ_F) and renormalization (μ_R) scales are set to $\mu_0 = \mu_F = \mu_R = m_t + m_H/2$. Pile-up and the underlying events are simulated by Pythia 8.1 [10] with the CTEQ61L set of parton distribution functions and AU2 underlying event tune. The Higgs boson mass is set to 125 GeV and the Top quark mass is set to 172.5 GeV.

The production cross section and the Higgs boson decay branching fractions together with their theoretical uncertainties are taken from the NLO theoretical calculations reported in Ref. [11]. The uncertainty from the QCD scale estimated by varying μ_0 by a factor of 2 from the nominal value is $^{+3.8\%}_{-9.3\%}$, while the uncertainty from the PDF set and the value of α_S is $\pm 8.1\%$.

The impact of the choice of the QCD scale on the simulation of the $t\bar{t}H$ event selection efficiency is estimated in two independent ways.

First, the factorisation and renormalisation scales μ_0 are varied by a factor of 2, as $\mu = 2\mu_0$ and $\mu = \mu_0/2$. The effects of these new scales are estimated via the application of event reweighting procedures on the nominal simulation using kinematic distributions at parton level. The weights used are dependent on the transverse momenta of both the $t\bar{t}H$ system and of the top quark, as described in Ref. [12].

Second, the choice of the factorisation and renormalisation scales, dependent on fixed ("static") parameters in the nominal simulation, is tested comparing its prediction with an alternative ("dynamic"), but still physics motivated choice $\mu_0 = (m_T^t m_T^{\bar{t}} m_T^H)^{\frac{1}{3}}$, which depends on kinematic variables. This comparison is performed via event reweighting of the nominal static simulation based on weights derived as a function of the $t\bar{t}H$ transverse momentum [12]. In order to take the difference between the choices of scale as systematic uncertainties, a symmetric envelope around the nominal simulation is built applying the weights and also their inverses.

Fig. 4 shows the impact of the different choices for the factorization and renormalization scales on the jet and b-jet multiplicities in events with 2 SS leptons. Similar variations are seen also in the other event categories. In order to not double-count the variations on the total cross section the predictions from the different QCD scales are normalised to the same total cross section. That means that the observed differences are only coming from the event selection. Significant variations on the jet multiplicities can be seen and these translate into different predictions on the signal event yields in the signal regions. Such differences, listed in Table 8, are taken as theoretical systematic uncertainties in addition to the ones affecting the total $t\bar{t}H$ production cross section. The "Static" uncertainties come from the variations by a factor of 2 from the nominal scale and they are correlated with the uncertainties on the total cross section, which are estimated with the same procedure. The "Dynamic" uncertainties come from the difference between the nominal and the alternative dynamic scale and are treated as an independent source of theoretical uncertainty.

The uncertainty of the $t\bar{t}H$ event selection due to the PDF sets is estimated comparing the predictions with three different PDF sets, varying each set within errors and taking the width of the envelope as systematic uncertainty. The recommended sets are `CT10`, `MSTW2008nlo68cl` and `NNPDF21_100`. We

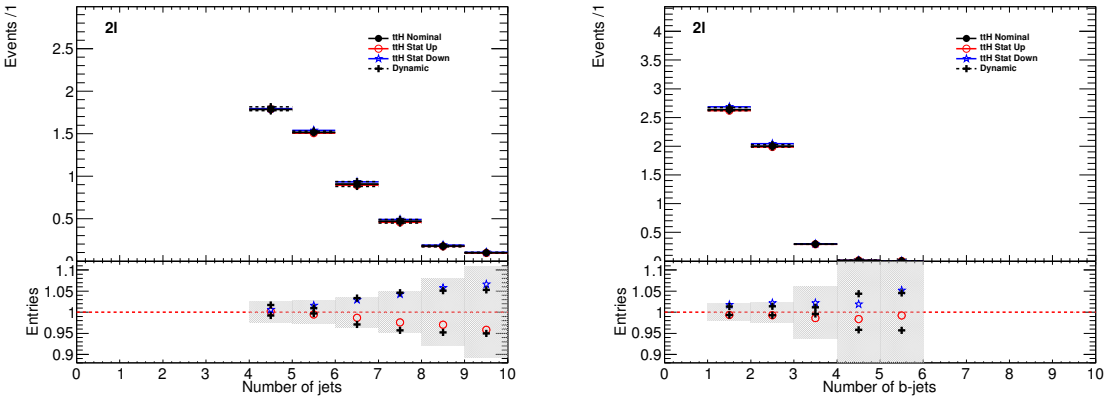

(a) jet multiplicity

(b) b-jet multiplicity

Figure 4: Effects on the jet multiplicities in 2 SS lepton $t\bar{t}H$ events from different choices of the factorization and renormalization scales. "Static" refers to the variations by a factor of 2 of the nominal μ_0, while "Dynamic" refers to the alternative choice of μ_0 which depends on the event kinematic. The grey band in the lower panels represents the statistical uncertainty of the nominal sample.

Table 8: Theoretical uncertainties of the signal event yields in the signal regions due to the impact of QCD scale uncertainties on the event selection.

QCD scale [%]	1l_2tau	2l4jets	2l≥5jets	2l_tau	3l	4l
Static	$^{+0.7}_{-0.1}$	$^{+0.6}_{-0.0}$	$^{+2.7}_{-1.3}$	$^{+2.7}_{-1.0}$	$^{+2.3}_{-0.8}$	$^{+0.9}_{-0.2}$
Dynamic	$^{+0.6}_{-0.0}$	$^{+1.7}_{-0.8}$	$^{+2.0}_{-2.6}$	$^{+1.7}_{-1.1}$	$^{+1.7}_{-1.1}$	$^{+0.5}_{-0.0}$

Table 9: Uncertainties on $t\bar{t}H$ acceptance in signal regions due to PDF variation.

Sample	1l_2tau	2l 4j	2l 5j	2l_tau	3l	4l
$t\bar{t}H$	1.0%	0.3%	1.0%	0.9%	0.5%	1.4%

determine the change in the acceptance due to the PDF sets via the formula 1 to disentangle it from the change in production cross section.

$$\left(\frac{\text{Reweighted yield in SR}}{\text{Reweighted total number of events}}\right)\left(\frac{\text{Original yield in SR}}{\text{Original total number of events}}\right)^{-1} - 1 \qquad (1)$$

Fig. 5 shows the estimated PDF systematic uncertainties as a function of the jet multiplicity in $t\bar{t}H$ events with at least two leptons. The uncertainties are compatible with the uncertainty on the production cross section estimated in Ref. [11] and indicated by the dashed red lines in the lower panel. Table 9 shows the half-width of the envelope of the acceptance under all eigenvector variations of the three PDF sets. No significant dependence on the event topology is observed, so that the PDF systematic uncertainty on the $t\bar{t}H$ event selection is neglected.

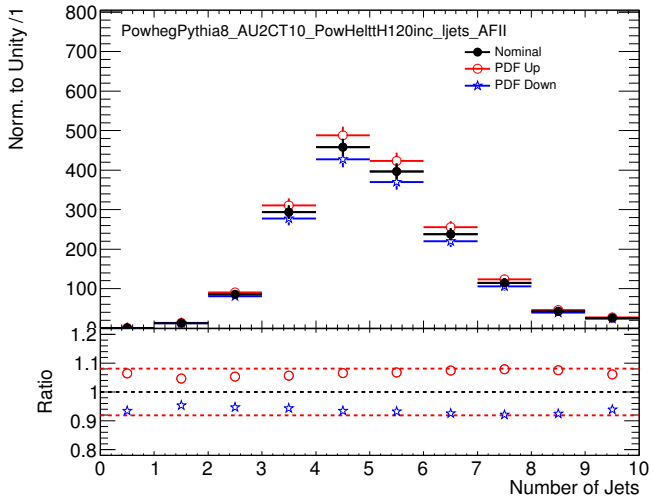

Figure 5: PDF systematic uncertainty on the jet multiplicities in $t\bar{t}H$ events with at least 2 leptons. The dashed red lines in the lower panel indicate the systematic uncertainty on the $t\bar{t}H$ production cross section.

3.2 $t\bar{t}V$ Production

Samples of $t\bar{t}V$ ($V = W, Z$) are generated with the MADGRAPH v5 LO generator [13] and the CTEQ6L1 PDF set. PYTHIA 6.425 with AUET2B tune is used for showering.

NLO cross section calculations have been performed for $t\bar{t}W$ [14] and for both $t\bar{t}W$ and $t\bar{t}Z$ [15] at $\sqrt{s} = 8$ TeV. These calculations include theoretical uncertainties on the cross section due to the choice of renormalisation and factorisation scale and in [14] the theoretical uncertainty due choice of PDF is also considered.

Process	σ_{NLO} [fb]	Scale Uncertainty [%]		PDF Uncertainty [%]		Total symmetrised uncertainty [%]
$t\bar{t}W^+$	144.9	+10	-11	+7.7	-8.7	13.3
$t\bar{t}W^-$	61.4	+11	-12	+6.3	-8.4	13.6
$t\bar{t}Z$	206.7	+9	-13	+8.0	-9.2	14.0

Table 10: NLO cross section and theoretical uncertainty calculations derived from `MadGraph5_aMC@NLO`.

Table 11: Theoretical uncertainties of the $t\bar{t}W$ and $t\bar{t}Z$ event yields in the signal regions due to the impact of QCD scale uncertainties on the event selection.

QCD scale [%]	1l_2tau	2l4jets	2l≥5jets	2l_tau	3l	4l
$t\bar{t}Z$	$^{+0.1}_{-0.2}$	$^{+1.6}_{-1.8}$	$^{+3.1}_{-3.0}$	$^{+1.7}_{-1.7}$	$^{+1.1}_{-1.2}$	$^{+0.5}_{-0.5}$
$t\bar{t}W$	$^{+1.8}_{-2.2}$	$^{+3.3}_{-3.5}$	$^{+0.5}_{-0.7}$	$^{+1.3}_{-1.7}$	$^{+0.4}_{-0.4}$	—

It is difficult to directly compare these calculations as they differ in several aspects; the choice of central scale; the definition of the scale uncertainty envelope; the choice of PDF; the inclusion (or not) of the PDF uncertainty calculation and only [15] has a prediction for $t\bar{t}Z$. As a result of the limitations of/differences between the two calculations, `MadGraph5_aMC@NLO` [16] is used to evaluate the cross sections and uncertainties with more optimal and consistent set of parameter choices. The uncertainties are calculated using the internal scale and PDF reweighting that is available with `MadGraph5_aMC@NLO`. The prescription for the scale envelope is taken from [15]: the central value $\mu_0 = \mu_R = \mu_F = m_t + m_V/2$ and the uncertainty envelope is $[\mu_0/2, 2\mu_0]$. The PDF uncertainty prescription used is the recipe from [14]: calculate the PDF uncertaintly using the `MSTW2008nlo` [17] PDF for the central value and then the final PDF uncertainty envelope is derived from three PDF error sets each with different α_S values (the central value and the upper and lower 90% CL values). The final NLO cross section central values and uncertainties are given in Table 10.

As a cross check, a comparison between [14] and [15] and the calculations with `MadGraph5_aMC@NLO` using the same settings is reported in Appendix C and gives consistent results.

The uncertainty of the simulation of the $t\bar{t}V$ production in the event selection is estimated varying the scale of the QCD emissions in the LO MADGRAPH v5 generator (the so-called `alpsfact` parameter). The effect of varying this parameter is estimated via event reweighting of the nominal samples. The weights are derived as a function of the $t\bar{t}V$ transverse momentum and are documented in Ref. [18].

Fig. 6 shows the impact of this uncertainty on the jet multiplicity distributions in 2 SS lepton $t\bar{t}W$ and $t\bar{t}Z$ events, separately. Similar to the QCD scale uncertainties on $t\bar{t}H$ events, the resulting $t\bar{t}V$ event yield variations, listed in Table 11 are taken as systematic uncertainties.

The uncertainty on the acceptance for $t\bar{t}V$ due to PDF choice is evaluated separately from the uncertainty on the overall cross section. This is complicated slightly because the standard simulation uses the `CTEQ6L1` leading order PDF, while the PDF eigenvector sets we compare with are next to leading order (`CT10`, `MSTW2008nlo`, and `NNPDFnlo 2.1`). We ignore the overall offset of the NLO PDFs relative to the LO one and only determine the width of the envelope of NLO PDFs. Formula 1 is used to determine the change in the acceptance. Table 12 shows the half-width of the envelope of the acceptance under all eigenvector variations of the three PDF sets.

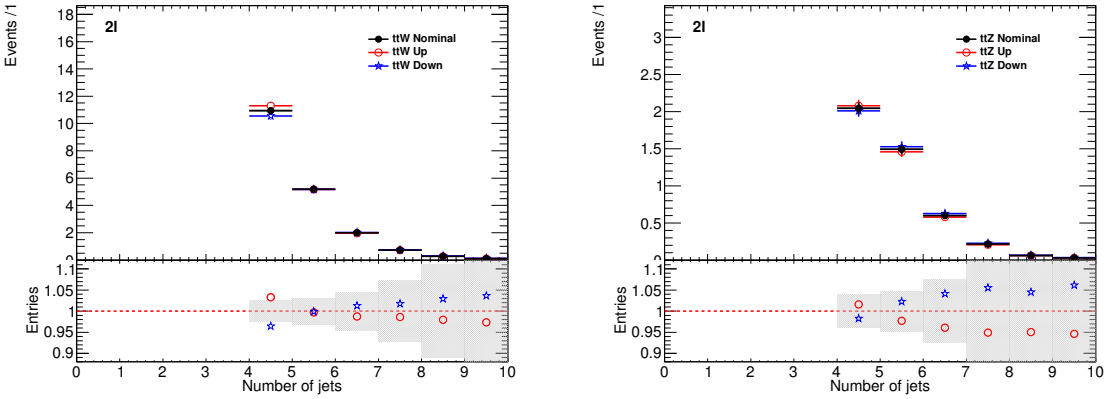

(a) jet multiplicity in $t\bar{t}W$ events

(b) jet multiplicity in $t\bar{t}Z$ events

Figure 6: Effects on the jet multiplicities in 2 SS lepton $t\bar{t}V$ events from QCD scale uncertainties. The grey band in the lower panels represents the statistical uncertainty of the nominal sample.

Table 12: Uncertainties on $t\bar{t}V$ acceptance in signal regions due to PDF variation. There are insufficient statistics for $t\bar{t}W$ in the 4l region to derive an uncertainty.

Sample	1l_2tau	2l 4j	2l 5j	2l_tau	3l	4l
$t\bar{t}Z$	2.7%	1.5%	2.3%	0.9%	1.4%	0.9%
$t\bar{t}W$	4.8%	1.1%	2.5%	1.7%	3.6%	—

3.3 Summary

Tab.13 gives the summary of the theoretical systematics that are included in the analysis.

Type	Description	Name	Uncertainty	Status
		Signal (ttH)		
QCD Scale	Cross Section (Dynamic Scale)	QCDscale_XS_ttH	+3.8% −9.3%	✓
	Analyses Acceptance	QCDscale_Acceptance_ttH	0.-2.6% (Table 8)	✓
PDF+α_S	Cross Section	pdf_ttH	± 8.1%	✓
	Analyses Acceptance	pdf_Acceptance_ttH	Negligible (Table 9)	✗
		ttW (Irreducible background)		
QCD Scale	Cross Section (Dynamic Scale)	QCDscale_XS_ttW	±15%	✓
	Analyses Acceptance	QCDscale_Acceptance_ttW	0.4-3.5% (Table 11)	✓
PDF+α_S	Cross Section	pdf_ttW	± 13%	✓
	Analyses Acceptance	PDF_Acceptance_ttW	1.1-4.8% (Table 12)	✓
		ttZ (Irreducible background)		
QCD Scale	Cross Section (Dynamic Scale)	QCDscale_XS_ttZ	±12%	✓
	Analyses Acceptance	QCDscale_Acceptance_ttZ	0.1-3.1% (Table 11)	✓
PDF+α_S	Cross Section	pdf_ttZ	± 9%	✓
	Analyses Acceptance	PDF_Acceptance_ttZ	0.9-2.7% (Table 12)	✓
		VV Backgrounds		
Cross Sections	WZ Processes	WZxsec	± 50%	✓
(Scale ⊕PDF)	ZZ processes	ZZxsec	± 25%	
	WW processes	WWxsec	± 25%	✓
	$\gamma\gamma$, Wγ* and Zγ* Processes	ggVgxsec	± 25%	✓
		$t\bar{t}$		
Cross Section		ttbarxsec	± 30%	✓

Table 13: Summary of theoretical systematics to be included in the analysis, with their type, description, name, values and uncertainties, and status of inclusion in the final results. The cross section uncertainties for signal are taken from the yellow report values for M_{H}=125 GeV. The acceptance uncertainties were determined for each channel selection and are given in dedicated tables. The reducible background uncertainties from MC are not relevant when the process is included in the fake estimates.

4 2 lepton Same-Sign channel

In this channel, events must have axactly two leptons. Leptons being electrons or muons. Events with taus are rejected. The two leptons must have the same charge leading to three possible signal regions $e^{\pm}e^{\pm}$, $e^{\pm}\mu^{\pm}$ and $\mu^{\pm}\mu^{\pm}$. This categorisation is used due to the different lepton efficiencies and purities of electrons and muons.

In order to reject the two main background processes, $t\bar{t}$ and $t\bar{t}V$, events must have at least four jets. The signal region is splitted in two: events with exactly 4 jets and events with at least 5 jets. This categorisation is justified by the different signal purities in these two regions.

In order to reject di-bosons and single boson channels, at least one b-jet is required.

- pass event cleaning
- passed trigger: EF_mu24i_tight or EF_mu36_tight or EF_e24vhi_medium1 or EF_e60_medium1
- exactly two tight leptons in the event
- at least one trigger matched lepton
- lepton $p_{\mathrm{T}} > 25$ GeV for leading lepton
- lepton $p_{\mathrm{T}} > 20$ GeV for subleading lepton
- No third lepton with $p_{\mathrm{T}} > 10$ GeV.
- Same sign of reconstructed charge of the two leptons
- number of good jets 4 or ≥5 jets
- number of good b-jets ≥ 1
- No hadronic tau

Table 14: Resulting event numbers obtained from MC in the same-sign channel after the full signal region selections.

	≥ 5 jets			4 jets		
	$e^{\pm}e^{\pm}$	$e^{\pm}\mu^{\pm}$	$\mu^{\pm}\mu^{\pm}$	$e^{\pm}e^{\pm}$	$e^{\pm}\mu^{\pm}$	$\mu^{\pm}\mu^{\pm}$
$t\bar{t}H$	0.73 ± 0.03	2.13 ± 0.05	1.41 ± 0.04	0.44 ± 0.02	1.16 ± 0.03	0.74 ± 0.03
$t\bar{t}V$,tV	2.60 ± 0.13	7.42 ± 0.17	5.01 ± 0.16	3.05 ± 0.13	8.39 ± 0.24	5.79 ± 0.20
VV	0.48 ± 0.25	0.37 ± 0.23	0.68 ± 0.30	0.77 ± 0.27	1.93 ± 0.80	0.54 ± 0.30
$t\bar{t}$, tX (MC)	1.31 ± 0.67	2.55 ± 0.84	1.76 ± 0.67	4.99 ± 1.19	8.19 ± 1.41	3.70 ± 1.03
Z+jets (MC)	0.16 ± 0.16	0.28 ± 0.20	0.12 ± 0.12	1.37 ± 0.78	0	0.23 ± 0.23
fake leptons (DD)	2.31 ± 0.97	3.87 ± 1.01	1.24 ± 0.41	3.43 ± 1.38	6.82 ± 1.63	2.38 ± 0.78
Q misid (DD)	1.10 ± 0.09	0.85 ± 0.08	–	1.82 ± 0.11	1.39 ± 0.08	–

The yields obtained from the simulation are provided in Table 14 together with the background due to fake leptons and to charge mis-identification of electrons as derived from the data and described in [19].

5 2 lepton Same-Sign channel with hadronic tau

5.1 Signal region selection

In this channel three flavours of leptons are considered. However, electrons and muons are referred as leptons, and hadronic taus as taus. Each event is required to have exactly two same sign leptons. In case the two selected leptons are both electrons, a Z-veto is applied in order to reduce possible remaining Z+jets background pollution from charge mis-identification. Due to a high signal jet multiplicity, at least four jets and at least one b-jet are required in the events. Finally, exactly one hadronic tau is required. The reconstructed charge of the hadronic tau has to be opposite sign to the lepton. The selection of the signal region is summarised as follows:

- pass event cleaning
- passed trigger: EF_mu24i_tight or EF_mu36_tight or EF_e24vhi_medium1 or EF_e60_medium1
- exactly two tight leptons in the event
- at least one trigger matched lepton
- lepton $p_T > 25$ GeV for leading lepton
- lepton $p_T > 15$ GeV for subleading lepton
- same sign of reconstructed charge of the two leptons
- Z veto: (invariant mass of any SS electron-electron pair must be outside [81 GeV, 101 GeV])
- number of good jets ≥ 4
- number of good b-jets ≥ 1
- exactly one hadronic tau
- opposite charge of hadronic tau to the leptons

5.2 Expected MC backgrounds

The MC event yields obtained with the signal region selection above are summarised in Table 15.

Table 15: Resulting event numbers obtained from MC in the 2lSS+tau channel after the full signal region selection.

Process	MC event yield
ttH signal	0.47±0.02
$t\bar{t}$	0.70±0.38
Z+jets	0.00±0.00
W+jets	0.00±0.00
ttZ	0.44±0.05
ttW	0.41±0.04
VV	0.11±0.10

352 ### 5.3 Expected data-driven backgrounds

353 The total estimated fake background in the signal region is obtained to be $N_{fakes} = 0.46 \pm 0.59$ events,
354 including statistical and systematic uncertainties (see Note 2).

355 # 6 3 lepton channel

6.1 Signal region selection

The event selections defining the signal region for the 3 lepton channel, presented in Note1 [**?**], are listed here as a reminder to the reader:

- three tight leptons, the sum of the charges of which should be ± 1;
- the event must have passed one of the following triggers: `EF_e24vhi_medium1, EF_e60_medium1, EF_mu24i_tight, EF_mu36_tight` and one of the leptons has to be matched to an EF ROI;
- N(b-tags, MV1) ≥ 1 and N(jets, $p_T > 25$ GeV, $|\eta| < 2.5$) ≥ 4 **OR**
- N(b-tags, MV1) ≥ 2 and N(jets, $p_T > 25$ GeV, $|\eta| < 2.5$) = 3
- Invariant mass of two leptons, if of same flavor and opposite charge, should not be in the range [81, 101] GeV, to suppress the $t\bar{t}Z$ and Z+jets contribution (Z veto).

6.1.1 Signal region definition studies

Several different SR definitions were considered *a priori*, before deciding to adopt the one described above. The choice was made based mainly on the expected reach of the channel in terms of limit on $\frac{\sigma}{\sigma_{SM}}$. Table 16 shows the expected limit for various options.

SR definition	Expected limit (median), stat only	Expected limit (median), stat $\oplus$ syst
one SR	3.15722	3.26021
split (4ji,1bi) + (3je,2bi)	3.14786	3.24964
split (4ji,1be) + (3ji,2bi)	3.15365	3.25058
split Zdep + Zenr	3.11811	3.21618

Table 16: . Expected limit, extracted from the signal region fit median, on $\frac{\sigma}{\sigma_{SM}}$ for different signal region definitions. Here "nji/e" stands for $\geq/=$ n jets; "mbi/e" stands for $\geq/=$ m b-tags. "Zdep" stands for "Z depleted", where events with an opposite-sign, same-flavour lepton pair are discarded. In the Zenr ("Z enriched") sub-region, only those events are selected instead.

The option appearing as "Zdep + Zenr" aims at exploting the difference in $t\bar{t}Z$ content between the two sub-regions.

The values of the systematic uncertainties used are 30% for the top quark processes yield and 20% for $t\bar{t}V$ Ċonsiderations related to the statistical uncertainty with which the top fakes could be estimated in the signal sub-regions also played a role: one inclusive SR was chosen because the other options would only marginally push down the limit, but splitting would cost in terms of sample size of the top quark-dominated CR from where to estimate the fakes. Namely, a more realistic systematic uncertainty on the top fakes of "split Zdep + Zenr" would be 50% overall; that value brings the limit up to 3.33418.

6.2 Dominant background processes

The main irreducible background process for this channel is the associated production of a top quark pair and a vector boson W or Z, $t\bar{t}V$, where the top quark pair can decay either in one lepton and quarks, and the other two prompt leptons come from the Z boson; or it decays di-leptonically and the last prompt lepton comes from the W boson decay. This category, which includes also virtual photon $t\bar{t}\gamma^*$ contributions, is also the most important background overall. The related yield in the SR is taken

384 from MC for all the listed processes (see Note 2 []) and validated against data in dedicated regions (see
385 Section **??**). In total 7.21 ± 0.24 events are expected from the $t\bar{t}V$ category in the 3 lepton SR.
386 Events of top quark pair creation decaying di-leptonically and with a non-prompt lepton from a heavy
387 flavour (mainly b-quark) decay constitute a reducible background which ranks second in importance
388 among the background processes for this channel. Its yield in the SR is estimated in a data-driven way,
389 with techniques and results reported in []. In total 2.62 ± 0.51 events are expected from the top quark
390 fakes category in the 3 lepton SR.

7 4 lepton channel

7.1 Signal region selection

In the four lepton signal region, selected events must have exactly four leptons with a total charge of zero. At least one of these leptons much be matched to one of the applied single lepton trigger. The leading and sub-leading leptons are required to have a p_{T} of 25 and 15 GeV respectively. In order to suppress background contributions from low-mass resonances and Drell-Yan radiation, all opposite-sign-same-flavour (OS-SF) lepton pairs are required to have a dilepton invariant mass of at least 10 GeV. The quadlepton invariant mass is required to be between 100 and 500 GeV. This choice of mass window suppresses background from the on-shell $Z \to 4\ell$ peak and exploits the high-mass differences between the signal and the dominant $t\bar{t}Z$ background. Events containing an OS-SF lepton pair within 10 GeV of the Z boson mass are discarded. This Z-veto procedure greatly reduces background contributions from ZZ production as well as $t\bar{t}Z$ and while it also affects the signal by vetoing $H \to ZZ^*$, $Z \to \ell^+\ell^-$, these events constitute a small amount of the total expected signal. Finally, selected events are required to have at least two jets, at least one of which must be tagged as a b-quark initiated jet using the MV1 70% working point.

The contribution from $t\bar{t}Z$ comprises approximately 75% of the total background in the inclusive signal region. A signal region categorisation which factorises $t\bar{t}Z$ from the remaining backgrounds is thus beneficial. The signal region is accordingly divided into two categories based on the presence of OS-SF lepton pairs in the final state. The Z-depleted region contains events with zero OS-SF lepton pairs ($e^{\pm}e^{\pm}\mu^{\mp}\mu^{\mp}$) while the remaining events comprise the Z-enriched region ($e^+e^-\mu^+\mu^-$, $eee\mu$, $\mu\mu\mu e$, $eeee$ and $\mu\mu\mu\mu$).

7.2 Expected MC backgrounds

The dominant backgrounds in the four lepton channel are estimated using Monte Carlo simulations described in detail in Note 1. Contributions from $t\bar{t}Z$ and tZ together total approximately 88% of the total background. ZZ production is the next largest background at approximately 9%. Finally, the remaining background contributions estimated from MC come from ggF $H \to 4\ell$ and $t\bar{t}WW$. The modelling and normalisation of on-shell ZZ is validated against data using a dedicated four lepton validation region (VR). Similarly, the off-shell modelling of four lepton events is investigated with an inclusive four lepton VR which excludes on-shell ZZ contributions. The $t\bar{t}Z$ modelling and normalisation is likewise validated with a three lepton VR. These VRs are outlined in Section 8 of this note.

7.3 Expected data-driven backgrounds

Various data-driven techniques are employed in this analysis to estimate backgrounds which arise from non-prompt or fake leptons which are not modelled well in MC. An in-situ method is used in the four lepton channel to estimate the events from $t\bar{t}$and Z+jets which may contribute to the signal region in this manner. However, due to the high lepton multiplicity in this channel, the expected contribution from fake lepton backgrounds is very small. Estimate procedures for this background contribution are extensively outlined in Note 2. Table REFERENCE lists the results of this procedure for the inclusive four lepton signal region.

Data yields are taken from control regions which have 2 tight leptons (those which pass all lepton selection criteria) and 2 anti-tight leptons (which explicitly fail one or a number of lepton selections). These data yields are then extrapolated to the SR using two successive extrapolations. First, the estimates are extrapolated in leptons using the lepton fake θ factors derived by the three lepton analysis. This step of the extrapolation is performed separately for each anti-tight lepton flavour and the contributions are

then summed. Finally, this estimate is extrapolated in jets by using a second extrapolation factor which is derived from two lepton events and corresponds to the efficiency of fake background events passing the N_{jet} selection of the SR. This final value is taken as the upper limit of the background contribution from fake leptons in the four lepton signal region. Both steps of the extrapolation are validated using MC closure tests which are documented thoroughly in Note 2.

7.4 Signal region results

The corresponding yields for this region are shown in Table 17. MC prediction yields from $t\bar{t}$and Z+jets samples are also included here for reference, however as discussed previously the yield for both of these backgrounds will be taken together from the data-driven estimate.

Table 17: Cutflow including unblinded MC yield prediction for the four lepton inclusive signal region. The MC yields for $t\bar{t}$and Z+jets MC samples are included for reference however ultimately these predictions some instead from the data-driven fake estimate

	$t\bar{t}H$	$t\bar{t}WW$	tZ	$t\bar{t}Z/\gamma^*$	VV	H (ggF)	$t\bar{t}$/t + X	Z+jet	Sum Bkg.
Preselection	0.44 ± 0.01	0.03 ± 0.00	0.60 ± 0.03	4.70 ± 0.12	201.03 ± 0.87	4.42 ± 0.06	0.17 ± 0.05	0.35 ± 0.20	211.29 ± 0.90
100 < $M_{4\ell}$ < 500 GeV	0.42 ± 0.01	0.02 ± 0.00	0.55 ± 0.02	4.28 ± 0.11	173.98 ± 0.69	4.38 ± 0.06	0.16 ± 0.04	0.35 ± 0.20	183.70 ± 0.73
$M^{xy}_{\ell\ell}$ > 10 GeV	0.41 ± 0.01	0.02 ± 0.00	0.54 ± 0.02	4.18 ± 0.11	165.24 ± 0.61	4.05 ± 0.06	0.14 ± 0.04	0.21 ± 0.15	174.38 ± 0.64
Z-veto	0.29 ± 0.01	0.01 ± 0.00	0.11 ± 0.01	0.64 ± 0.04	5.61 ± 0.15	1.45 ± 0.03	0.09 ± 0.03	0.10 ± 0.10	8.01 ± 0.19
$N_{\text{jet}} \geq 2$	0.24 ± 0.01	0.01 ± 0.00	0.05 ± 0.01	0.50 ± 0.04	0.52 ± 0.03	0.17 ± 0.01	0.05 ± 0.02	0.00 ± 0.00	1.30 ± 0.06
$N_{\text{b-jet}} \geq 1$	0.20 ± 0.01	0.01 ± 0.00	0.05 ± 0.01	0.44 ± 0.04	0.05 ± 0.01	0.01 ± 0.00	0.02 ± 0.01	0.00 ± 0.00	0.57 ± 0.04

The four lepton inclusive signal region has a predicted signal significance of approximately $\sigma = 0.26$, while the SR categorisations discussed in the preceding sub-sections offer small improvements to this significance.

8 1 lepton and 2 hadronic tau channel

8.1 Signal region selection

8.2 Expected MC backgrounds

8.3 Expected data-driven backgrounds

8.4 Signal region results

9 Control regions

CR	Selection
Inclusive OS dilepton (ee, $e\mu$, $\mu\mu$)	2 OS leptons, $p_{\mathrm{T}} > 25$ GeV, $M(\ell^+\ell^-) > 40$ GeV for ee and $\mu\mu$, with 2ℓ and 3ℓ-style cuts for the muons and electrons Demonstrate normalization of Z, lepton scale factors
Top dilepton (ee, $e\mu$, $\mu\mu$)	As for inclusive OS, but ≥ 2 jets and ≥ 1 MV1 70% btags, ± 10 GeV veto around Z mass Demonstrate normalization of top: btag scale factors
WZ	3ℓ lepton selection, require one OS SF pair within 5 GeV of Z, other lepton has $M_T(\ell, E_{\mathrm{T}}^{\mathrm{miss}}) > 40$ GeV Verify WZ normalization, njet spectra
$W\ell\ell$ off-shell	As above but Z cut reversed; one lepton with $M_T(\ell, E_{\mathrm{T}}^{\mathrm{miss}}) > 40$ GeV Verifies off-shell modeling
$t\bar{t}Z$	3ℓ lepton and jet selection, require one OS SF pair within 5 GeV of Z Verify $t\bar{t}Z$ normalization, modeling
ZZ	4ℓ lepton selection, require one OS SF pair within 5 GeV of Z and another within 10 GeV Verify ZZ normalization, njet spectra
4ℓ inclusive	As above but exclude ZZ candidates Verify off-shell 4ℓ modeling

Table 18: Description of the control regions defined and the background each of them is designed for.

Table 19: Predicted and observed yields in various control regions. The control regions are as defined in Table 9. The "OS dilepton" and "top dilepton" yields combine the ee, $e\mu$, and $\mu\mu$ final states. The "OS dilepton" and "top dilepton" yields are for the 2ℓ-type lepton cuts; others are for 3ℓ-type cuts. All certainties shown in the table are statistical only. For all MC yields, the uncertainty reflects the size of the MC sample; for the Data/MC ratio, the first uncertainty shown is from data statistics and the second from MC statistics.

	OS dilepton	top dilepton	WZ	$W\ell\ell$
Diboson	28330 ± 45	286 ± 5	1159 ± 9	391 ± 5
tZ	89 ± 1	10.7 ± 0.3	12.5 ± 0.3	3.07 ±0.13
ttW	98 ± 1	73.0 ± 0.7	0.72 ± 0.07	8.74 ± 0.25
Other $t\bar{t}$+X	2.02 ± 0.02	1.62 ± 0.02	0.03 ± 0.00	0.17 ± 0.01
ttll	137.6 ± 0.3	57.3 ± 0.2	19.7 ± 0.1	4.65 ± 0.05
Single top	6448 ± 21	2086 ± 12	0.30 ± 0.13	3.1 ± 0.5
tt	67530 ± 140	42100 ± 110	3.0 ± 0.9	39 ± 3
Z+jets	5623 ± 11	4710 ± 60	31 ± 5	118 ± 15
ggF $H \to 4\ell$	11.0 ± 0.1	0.04 ± 0.01	1.08 ± 0.03	1.14 ± 0.03
ttH	46 ± 1	36.7 ± 0.5	0.41 ± 0.04	2.43 ± 0.13
Total MC	10138400 ± 5600	49320 ± 120	1228 ± 10	569 ± 17
Data	10691661	50742	1371	563
Data/MC	1.05 ± 0.00 ± 0.00	1.03 ± 0.00 ± 0.00	1.12 ± 0.03 ± 0.01	0.99 ± 0.04 ± 0.03

	WZ+HF	$t\bar{t}Z$	ZZ	4ℓ non-ZZ
Diboson	23.7 ± 1.2	3.8 ± 0.5	114.7 ± 0.5	178.86 ± 0.63
tZ	8.26 ± 0.21	2.51 ± 0.10	0.03 ± 0.00	0.59 ± 0.03
ttW	0.59 ± 0.06	0.22 ± 0.03	0.00 ± 0.00	0.00 ± 0.00
Other $t\bar{t}$+X	0.02 ± 0.00	0.02 ± 0.00	0.00 ± 0.00	0.03 ± 0.00
ttll	15.90 ± 0.09	13.93 ± 0.09	0.21 ± 0.01	3.35 ± 0.04
Single top	0.06 ± 0.06	0.00 ± 0.00	0.00 ± 0.00	0.00 ± 0.00
$t\bar{t}$	2.08 ± 0.72	0.12 ± 0.12	0.00 ± 0.00	0.61 ± 0.43
Z+jets	0.70 ± 0.33	0.56 ± 0.32	0.00 ± 0.00	0.33 ± 0.23
ggF $H \to 4\ell$	0.03 ± 0.00	0.00 ± 0.00	0.00 ± 0.00	4.09 ± 0.06
ttH	0.33 ± 0.04	0.33 ± 0.03	0.00 ± 0.00	0.44 ± 0.01
Total MC	51.3 ± 1.5	21.1 ± 0.6	114.9 ± 0.5	188.2 ± 0.7
Data	60	30	111	217
Data/MC	1.17 ± 0.15 ± 0.03	1.42 ± 0.26 ± 0.03	0.97 ± 0.09 ± 0.00	1.15 ± 0.08 ± 0.00

9.1 Inclusive dilepton control regions

9.2 ttbar control regions

9.3 WZ control regions

The selections to check the level of accuracy of the simulation in reproducing the di-boson WZ process, both in terms of overall normalization and in the shape of the main variables, are as presented in Table 9. Both inclusive and b-tagged samples are considered, to assess the goodness in simulating WZ+heavy flavour. A sample where all bosons decay leptonically is chosen, therefore with 3 leptons selected as in the $t\bar{t}H$ signal region. The two leptons with opposite sign charge will be compatible with coming from a Z boson, while no further selection is applied on e.g. number of jets or number of b-tags for the inclusive sample. The sample aimed at studying the WZ+HF production should have at least 1 jet which is b-tagged. We assign a conservative 50% systematic error to cover MC modeling based on these distributions and the agreement seen in similar $W + b$ and $Z + b$ analyses and use the MC central value for the final $W^{\pm}Z$ in the SR. More is discussed in Note 2.

9.3.1 Inclusive WZ control region

The yields in the inclusive WZ control region are provided in Table 20. The data-to-MC normalization factor in this sample is 1.11 ± 0.02, with a significant difference from unity. Most of this discrepancy comes from the 1 b-tag sample, which is the reason why a dedicated look is given to the 1 b-tag region.

Multiplicities of jets and b-tags, of electrons (the number of electrons+muons in the event is fixed to 3 by construction), and kinematic variables are presented in Figures **??-??** along with a bin-by-bin Data/MC comparison.

Process	$t\bar{t}H$	top	ttW	ttZ	4 tops
N(events)	0.89 ± 0.02	8.64 ± 0.33	1.60 ± 0.08	28.46 ± 0.28	-

ttWW	tZ	di-boson	Z+jets	Total MC	Data
0.04 ± 0.01	18.98 ± 0.23	1791.78 ± 3.27	181.42 ± 5.53	2031.56 ± 3.58	2246.00 ± 47.39

Table 20: Yields in the inclusive WZ control region after all cuts.

9.3.2 $W\ell\ell$ control region

9.3.3 WZ+HF control region

The yields in the WZ control+heavy flavour region are provided in Table 21. The data-to-MC normalization factor in this sample is 1.19 ± 0.13, with a difference from unity of about 1σ.

Multiplicities of jets and b-tags, of electrons (the number of electrons+muons in the event is fixed to 3 by construction), and kinematic variables are presented in Figures **??-??** along with a bin-by-bin Data/MC comparison.

9.4 ttZ control region

The $t\bar{t}V$ production is the most relevant irreducible background in this analysis, particularly important for the 3 lepton channel. While the production cross-section of the $t\bar{t}W$ and $t\bar{t}Z$ processes is similar (see e.g. C), obtaining a region to validate the rate of $t\bar{t}W$ with uncertainties comparable to the theory ones is

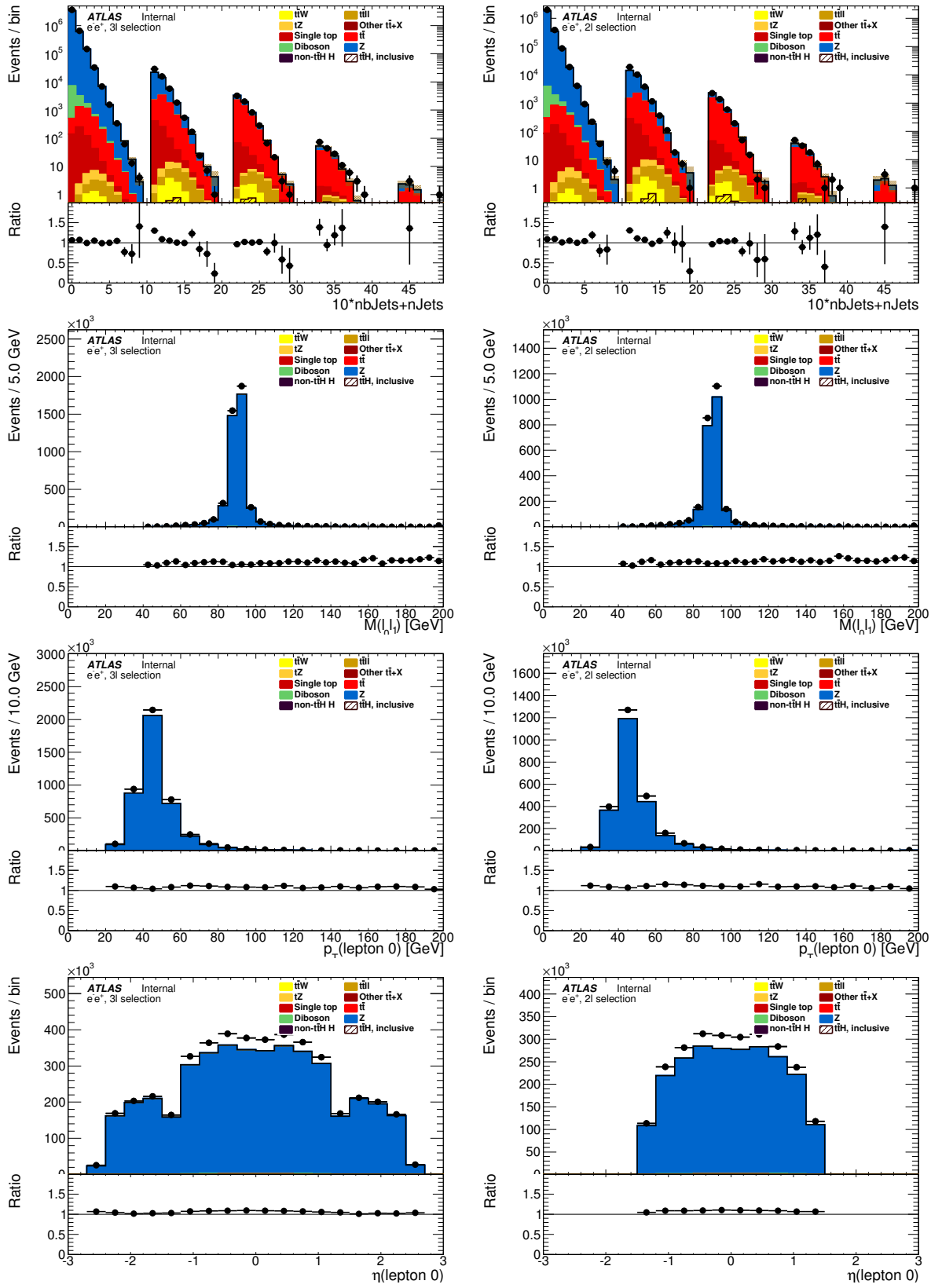

Figure 7: Distributions of (first row) jet and b-jet multiplicity; (second row) dilepton invariant mass; (third row) leading lepton p_{T}; and (bottom row) leading lepton η for the e^+e^- OS dilepton control region. Plots on the left show the 3ℓ lepton selection and those on the right show the 2ℓ selection.

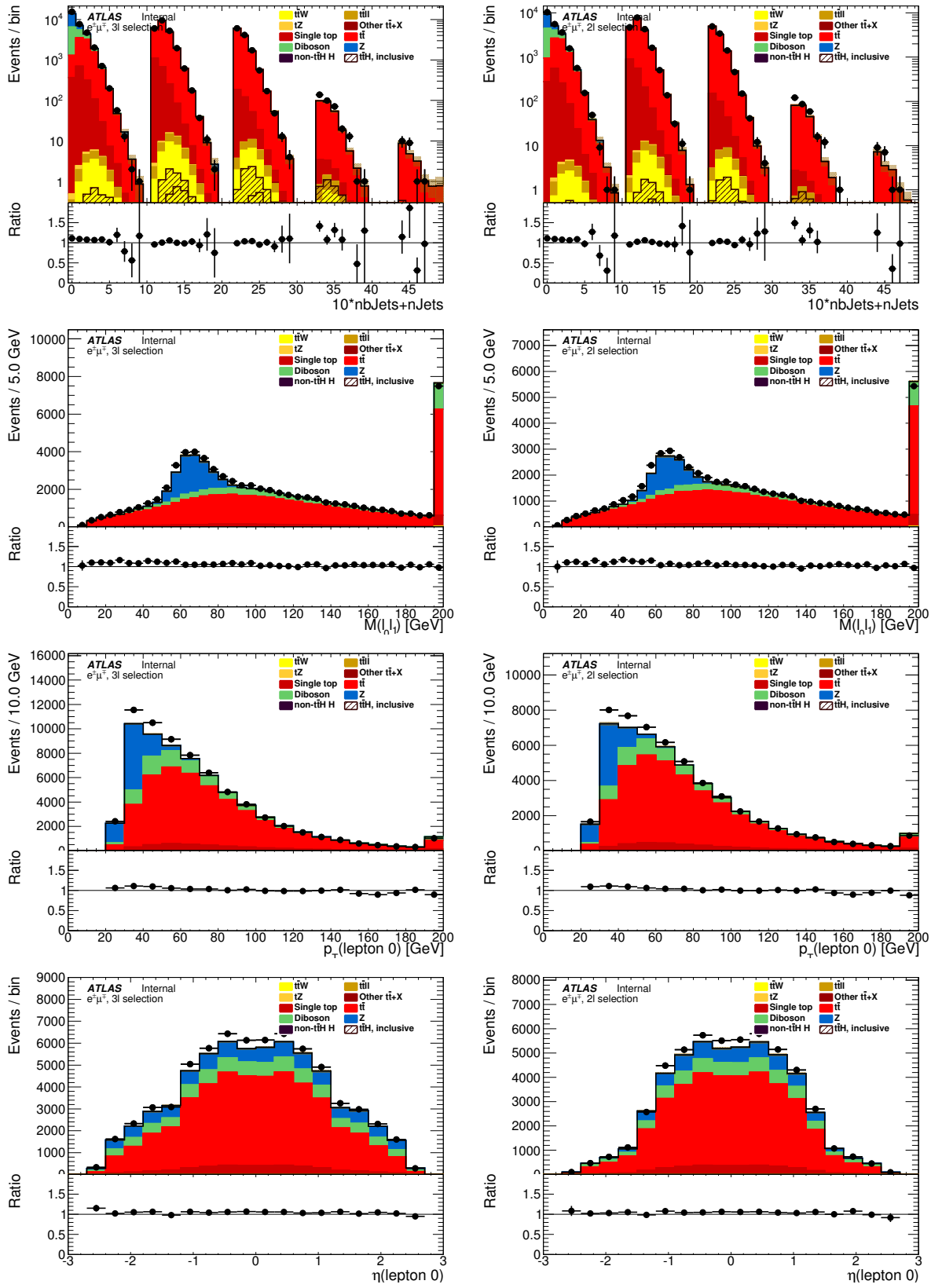

Figure 8: Distributions of (first row) jet and b-jet multiplicity; (second row) dilepton invariant mass; (third row) leading lepton p_{T}; and (bottom row) leading lepton η for the $e^{\pm}\mu^{\mp}$ OS dilepton control region. Plots on the left show the 3ℓ lepton selection and those on the right show the 2ℓ selection.

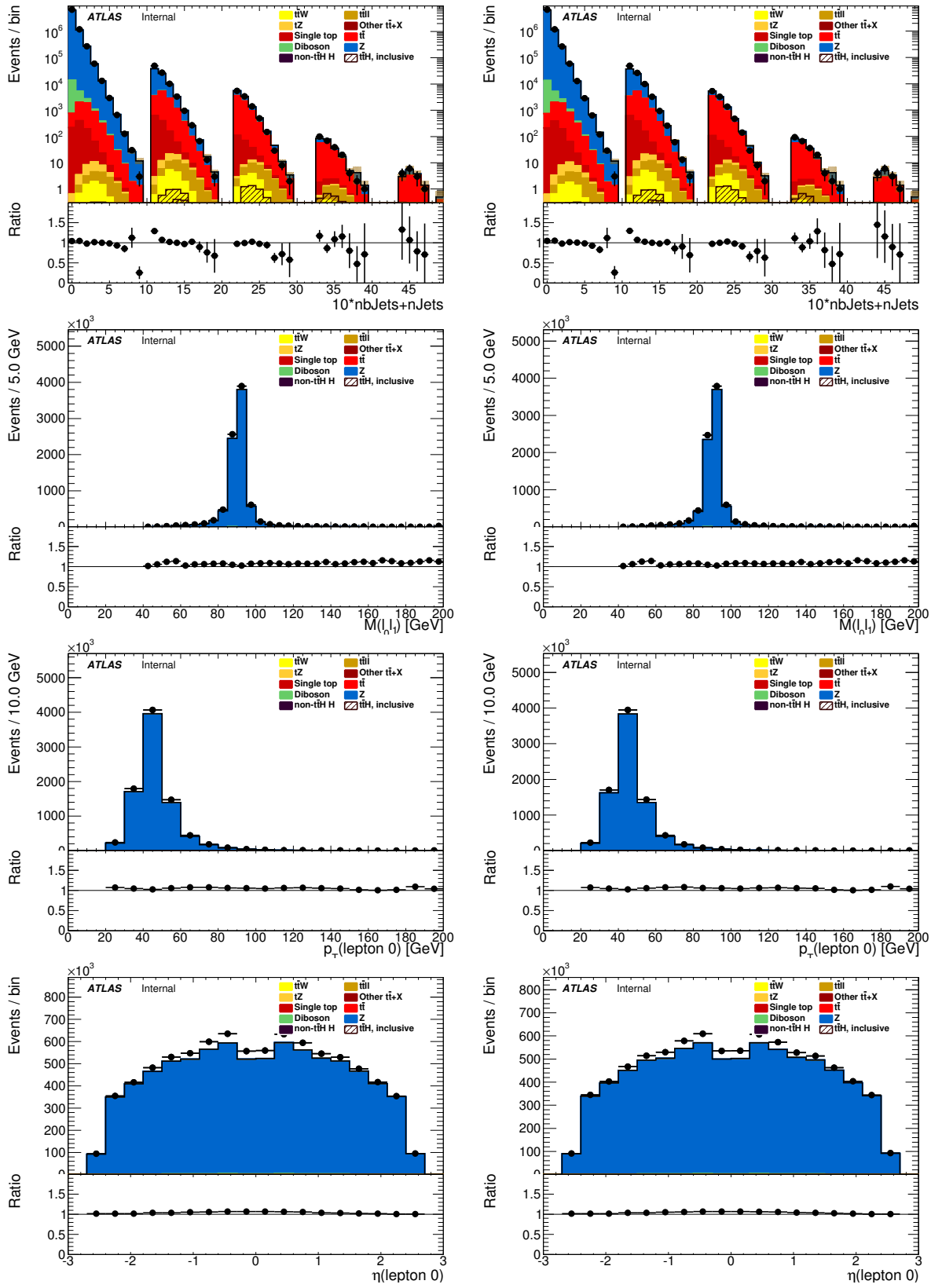

Figure 9: Distributions of (first row) jet and b-jet multiplicity; (second row) dilepton invariant mass; (third row) leading lepton p_{T}; and (bottom row) leading lepton η for the $\mu^{-}\mu^{+}$ OS dilepton control region. Plots on the left show the looser 3ℓ lepton selection and those on the right show the tighter 2ℓ selection.

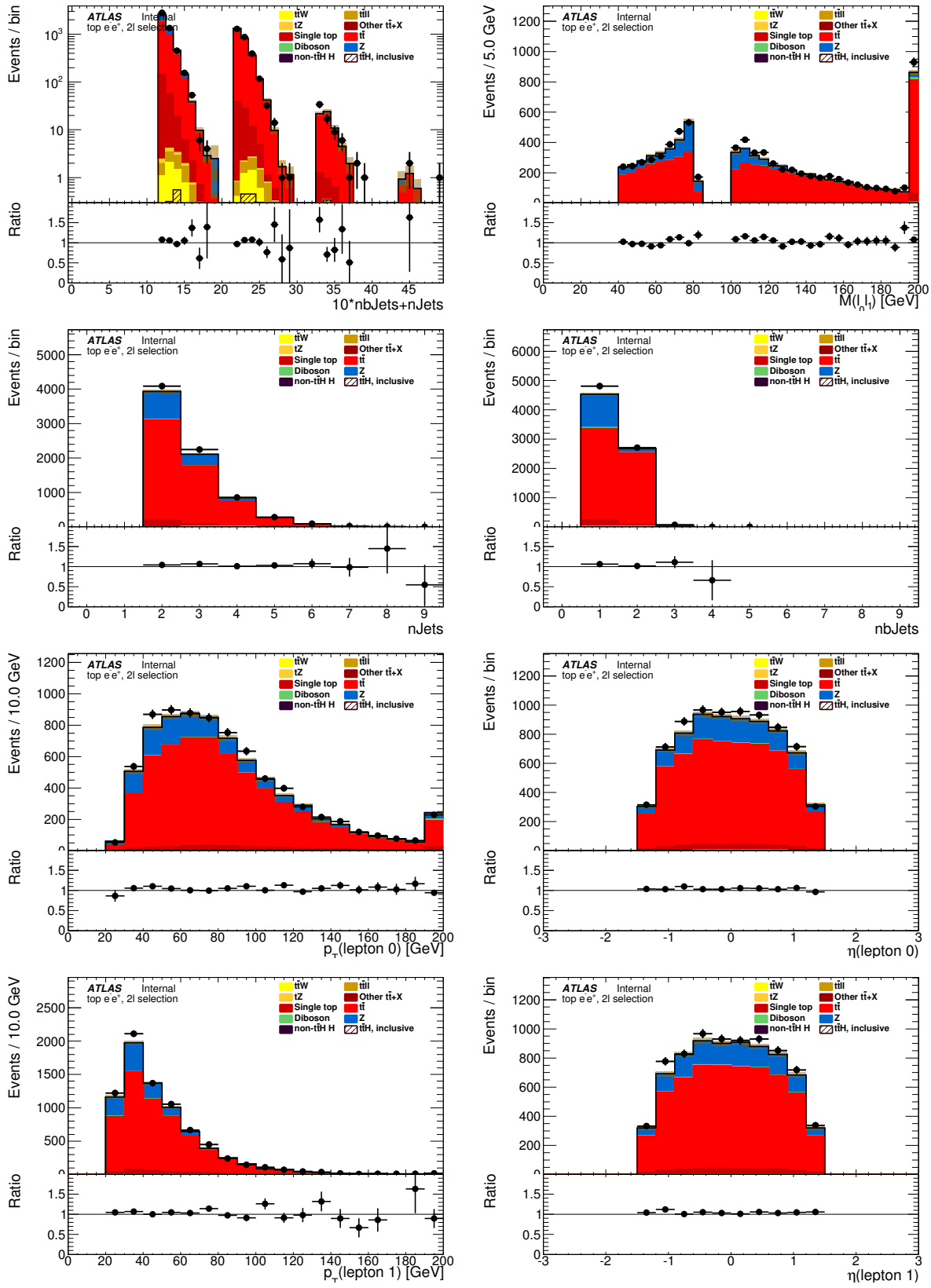

Figure 10: Distributions of (first row left) jet and b-jet multiplicity; (first row right) dilepton invariant mass; (second row) (left) jet and (right) b-jet multiplicity separately; (third row) (left) leading lepton p_{T} and (right) η; and (bottom row) (left) subleading lepton p_{T} and (right) η for the top $e^{+}e^{-}$ control region. Leptons are selected with the 2ℓ selection.

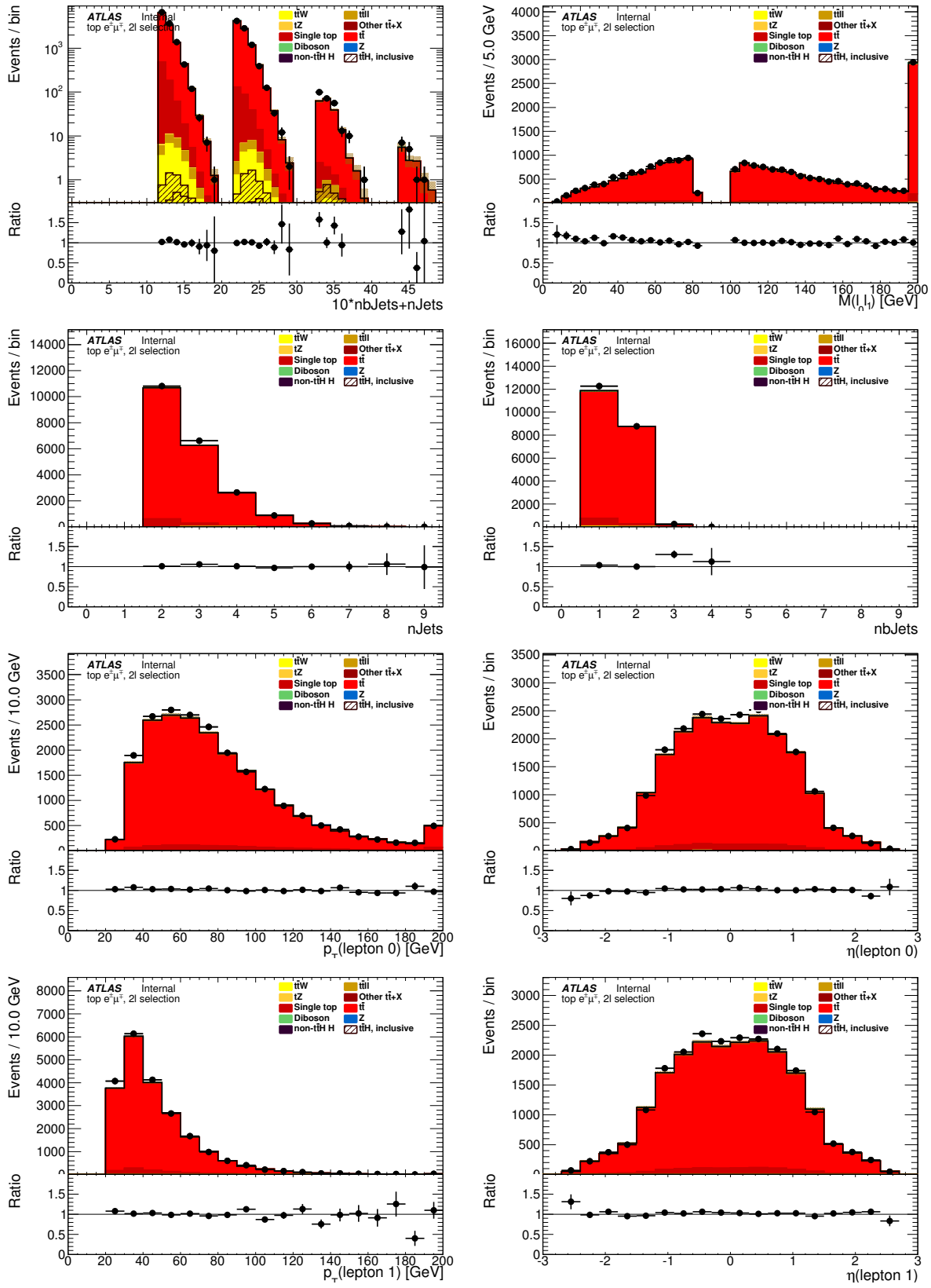

Figure 11: Distributions of (first row left) jet and b-jet multiplicity; (first row right) dilepton invariant mass; (second row) (left) jet and (right) b-jet multiplicity separately; (third row) (left) leading lepton p_{T} and (right) η; and (bottom row) (left) subleading lepton p_{T} and (right) η for the top $e^{\pm}\mu^{\mp}$ control region. Leptons are selected with the 2ℓ selection.

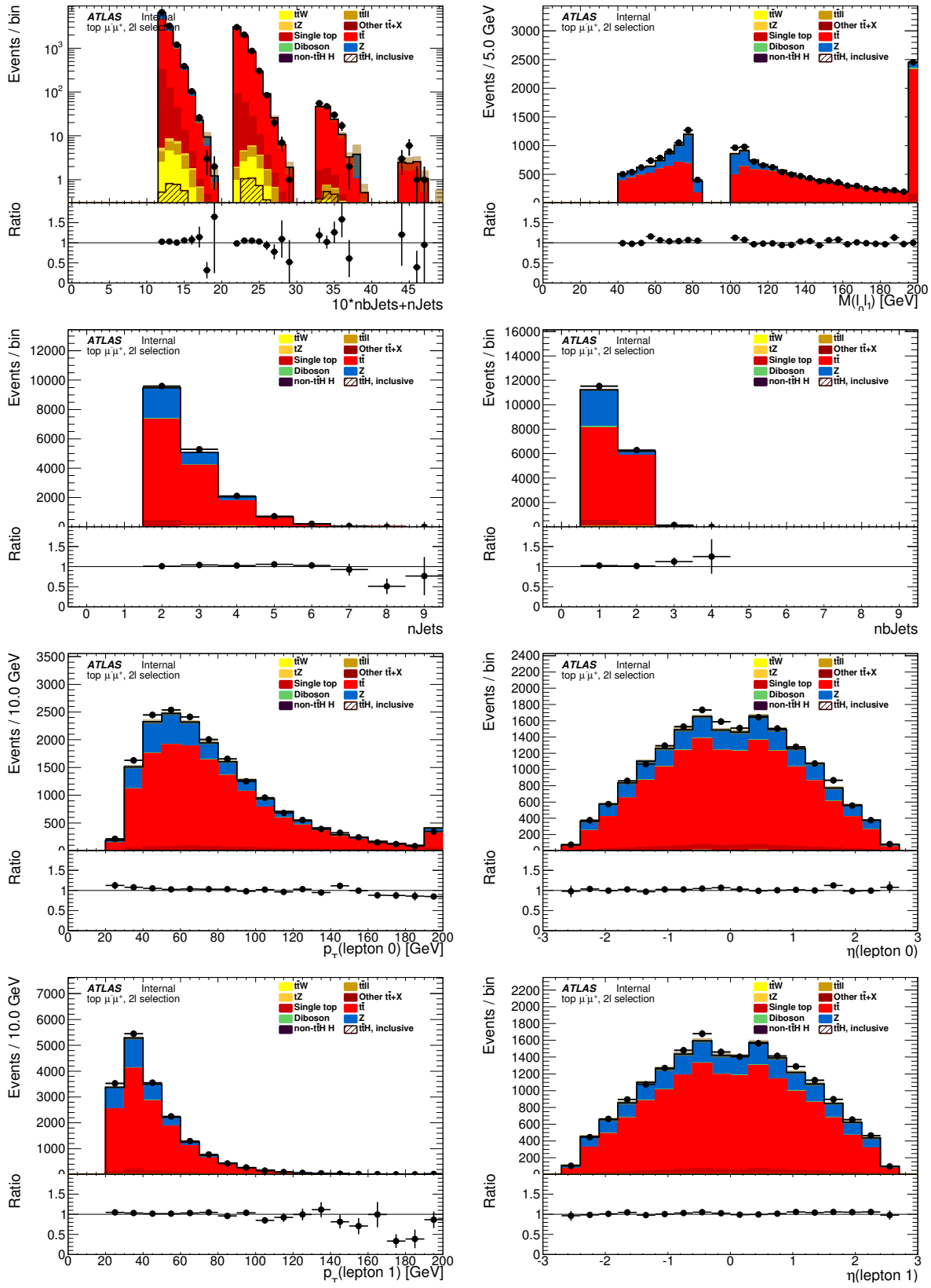

Figure 12: Distributions of (first row left) jet and b-jet multiplicity; (first row right) dilepton invariant mass; (second row) (left) jet and (right) b-jet multiplicity separately; (third row) (left) leading lepton p_{T} and (right) η; and (bottom row) (left) subleading lepton p_{T} and (right) η for the top $\mu^{+}\mu^{-}$ control region. Leptons are selected with the 2ℓ selection.

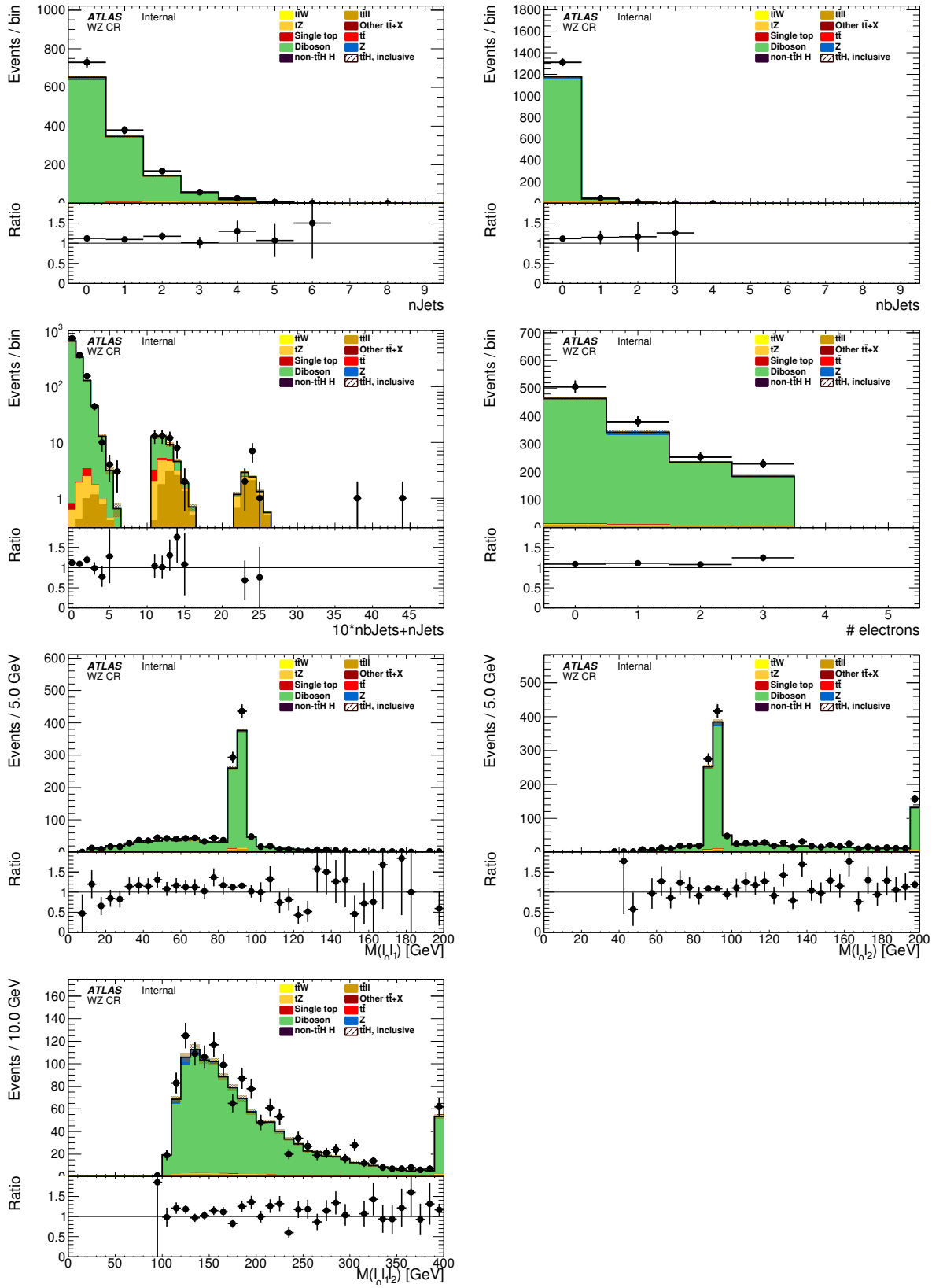

Figure 13: (Top row) jet and b-tag multiplicities; (second row) 10*n(b-tags)+n(jets) and electron multiplicity; (third row) invariant mass of opposite sign lepton pairs; (bottom row) invariant mass of the three lepton system in the inclusive *WZ* CR. Lepton 0 is the one with opposite charge with respect to lepton 1 and 2, where lepton 1 is closer in ΔR to lepton 0.

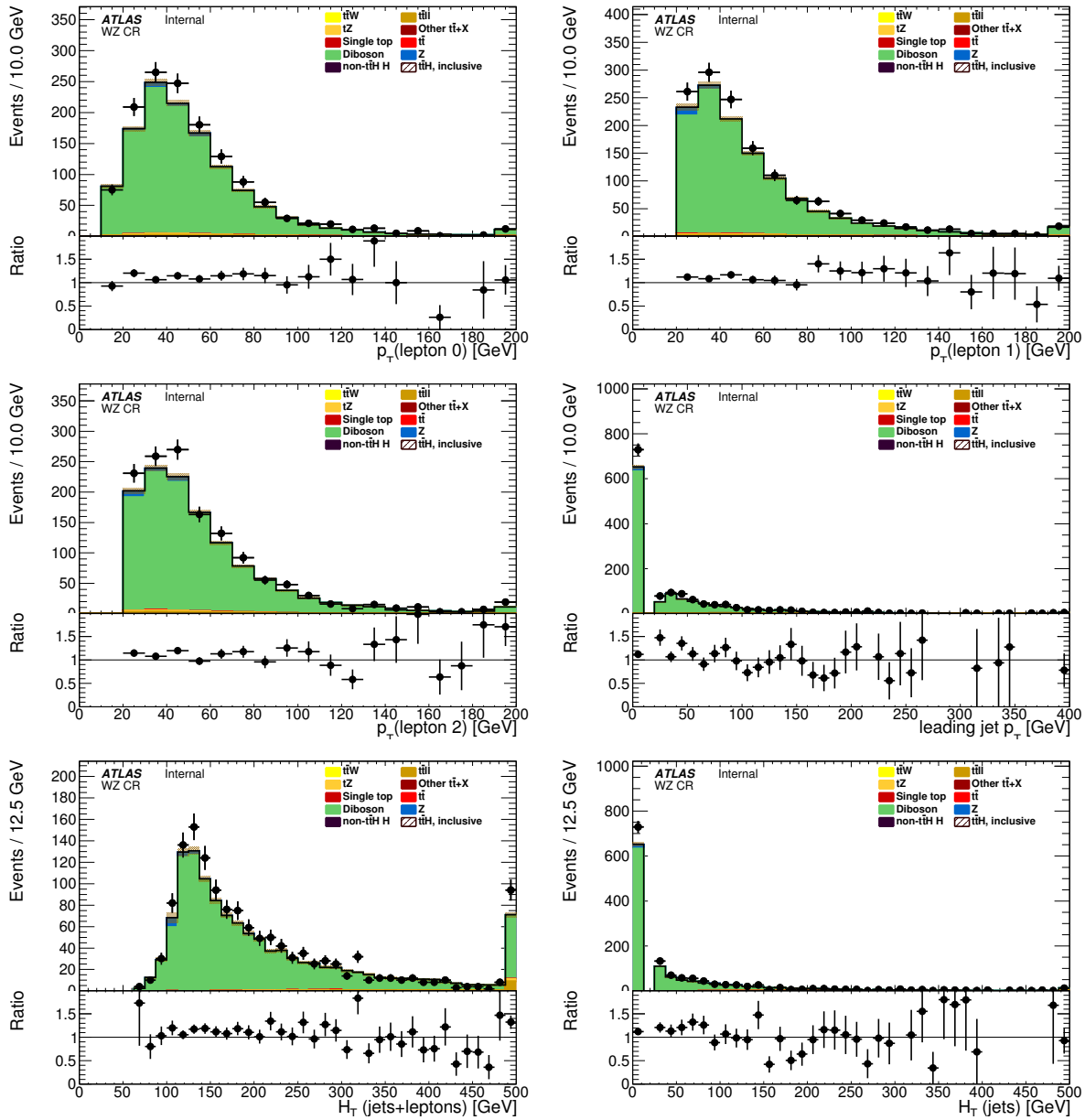

Figure 14: (Top row) Lepton 0 p_{T} (left) and lepton 1 p_{T} (right); (second row) lepton 2 p_{T} (left) and leading jet p_{T} (right); (third row) scalar sum of the p_{T} of selected leptons and jets in the event (left) and only of jets (right) for the inclusive WZ control region.

Process	$t\bar{t}H$	top	ttW	ttZ	4 tops
N(events)	0.68 ± 0.02	4.40 ± 0.24	1.30 ± 0.07	22.00 ± 0.25	-

ttWW	tZ	di-boson	Z+jets	Total MC	Data
0.02 ± 0.01	11.96 ± 0.18	37.18 ± 0.35	8.05 ± 1.11	86.32 ± 0.53	103.00 ± 10.15

Table 21: Yields in the WZ+heavy flavour control region after all cuts.

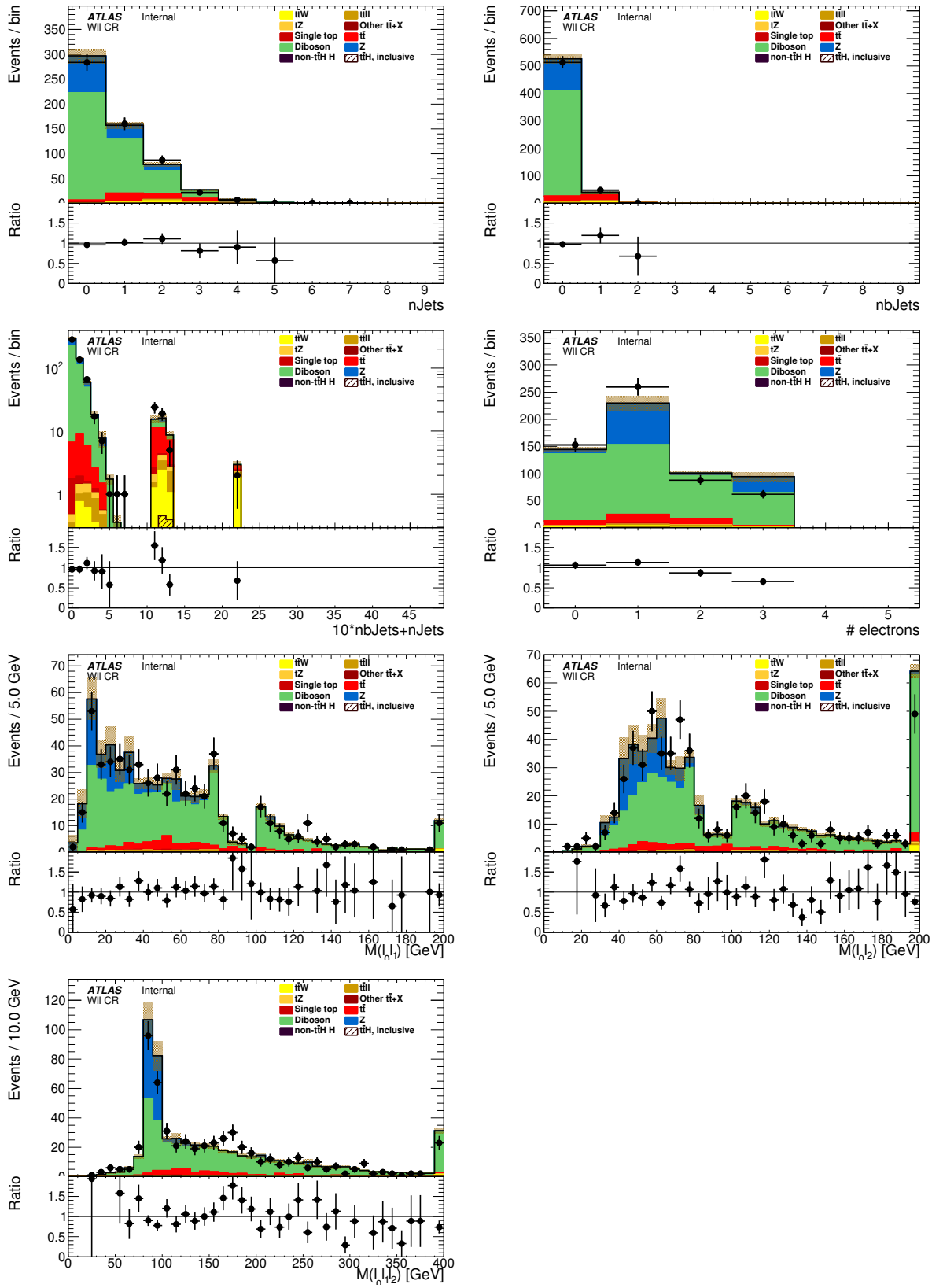

Figure 15: (Top row) jet and b-tag multiplicities; (second row) 10*n(b-tags)+n(jets) and electron multiplicity; (third row) invariant mass of opposite sign lepton pairs; (bottom row) invariant mass of the three lepton system in the inclusive $W\ell\ell$ CR. Lepton 0 is the one with opposite charge with respect to lepton 1 and 2, where lepton 1 is closer in ΔR to lepton 0.

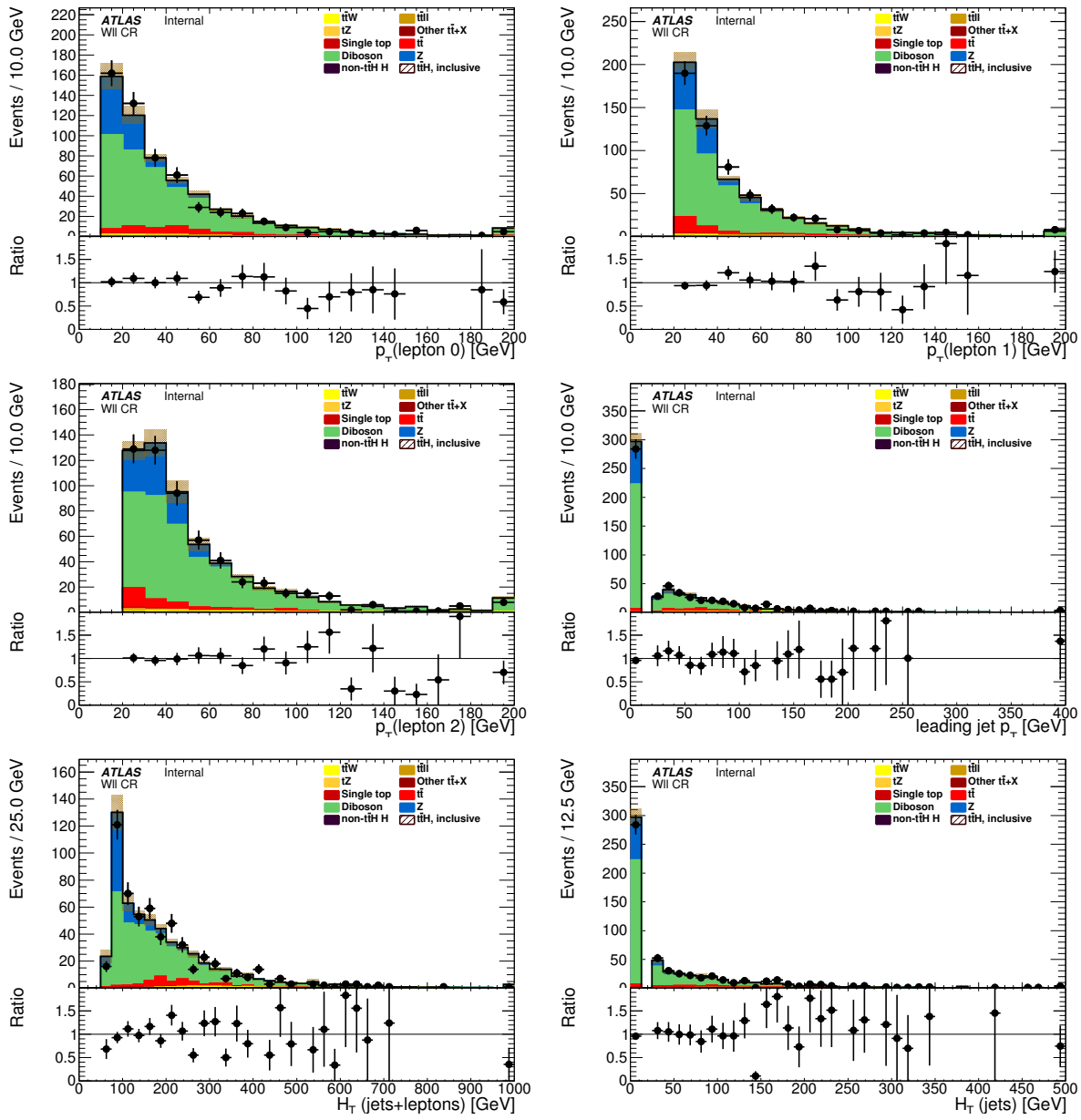

Figure 16: (Top row) Lepton 0 p_{T} (left) and lepton 1 p_{T} (right); (second row) lepton 2 p_{T} (left) and leading jet p_{T} (right); (third row) scalar sum of the p_{T} of selected leptons and jets in the event (left) and only of jets (right) for the inclusive $W\ell\ell$ control region.

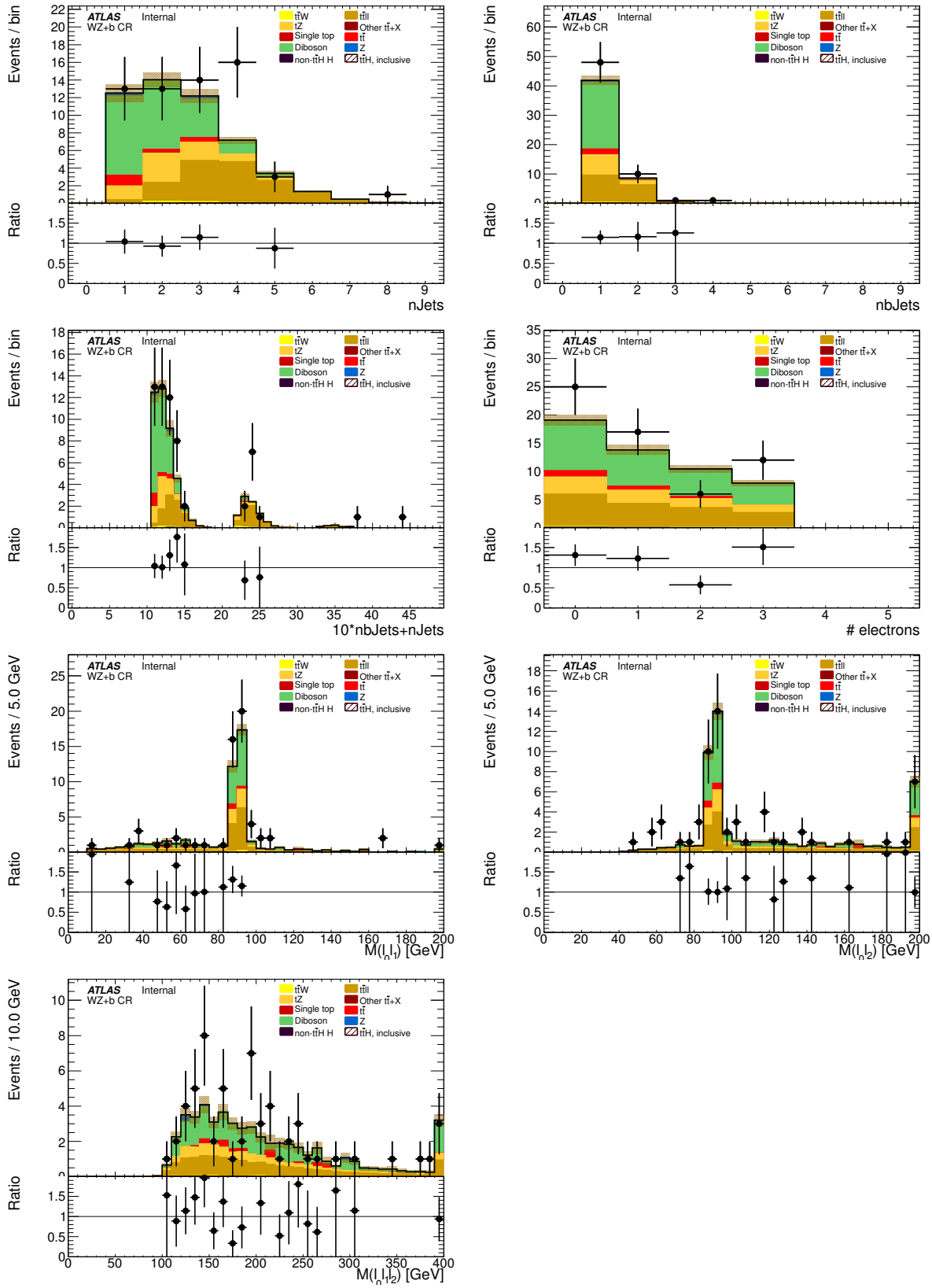

Figure 17: (Top row) jet and b-tag multiplicities; (second row) 10*n(b-tags)+n(jets) and electron multiplicity; (third row) invariant mass of opposite sign lepton pairs; (bottom row) invariant mass of the three lepton system in the WZ+1b CR. Lepton 0 is the one with opposite charge with respect to lepton 1 and 2, where lepton 1 is closer in ΔR to lepton 0.

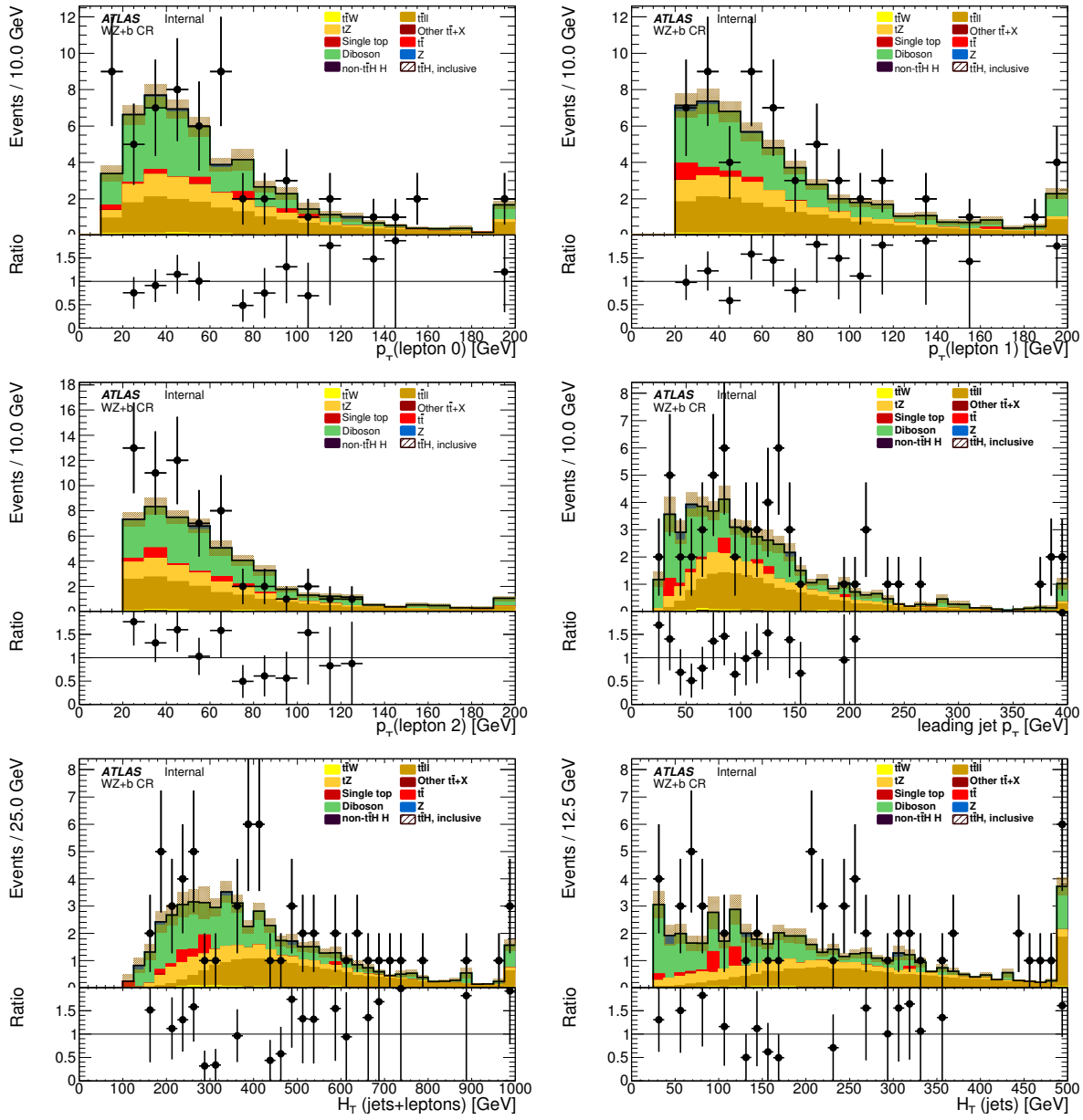

Figure 18: (Top row) Lepton 0 p_{T} (left) and lepton 1 p_{T} (right); (second row) lepton 2 p_{T} (left) and leading jet p_{T} (right); (third row) scalar sum of the p_{T} of selected leptons and jets in the event (left) and only of jets (right) for the WZ+1b control region.

not possible with the current data set. On the contrary, it is possible to use the Z boson candle to select a pure enough $t\bar{t}Z$ sample.

In the same manner as for WZ, also the selections to check the level of accuracy of the $t\bar{t}Z$ simulation, normalization and shape-wise, are as presented in Table 9. A region is defined which is very similar to the signal one, only with reverting the Z boson mass requirement to select events with at least one Z boson candidate.

The yields in the ttZ control region are provided in Table 22. The data-to-MC normalization factor in this sample is 1.26 ± 0.25, with a difference from unity of about 1σ. Most of this discrepancy comes from the 1 b-tag sample, which is the reason why a dedicated look is given to the 1 b-tag region.

Multiplicities of jets and b-tags, of electrons (the number of electrons+muons in the event is fixed to 3 by construction) are presented in Figure **??** along with a bin-by-bin Data/MC comparison. The kinematic features of the event are shown in Figures **??**-**??**.

Process	$t\bar{t}H$	top	ttW	ttZ	4 tops
N(events)	0.39 ± 0.01	0.22 ± 0.05	0.30 ± 0.03	13.58 ± 0.20	0.01 ± 0.01

ttWW	tZ	di-boson	Z+jets	Total MC	Data
0.01 ± 0.01	2.51 ± 0.06	4.05 ± 0.10	0.57 ± 0.28	22.15 ± 0.23	28.00 ± 5.00

Table 22: Yields in the ttZ control region after all cuts.

9.5 ZZ control region

A four lepton control region is used to invesigate the on-shell modeling and overall normalization of the ZZ MC simulation used for the estimate of this background. Preselection of events for this region is identical to the four lepton signal region definition. This includes selecting exactly 4 leptons with a total charge of zero, trigger matching and p_{T} requirements and a low-mass cut of $M_{\ell\ell}^{xy} > 10$GeV on OS-SF lepton pairs. Leptons are then organized into OS-SF lepton pairs with a dilepton invariant mass within 10 GeV of the Z boson mass. Events without two distinct pairs of leptons meeting this criterion are discarded. The best Z-candidate pair is required to have an invariant mass within 5 GeV of the Z boson mass. This selection yields a ZZ control region which is upwards of 99% pure.

The lepton kinematic distributions are shown in Figure 21 along with a bin-by-bin Data/MC comparison. Similarly, Figures 22 and 23 show the dilepton invariant mass distributions of each lepton pairing and kinematic distributions for the reconstructed Z-candidate lepton pairs respectively. Finally, Figure 24 shows event-level distributions including lepton and jet multiplicities.

9.6 Inclusive 4ℓ control region

Orthogonal to the ZZ control region, a separate four lepton region is used to verify the modeling of off-shell 4ℓ events. The standard four lepton event preselection described previously is used and leptons are organized into Z-candidate pairs as in the ZZ CR. Events with two distinct Z-candidate lepton pairs are discarded. This selection yields a region which is dominated by ZZ^* (where Z^* here refers to an off-shell Z boson or photon), and which also includes sizeable contributions from $t\bar{t}Z$ and $H \to ZZ^*$ An excess of data is noted when one lepton pair is reconstructed as a Z-candidate.

The lepton kinematic distributions are shown in Figure 25 along with a bin-by-bin Data/MC comparison. Figure 26 shows the dilepton invariant mass distributions for each lepton pairing, while Figure 27 includes kinematic distributions for a reconstructed Z-candidate lepton pair along with the remaining

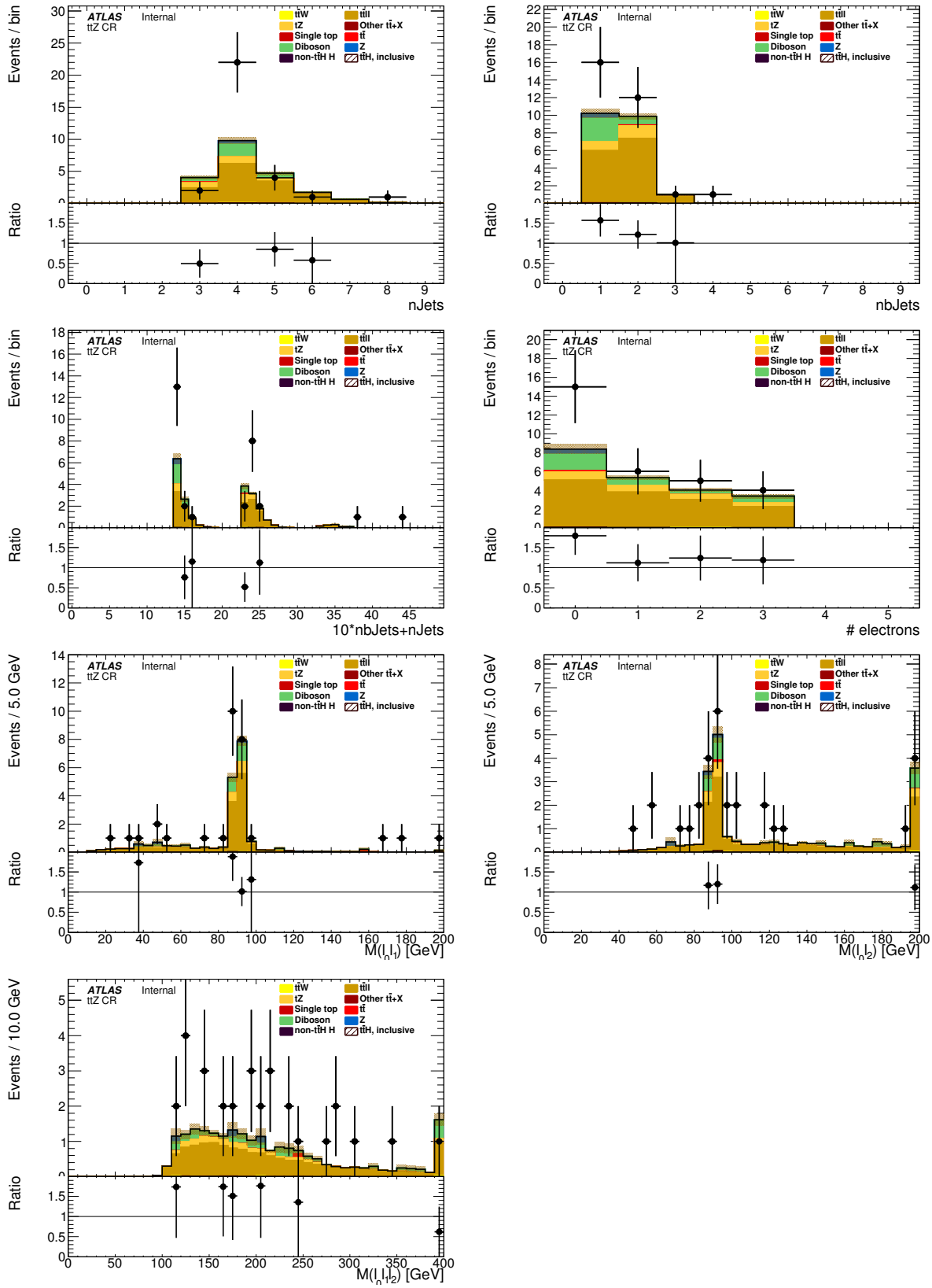

Figure 19: Top row) jet and b-tag multiplicities; (second row) 10*n(b-tags)+n(jets) and electron multiplicity; (third row) invariant mass of opposite sign lepton pairs; (bottom row) invariant mass of the three lepton system in the ttZ CR. Lepton 0 is the one with opposite charge with respect to lepton 1 and 2, where lepton 1 is closer in ΔR to lepton 0.

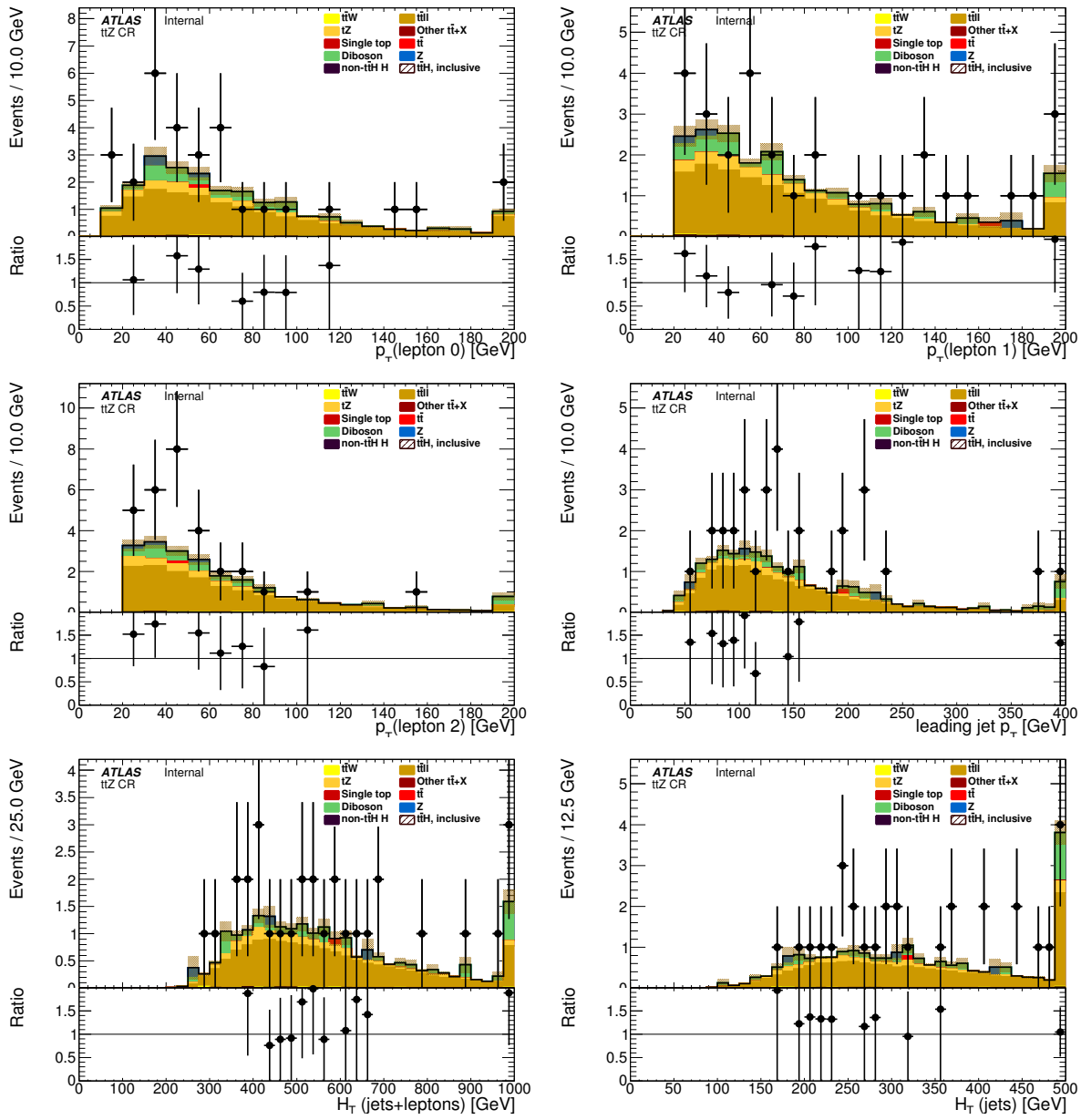

Figure 20: (Top row) Lepton 0 p_{T} (left) and lepton 1 p_{T} (right); (second row) lepton 2 p_{T} (left) and leading jet p_{T} (right); (third row) scalar sum of the p_{T} of selected leptons and jets in the event (left) and only of jets (right) for the ttZ control region.

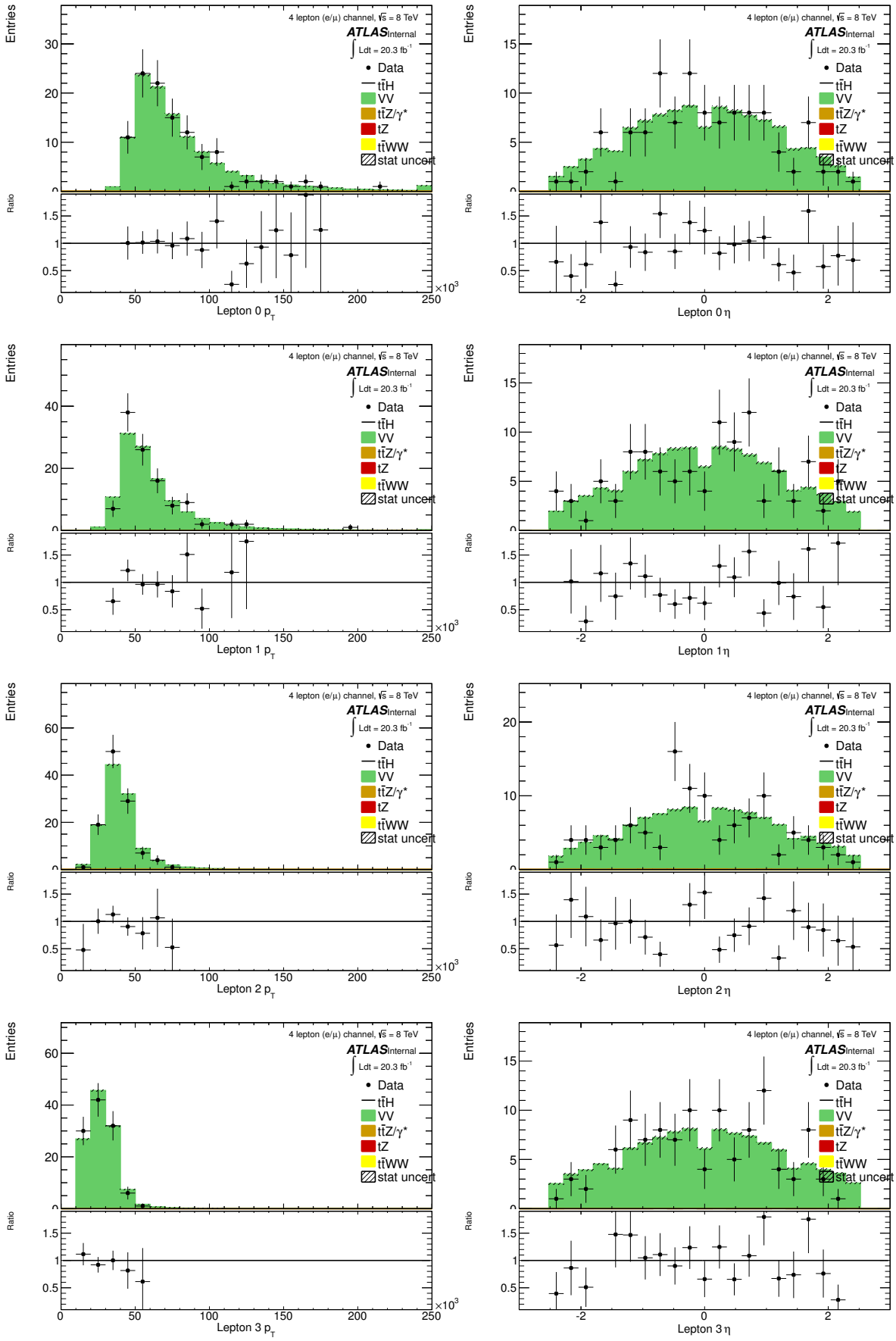

Figure 21: Lepton kinematic distributions for the ZZ control region. p_{T} and η distributions for each of the four leptons. Leptons are ordered in decreasing p_{T}, with lepton 0 having the highest p_{T}

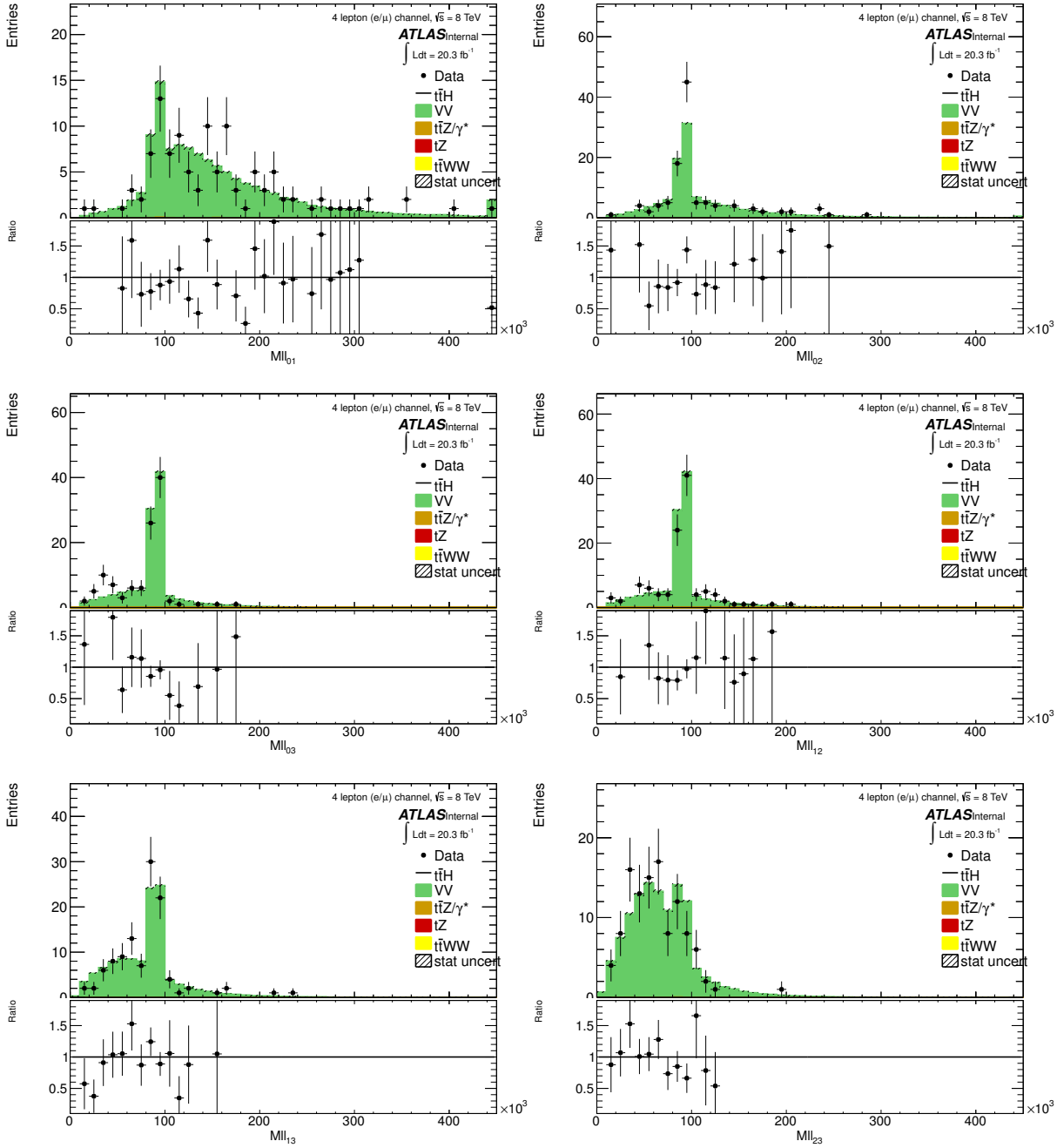

Figure 22: Invariant mass distributions for the *ZZ* control region. Dilepton invariant mass of each of the six possible pairs of leptons

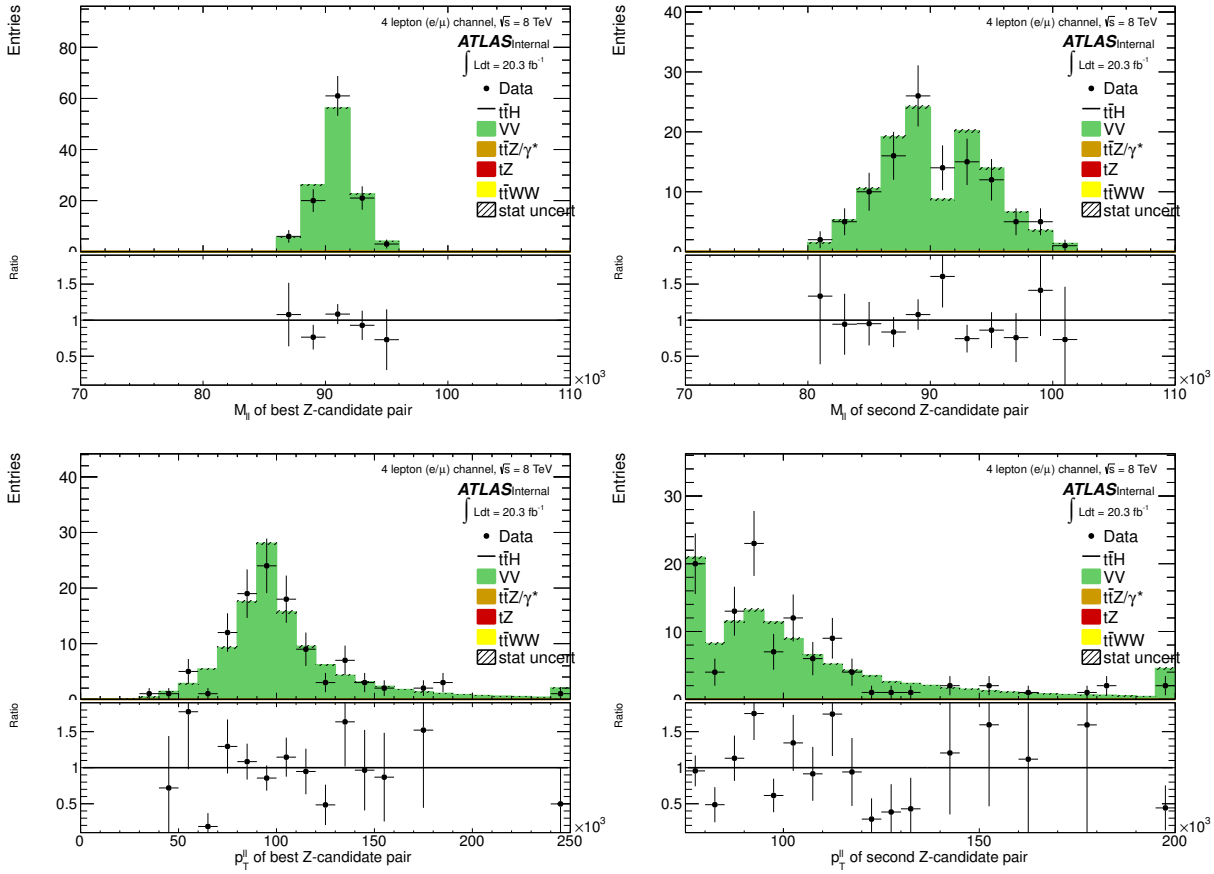

Figure 23: Z-candidate distributions for the *ZZ* control region. From top left to bottom right: dilepton invariant mass of the best Z-candidate lepton pair, dilepton invariant mass of the second Z-candidate lepton pair, dilepton p_{T} distributions for the best and second Z-candidate lepton pairs

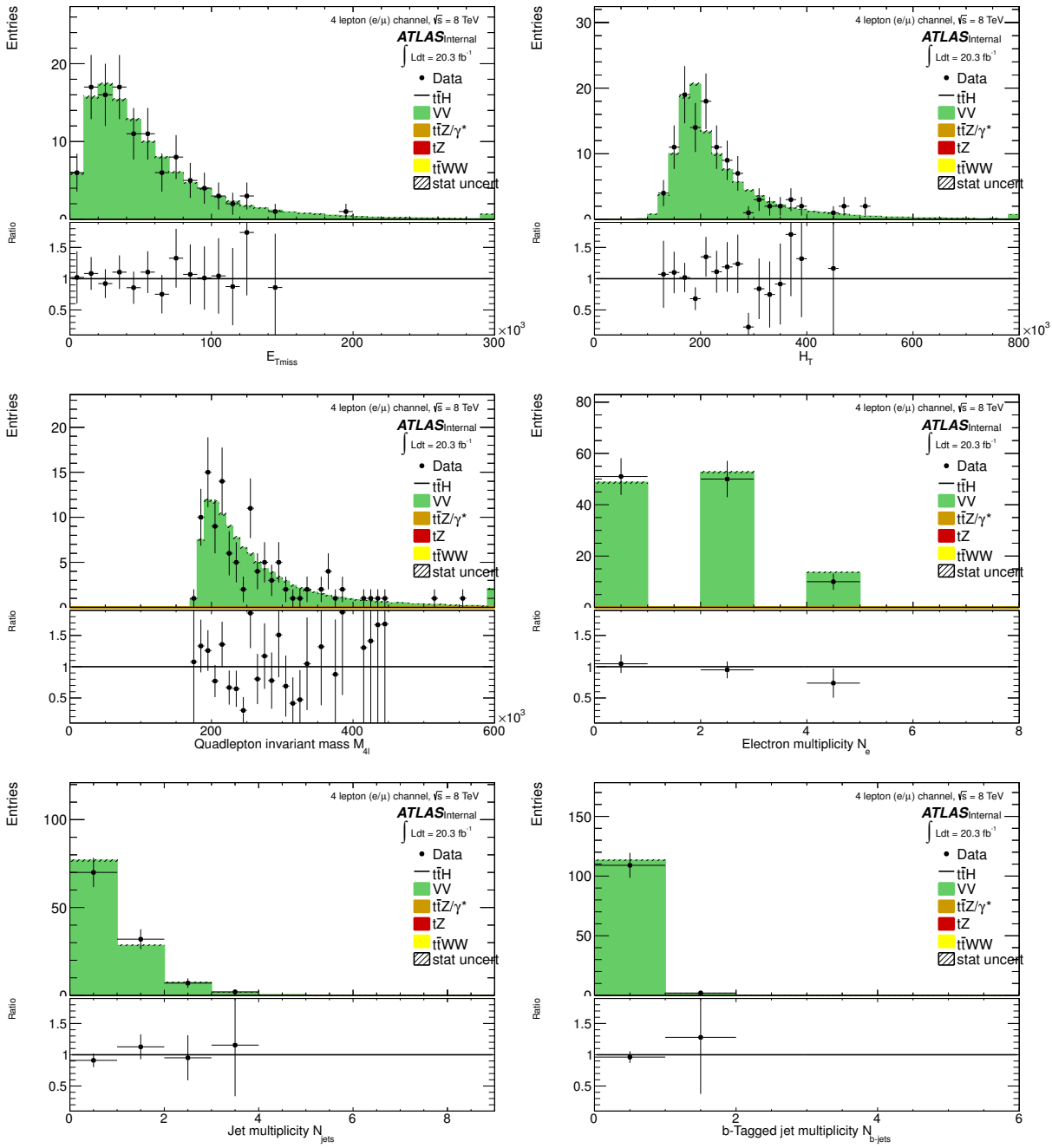

Figure 24: Event-level distributions for the ZZ control region. From top left to bottom right: the missing transverse energy and H_T distributions, quadlepton invariant mass distribution, electron multiplicity, total jet and b-tagged jet multiplicities

(non-Z-candidate) pair. Finally, event-level distributions including lepton and jet multiplicities are shown in Figure 28.

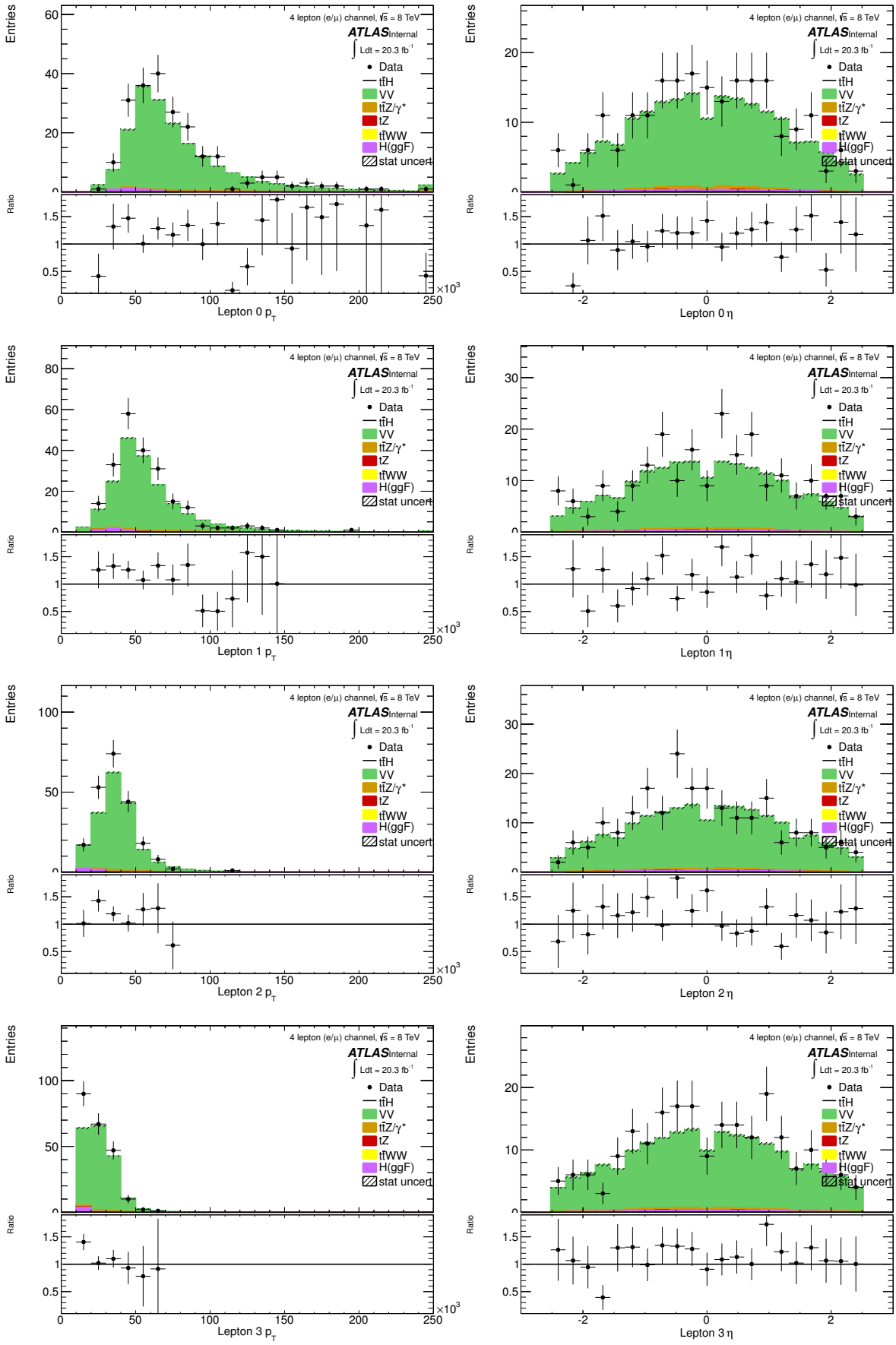

Figure 25: Lepton kinematic distributions for the 4ℓ control region. p_{T} and η distributions for each of the four leptons. Leptons are ordered in decreasing p_{T}, with lepton 0 having the highest p_{T}

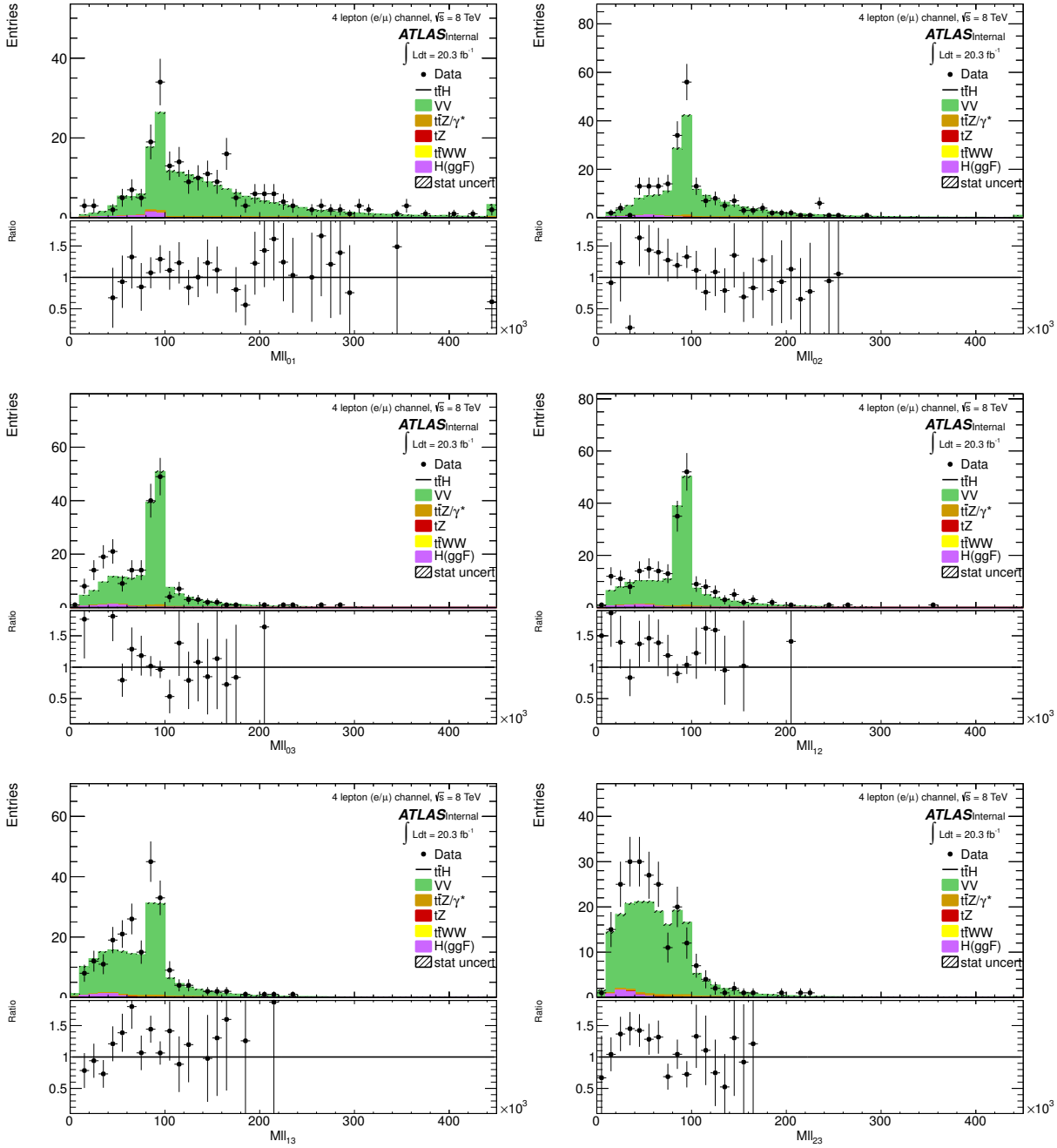

Figure 26: Invariant mass distributions for the 4ℓ control region. Dilepton invariant masses for each of the six possible pairs of leptons

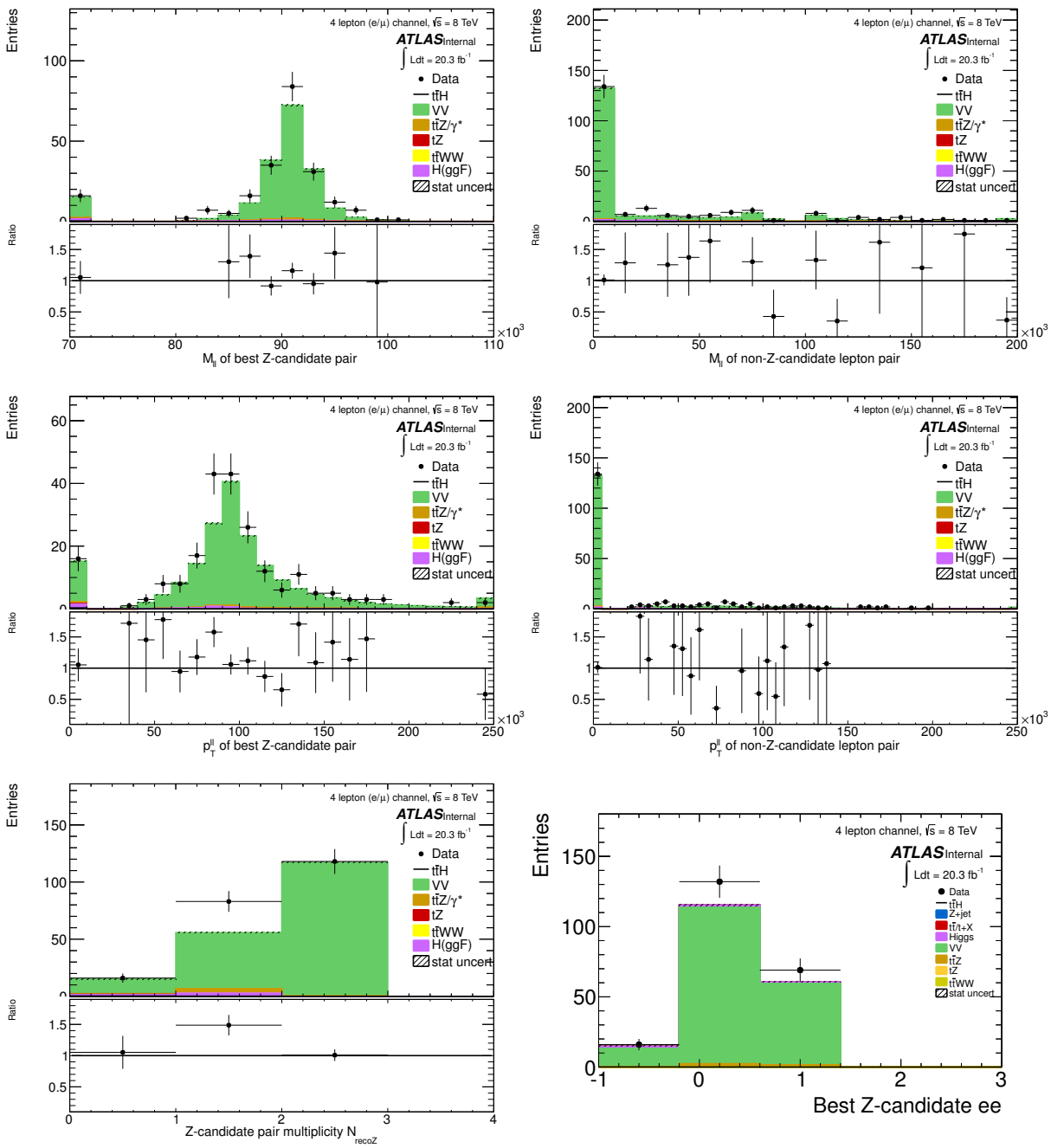

Figure 27: Z-candidate distributions for 4ℓ control region. From top left to bottom right: dilepton invariant mass of the Z-candidate lepton pair, dilepton invariant mass of the remaining (non-Z-candidate) lepton pair, dilepton p_{T} distributions for the Z-candidate and remaining lepton pairs, the multiplicity of Z-candidate lepton pairs and the electron flavour flag of the Z candidate. The electron flavour tag is -1 for events with no Z-candidate

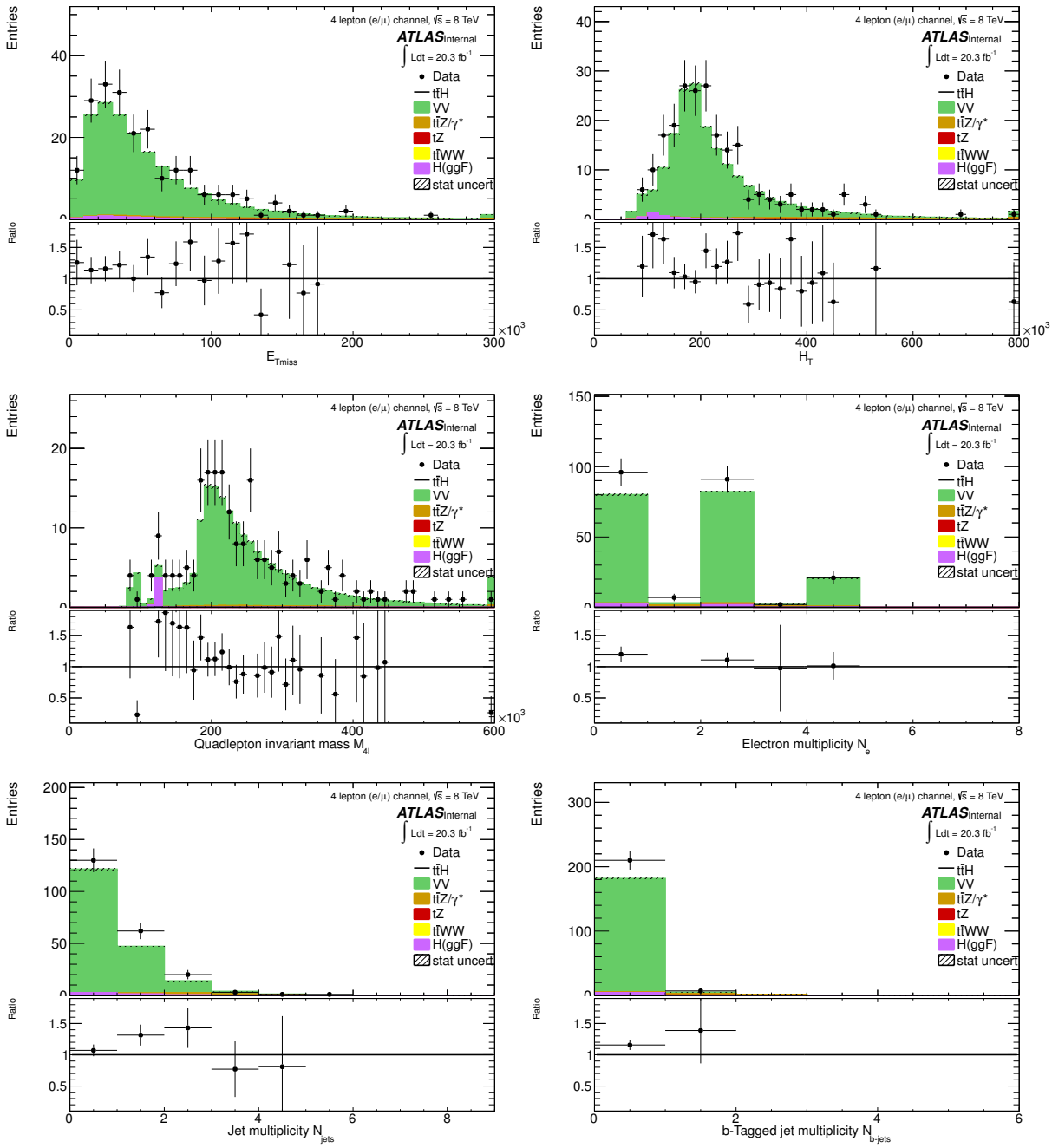

Figure 28: Event-level distributions for 4ℓ control region. From top left to bottom right: the missing transverse energy and H_T distributions, quadlepton invariant mass distribution, electron multiplicity, total jet and b-tagged jet multiplicities

10 Results

10.1 Statistical procedure

The results from this note follow the statistical procedure summarised in Ref. [20]. The Parameter Of Interest (POI) is the signal strength parameter μ, defined as the ratio between the observed number of events and the expected number of signal events from the Standard Model (SM) Higgs boson hypothesis. The Nuisance Parameters (NP) of the fit correspond to the theoretical and experimental systematics described in Sec. 2.6 and **??**, as well as the uncertainty linked to the data-driven fake estimates methods.

A profile likelihood ratio based test statistic $\lambda(\mu)$ is used to test different hypothesised values of μ. The background-only hypothesis is tested with $\lambda(0)$ and a signal plus background hypothesis is tested with $\lambda(\mu)$.

All channels are counting experiments, which means that instead of a distribution shape, it is only the signal and background yields that are fitted in the signal regions, and possibly in control regions.

The modified frequentist procedure, CL_s, is used to derive exclusion limits of μ. A hypothetical SM Higgs boson with a mass M_{H} is claimed to be excluded at 95% CL when CL_s is less than 0.05 for $\mu = 1$.

For the moment, in this note, only Asimov datasets are fitted since data in the Signal Region (SR) are blinded.

10.2 Inputs checks

Tables 23 to 26 show a summary of inputs, yields and fake estimates to the statistical study for each channel.

Channel	ttH	top	ttW	ttZ	VV	Z+jets	Tot B
2lee5j	0.73 ± 0.03	1.31 ± 0.57	1.49 ± 0.11	1.11 ± 0.07	0.48 ± 0.25	0.16 ± 0.16	4.56 ± 1.17
2lem5j	2.13 ± 0.05	2.55 ± 0.84	5.02 ± 0.15	2.40 ± 0.11	0.37 ± 0.23	0.28 ± 0.20	10.62 ± 1.54
2lmm5j	1.41 ± 0.04	1.76 ± 0.67	3.92 ± 0.14	1.09 ± 0.08	0.68 ± 0.30	0.12 ± 0.12	7.57 ± 1.31
2lee4j	0.44 ± 0.02	4.99 ± 1.19	2.07 ± 0.12	0.96 ± 0.08	0.77 ± 0.27	1.37 ± 0.78	10.16 ± 2.43
2lem4j	1.16 ± 0.03	8.19 ± 1.41	6.27 ± 0.20	2.12 ± 0.12	1.93 ± 0.80	0.00 ± 0.00	18.51 ± 2.54
2lmm4j	0.74 ± 0.03	3.70 ± 1.03	4.76 ± 0.18	1.03 ± 0.08	0.54 ± 0.30	0.23 ± 0.23	10.26 ± 1.82
3l	2.34 ± 0.04	1.21 ± 0.51	2.72 ± 0.19	4.49 ± 0.15	0.89 ± 0.25	0.32 ± 0.23	9.63 ± 1.33
2ltau	0.47 ± 0.02	0.70 ± 0.38	0.41 ± 0.04	0.44 ± 0.05	0.11 ± 0.10	0.00 ± 0.00	1.66 ± 0.57
4lZenr.	0.19 ± 0.01	0.00 ± 0.00	0.01 ± 0.00	0.73 ± 0.05	0.08 ± 0.01	0.00 ± 0.00	0.83 ± 0.07
4lZdep.	0.03 ± 0.00	0.00 ± 0.00	0.00 ± 0.00	0.00 ± 0.00	0.00 ± 0.00	0.00 ± 0.00	0.01 ± 0.00
1l2tau	0.88 ± 0.03	29.33 ± 2.90	0.66 ± 0.18	0.91 ± 0.08	0.62 ± 0.28	0.38 ± 0.31	31.90 ± 3.74

Table 23: All channels MC yields with their statistical errors. top includes ttbar, single top and four top processes. ttV processes includes also ttVV and tV processes. Remark: there is no events selected from gluon fusion Higgs or W+jets processes so it was removed from the table.

Channel	ttH	Fakes	Q Mis-ID	MC (non top)	Tot B
2lee5j	0.73 ± 0.03	2.33 ± 0.92	1.11 ± 0.09	3.08 ± 0.44	6.52 ± 1.45
2lem5j	2.13 ± 0.05	3.87 ± 0.88	0.85 ± 0.08	7.79 ± 0.50	12.51 ± 1.45
2lmm5j	1.41 ± 0.04	1.24 ± 0.31	-	5.69 ± 0.52	6.93 ± 0.82
2lee4j	0.44 ± 0.02	3.45 ± 1.36	1.82 ± 0.11	3.80 ± 0.46	9.07 ± 1.93
2lem4j	1.16 ± 0.03	6.83 ± 1.46	1.39 ± 0.08	10.26 ± 1.06	18.47 ± 2.60
2lmm4j	0.74 ± 0.03	2.39 ± 0.59	-	6.33 ± 0.57	8.72 ± 1.16
3l	2.34 ± 0.04	2.62 ± 0.00	-	8.42 ± 0.83	11.04 ± 0.83
2ltau	0.47 ± 0.02	0.47 ± 0.49	-	0.96 ± 0.19	1.43 ± 0.68
4lZenr.	0.19 ± 0.01	-	-	0.83 ± 0.07	0.83 ± 0.07
4lZdep.	0.03 ± 0.00	-	-	0.00 ± 0.00	0.00 ± 0.00
1l2tau	0.88 ± 0.03	16.98 ± 0.05	-	2.57 ± 0.84	19.55 ± 0.89

Table 24: Summary of final input yields with their statistical errors as used in the statistical framework. For all channels, data-driven fake estimates include ttbar, four tops and single tops MC estimates. For 2 leptons and 2 leptons + tau channels, W+jets, Z+jets components are also included.For the 2 leptons channels which have charge mis-identification estimates, the WW MC background is also included in the data-driven estimates. Because of its determination method, the statistical component on the 3 leptons fake estimates is considered as 0 here and further included in the systematic error given in a following table.

Contribution	Value	$\theta\mu\mu$ (stat)	$\theta\mu\mu$ (syst)	θee (stat)	θee (syst)	syst mis-ID
Fakes $\mu\mu$ 5j	1.24	±0.38	±0.45	±0.00	±0.00	±0.00
Fakes $\mu\mu$ 4j	2.39	±0.53	±0.69	±0.00	±0.00	±0.00
Fakes eμ 5j	3.87	±0.49	±0.74	±0.16	±0.49	∓0.42
Fakes eμ 4j	6.83	±0.72	±1.15	±0.19	±0.54	∓0.57
Fakes ee 5j	2.33	±0.00	±0.00	±0.19	±0.63	∓0.54
Fakes ee 4j	3.45	±0.00	±0.00	±0.24	±0.75	∓0.79
Q mis-ID eμ 5j	0.85	-	-	-	-	±0.34
Q mis-ID eμ 4j	1.39	-	-	-	-	±0.56
Q mis-ID ee 5j	1.11	-	-	-	-	±0.44
Q mis-ID ee 4j	1.82	-	-	-	-	±0.73

Table 25: Fakes and charge mis-Identification estimates and uncertainties for 2 leptons channel

Contribution	Value	stat error	syst error
Fakes 3 leptons	2.62	±0.00	±0.50
Fakes 2 leptons + τ	0.47	±0.49	±0.30
Fakes 4 leptons	-	± -	± -
Fakes 1 lepton + 2τ	16.98	±0.92	±3.40

Table 26: Fakes estimates and uncertainties for 3leptons, 2leptons+tau, 4leptons and 1lepton+2taus channel. No fake estimates for 4 leptons. For 3 leptons channel, both systematics and statistical components are included in the systematics error.

10.3 Exclusion limits

Channels		Stat	+Fakes Unc.	+Theory	+ Experimental
2l	2lee	8.13	8.43	8.74	8.86
	2lem	3.58	3.80	4.08	4.18
	2lmm	4.07	4.15	4.49	4.59
	2ltau	9.33	9.47	9.67	9.70
	All	2.22	2.39	2.72	2.80
3l		3.40	3.43	3.61	3.67
4l		15.16	15.16	15.44	15.55
1l2tau		11.40	13.57	13.91	13.93
All		1.72	1.82	2.09	2.17

Table 27: 95%CL limits on μ for all channels and combination with cumulative uncertainties.

Channels		Observed	Median Signal Injected	Median	68% CL Range	95% CL Range
2l	2lee	-	9.85	8.86	[5.94;12.31]	[4.24;15.88]
	2lem	-	5.10	4.18	[2.86;6.26]	[2.06;7.89]
	2lmm	-	5.54	4.59	[3.11;6.74]	[2.23;8.47]
	2ltau	-	11.03	9.70	[5.91;13.80]	[3.95;19.10]
	All	-	3.49	2.80	[1.93;3.73]	[1.40;4.79]
3l		-	4.65	3.67	[2.48;5.63]	[1.79;7.47]
4l		-	17.03	15.55	[9.48;24.39]	[6.22;32.26]
1l2tau		-	14.72	13.93	[9.72;20.42]	[7.12;25.54]
All		-	3.09	2.17	[1.50;3.19]	[1.09;3.97]

Table 28: Expected limits with their 68% and 95% CL errors, expected limits with signal injected, and observed limits (to be put once data unblinded).

10.4 Signal strength and profile likelihood scan

This section provides measurement of the signal strength and distributions of the profile likelihood scan of μ values, or Negative Log Likelihood (nll) for each sub-channel and their combination.

The signal strength measurement which results are given in Table 29 is for the moment performed on an asimov with μ=1 in order to track potential inconsistencies, as a sanity check. When replaced by data, this will give the measured mu value.

Figure **??** provides the profile likelihood as a function of the μ value : $2(nll(\mu, \hat{\hat{\theta}}_\mu) - nll^{min})$ where nll^{min} is the minimum of $\mathcal{L}(\hat{\mu}, \hat{\theta}_\mu)$ The distributions are smooth as expected, and naturally stop at the lowest μ value for which the pdf becomes negative. In particular, the pdf for the 4l Zdepleted region which has 0.03 signal events and 0.01 background events becomes negative below $\mu = -B/S = -0.3$. The plateau in the distributions after $\mu = 40$ is due to the parameter μ being limited between [-10.,40] in the workspace. Figures on the right show a scan of all μ values between those limits by steps of 0.1, while the Figures on the left show a zoom on the minimum which is 1.0 since a SM asimov is fitted. The intersection of the line at $nll = 1$ provides asymmetric errors around that minimum nll fitted value.

Channels		μ value
2l	2lee	$1.0^{+4.2}_{-3.4}$
	2lem	$1.0^{+2.1}_{-1.8}$
	2lmm	$1.0^{+2.3}_{-1.9}$
	2ltau	$1.0^{+4.3}_{-2.5}$
	All	$1.0^{+1.4}_{-1.3}$
3l		$1.0^{+1.8}_{-1.5}$
4l		$1.0^{+6.5}_{0.0}$
1l2tau		$1.0^{+6.8}_{-6.1}$
All		$1.000^{+1.138}_{-0.997}$

Table 29: μ measurement on a μ=1 asimov with all channels and combination with asymmetric minos errors after all sources of uncertainties have been taken into account.

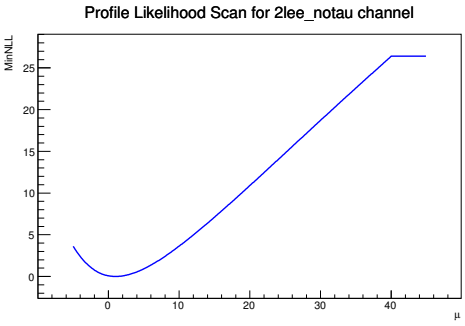

(a) 2lee

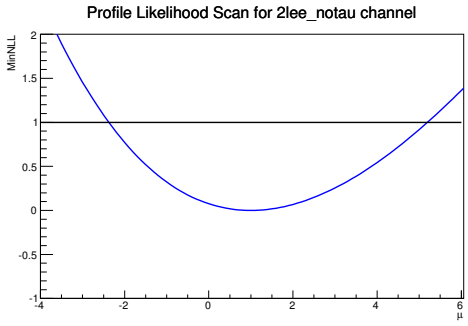

(b) 2lee, zoom

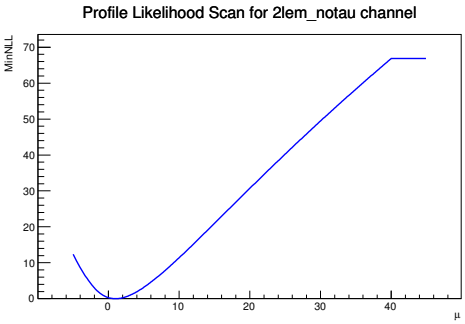

(c) 2lem

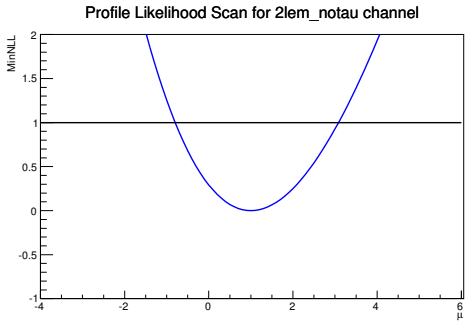

(d) 2lem, zoom

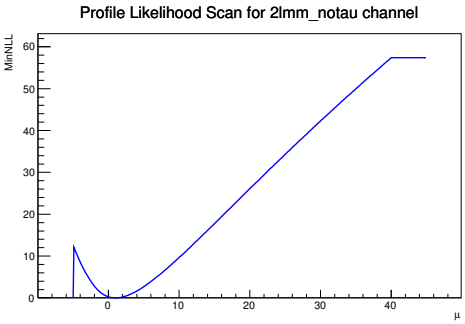

(e) 2lmm

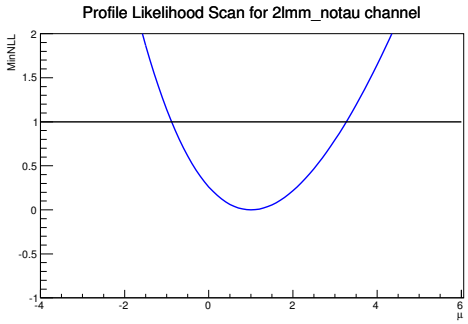

(f) 2lmm, zoom

Figure 29: Profile likelihood scan of μ values for 2lee, 2lem and 2lmm channels.

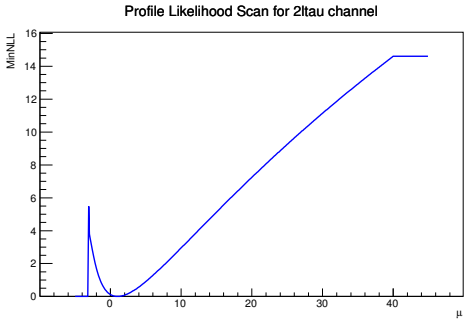

(a) 2ltau

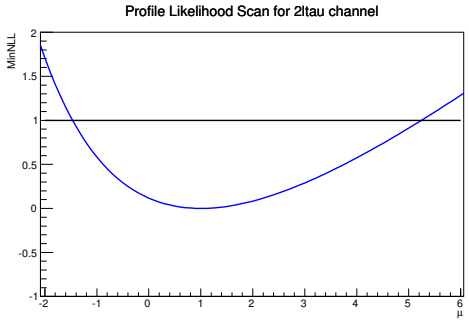

(b) 2ltau, zoom

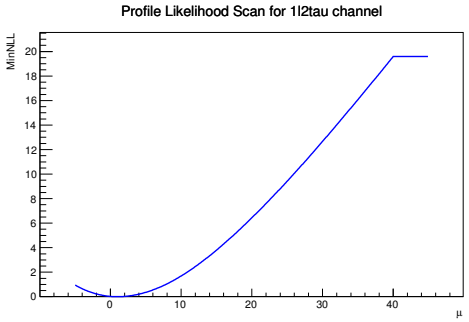

(c) 1l2tau

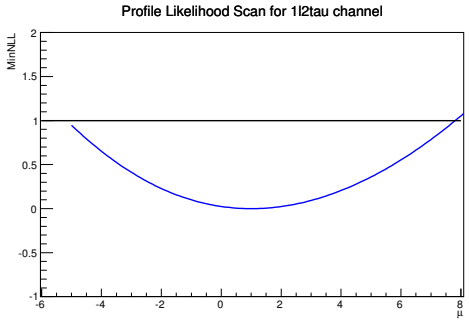

(d) 1l2tau, zoom

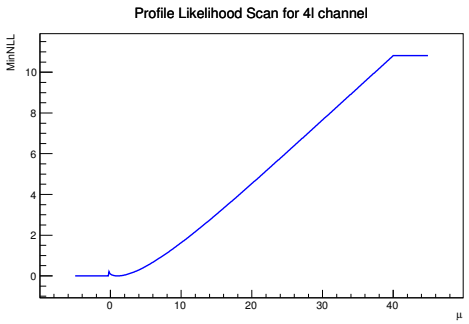

(e) 4l

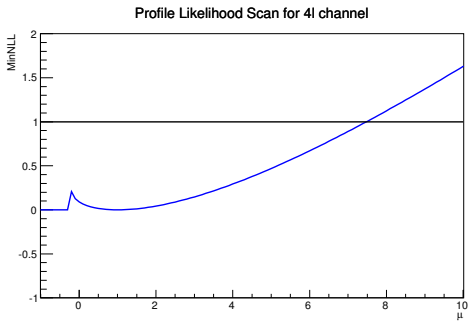

(f) 4l, zoom

Figure 30: Profile likelihood scan of μ values for 2ltau, 1l2tau combined and 4l channels.

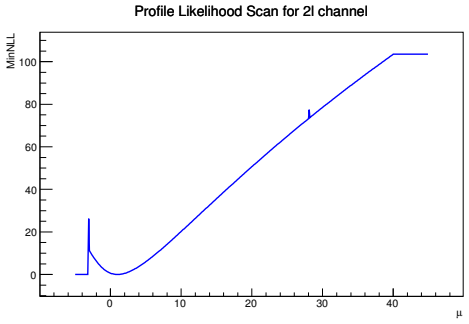

(a) 2l

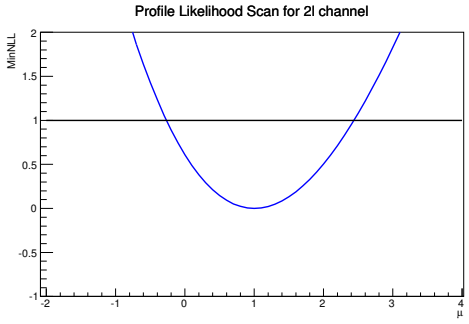

(b) 2l, zoom

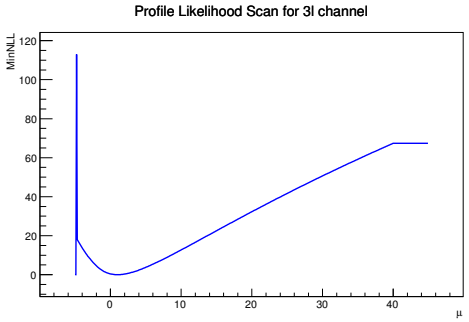

(c) 3l

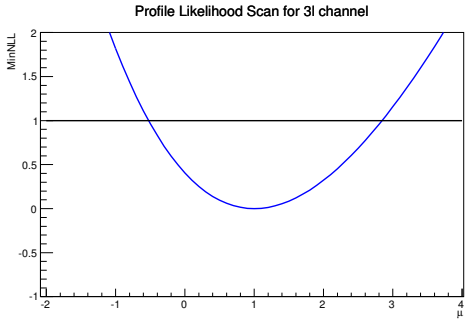

(d) 3l, zoom

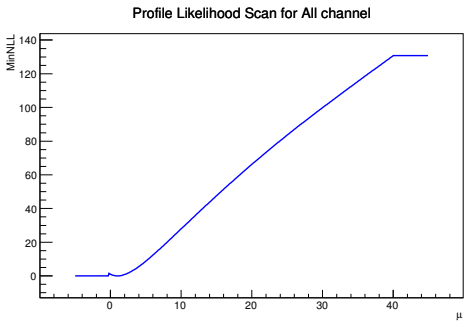

(e) All

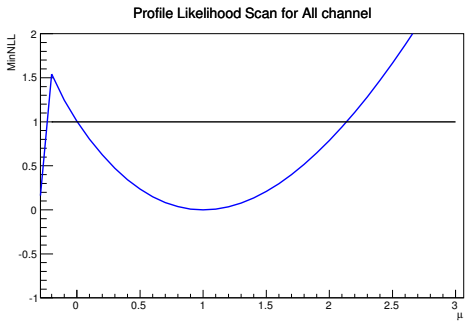

(f) All, zoom

Figure 31: Profile likelihood scan of μ values for all 2l combined, 3l and all channels combination.

10.5 Check of nuisance parameters impact and correlations

The ranking of all nuisance parameters considered for this analysis is give on Figure 32.

However, for more clarity, this ranking is also provided with significant parameters according to the pruning algorithm (see Section 10.6) and for sub-channels in Figures 33 to 37.

The correlation matrices for the most significant nuisance parameters (surviving pruning) are given for 2leptons, 3 leptons channels and all channels combined in Figures 38 and 39.

As expected and as presented on Figure 39 the leading parameters are most prone to show absolute correlations to the POI: between 11% and 26% for the QCD scale and pdf of the irreducible ttW and ttZ backgrounds and WZ cross section, 8% to 16% for the fake estimates uncertainties : θ_{ee}, $\theta_{\mu\mu}$ for 2l and the 2l, 2ltau and 1l2taus fake estimates uncertainties, and finally the relevant experimental systematics show up to 8% correlations.

The parameters ranking as a function of their impact on the POI do follow the expected order of importance for parameters, both in individual channels and for combined channels. When all channels are combined, the fake estimate uncertainty for the 2 leptons + tau channel shows a little constraint.

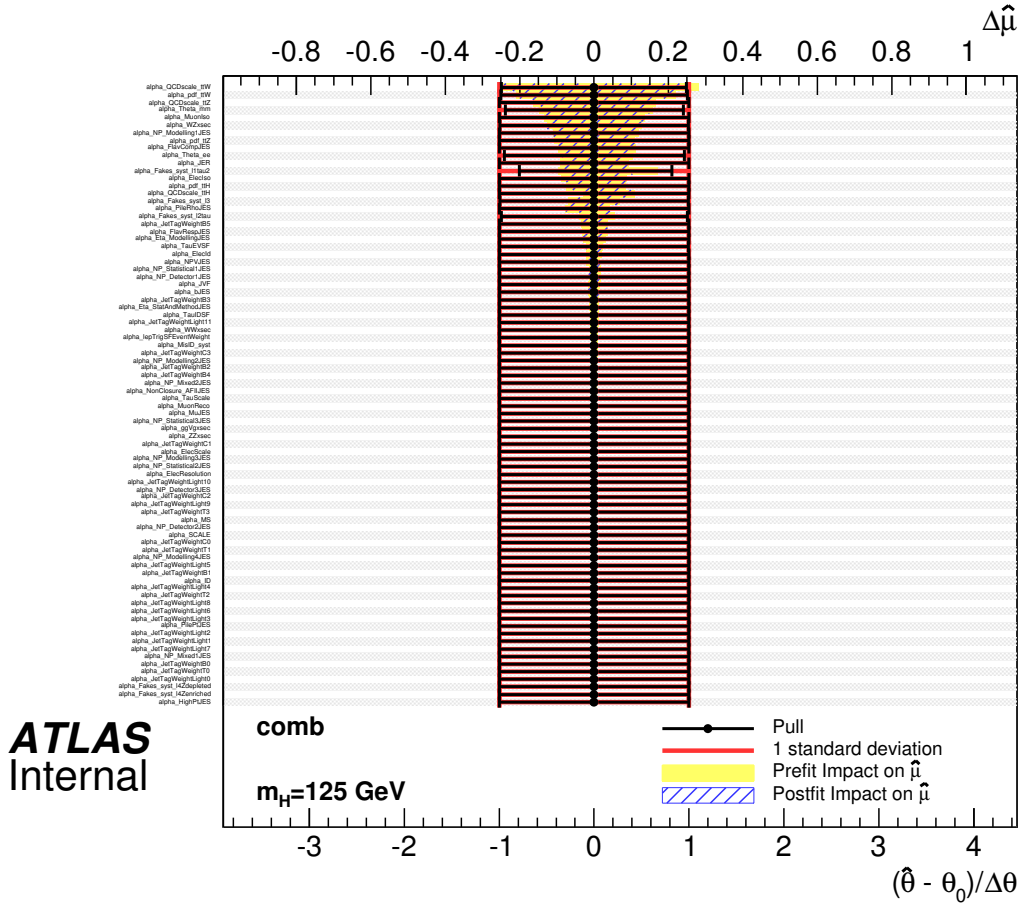

Figure 32: Ranking of all considered Nuisance Parameters (NP) for the all channels combined after fit to an Asimov data set with μ=1, before pruning

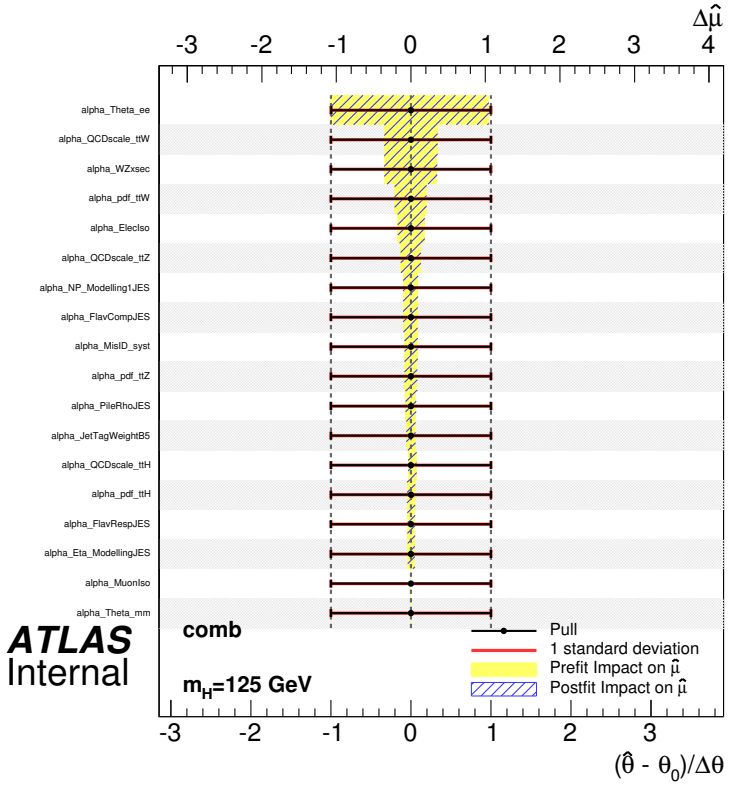

(a) 2lee channel

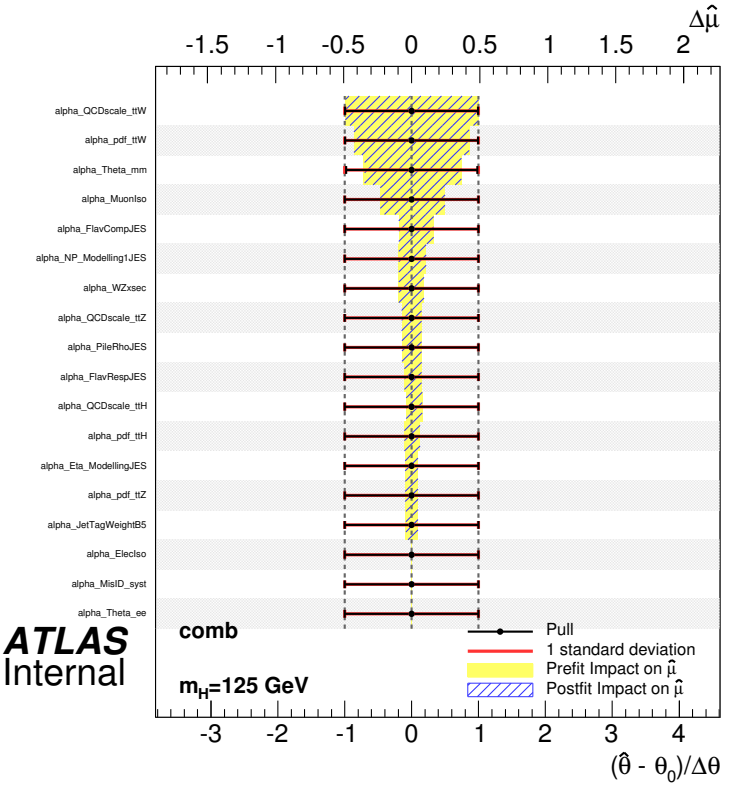

(b) 2lmm channel

Figure 33: Nuisance parameters ranking for 2lee and 2lmm (4 and 5 jets). Only non-prunable parameters were considered.

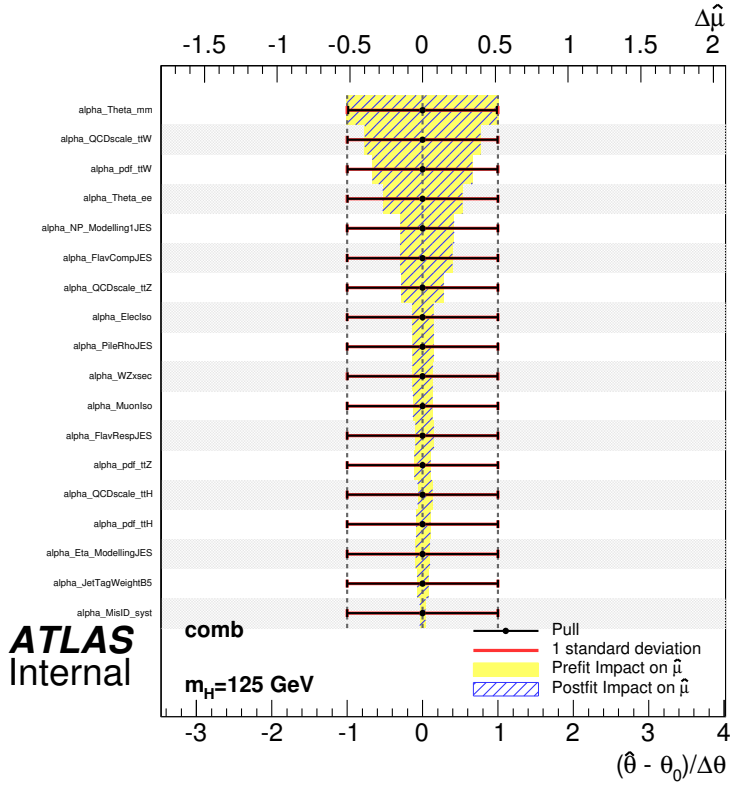

(a) 2lem channel

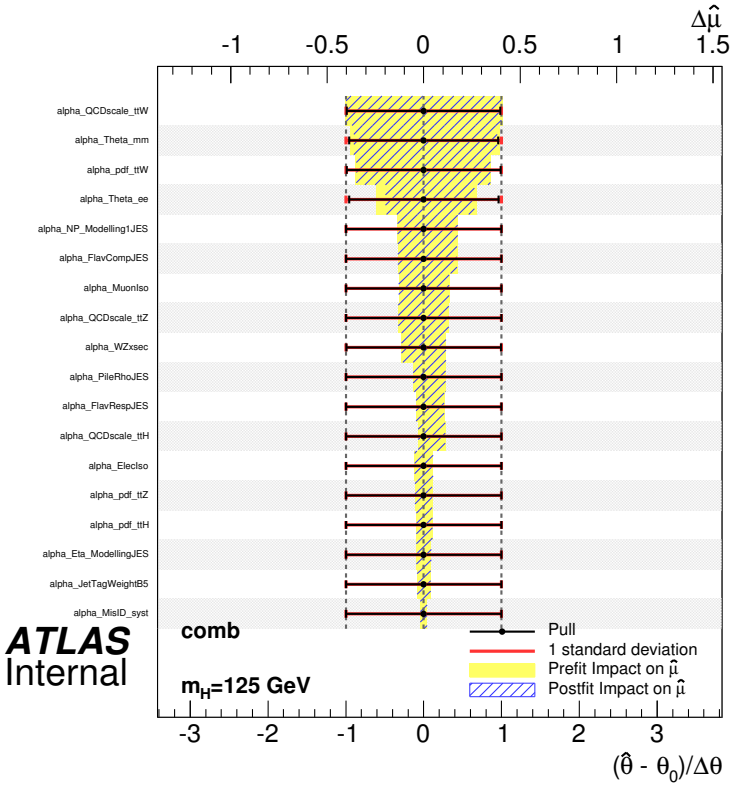

(b) 2l (ee, em, mm) channel

Figure 34: Nuisance parameters ranking for 2lem (4 and 5 jets) and inclusive 2 leptons channels without tau. Only non-prunable parameters were considered.

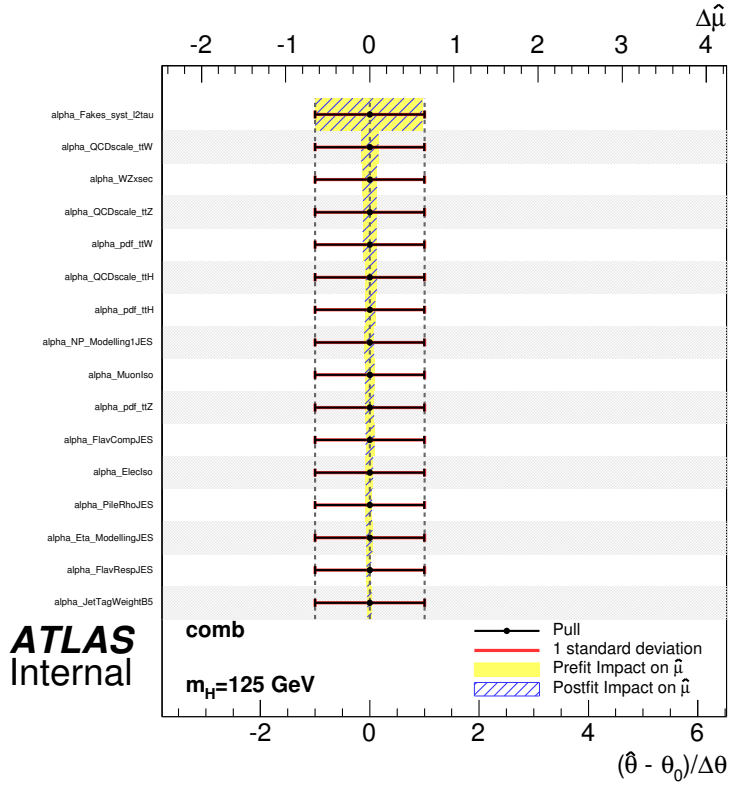

(a) 2ltau channel

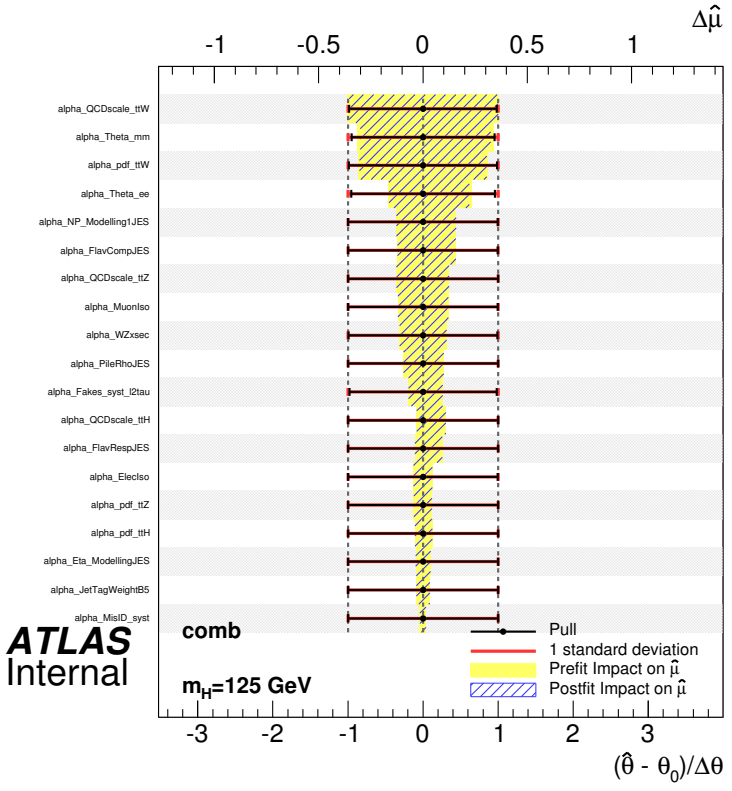

(b) All 2l (ee, em, mm, tau)channel

Figure 35: Nuisance parameters ranking for 2ltau and combined 2 leptons channels. Only non-prunable parameters were considered.

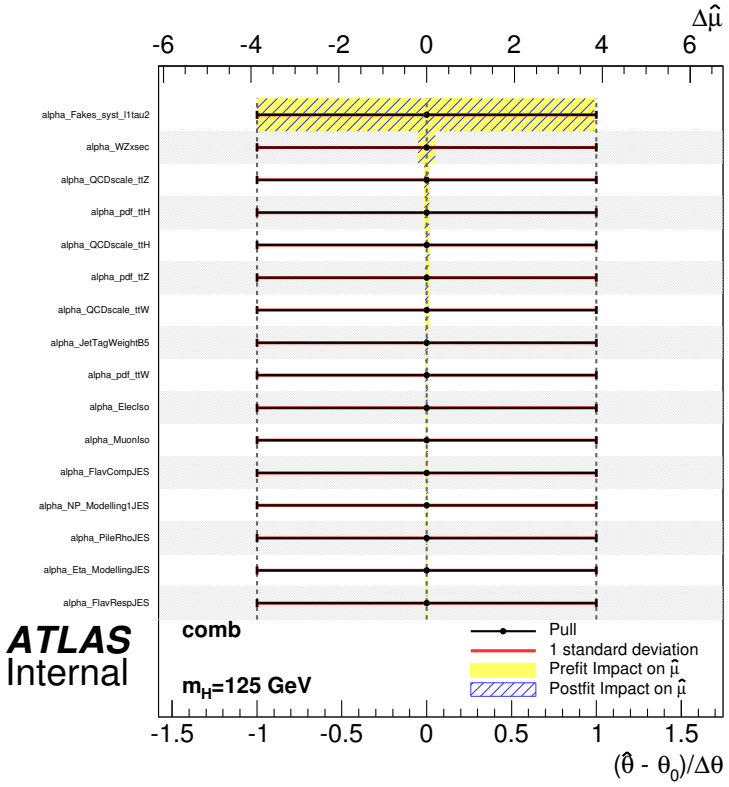

(a) 1l2tau channel

Figure 36: Nuisance parameters ranking for 4l and 1l2tau channels. Only non-prunable parameters were considered.

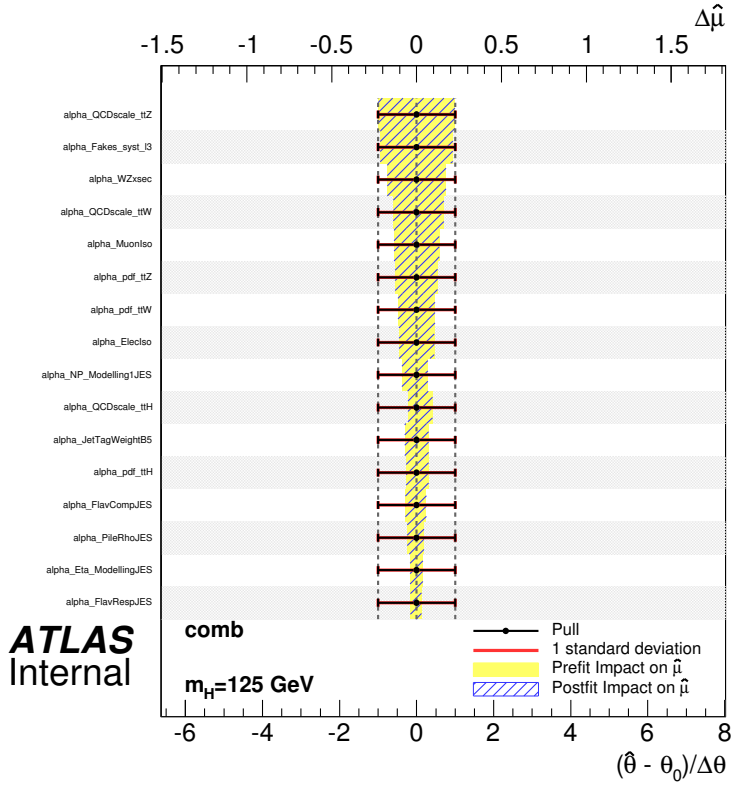

(a) 3l channel

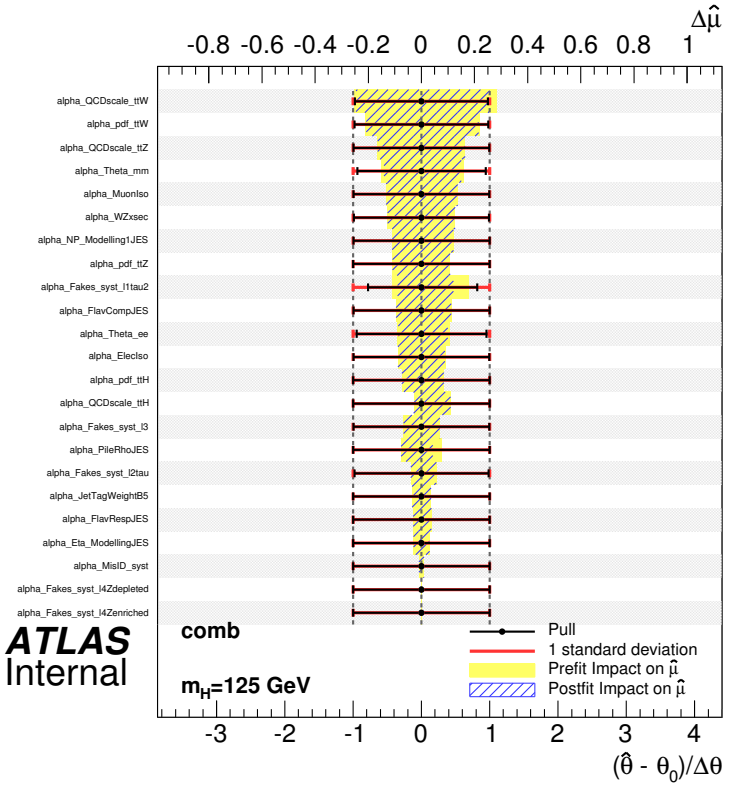

(b) combined channel

Figure 37: Nuisance parameters ranking for 3l and combined channels. Only non-prunable parameters were considered.

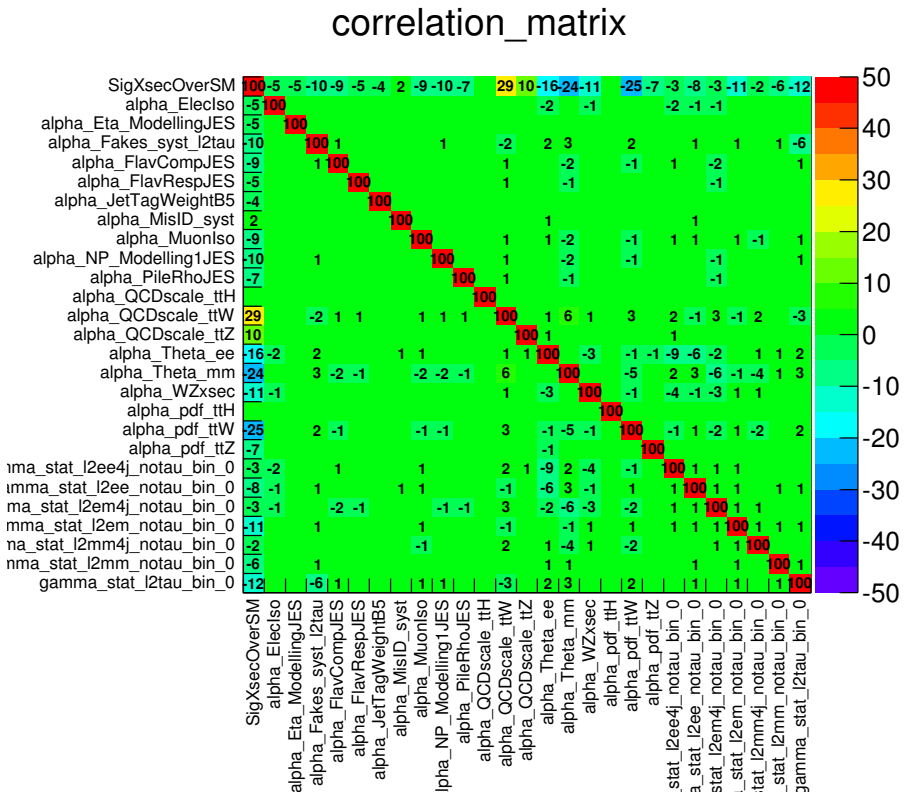

(a) 2l channels

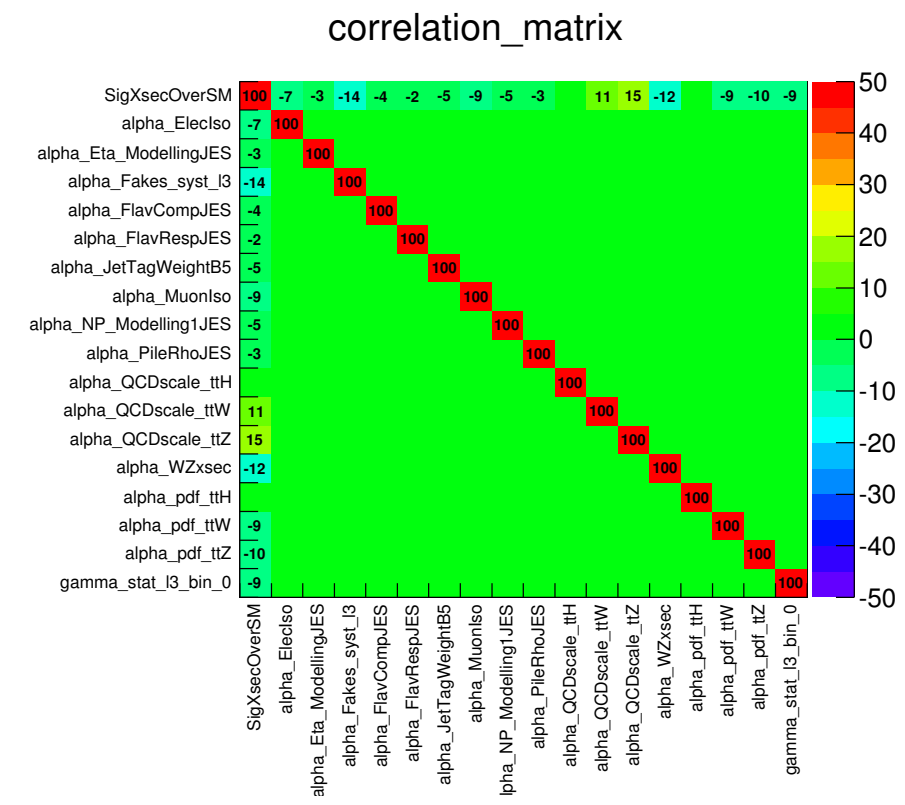

(b) 3l channel

Figure 38: Nuisance parameters ranking for 2l and 3l channels. Only non-prunable parameters were considered.

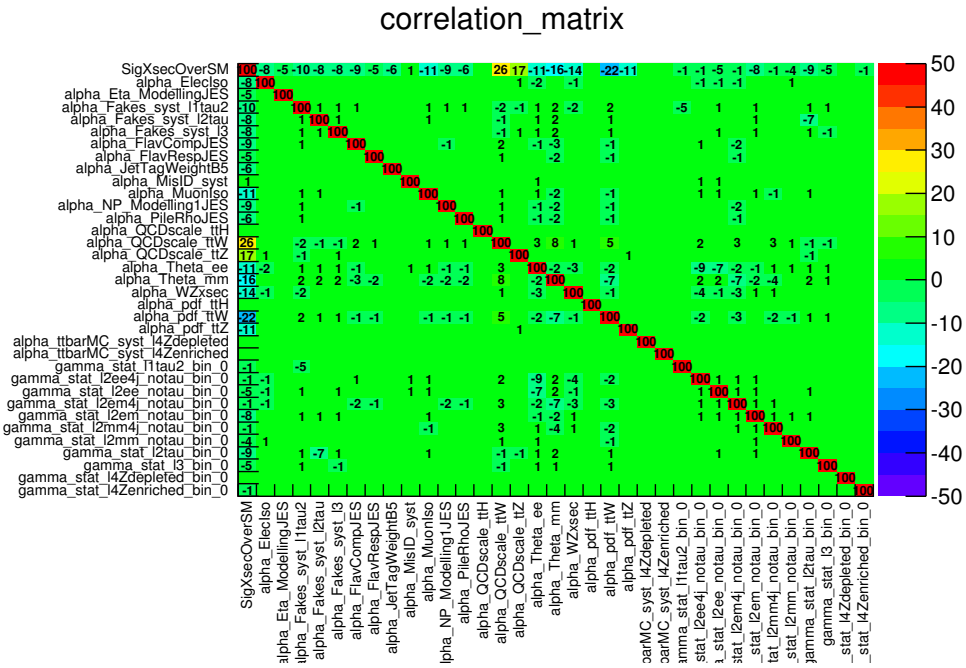

Figure 39: Correlation matrix (percentage) for the all channels combined after fit to an Asimov data set with μ=1, for relevant systematics surviving pruning.

10.6 Pruning

The pruning if nuisance parameters pruning can be considered in order to reduce computational time and fit instabilities. This section investigates the possibility of pruning nuisance parameters by the iterative removal of NP which changes the Hesse error on POI the least. The procedure is the iterative removal of NP which changes the Hesse error on POI the least when removed until the threshold is reached. Allowing the 2nd non-significant digit after rounding to vary by up to 5 units is considered a safe threshold.

Table 10.6 shows the list of nuisance parameters surviving the pruning algorithm, and specifies in which sub-channel it has been considered useful. In particular, cross section uncertainties on WW, ZZ, $Z\gamma^*$, $W\gamma^*$ and $\gamma\gamma$, all set to a conservative 25%, are considered negligible in the fit for all analysis. However, it has been decided every MC used in the fit should have a corresponding theory uncertainty and these parameters will therefore not be removed from the fit. In the same fashion, the uncertainty form charge mis-identification estimates in 2 leptons channels is greatly reduced from a 100% anti-correlation in its effect on the charge and identification fakes (see Tab. 25), resulting in an effective low impact on the POI and possible pruning. The charge mis-ID will however not be pruned in the analysis.

Finally, the pruning procedure shows the only significant experimental systematics are the muon and electron isolation scale factors: MuonIso and ElecIso, the eta modelling component of the JES Eta_ModellingJES, flavour related component of the JES: FlavCompJES and FlavRespJES, the b-tagging efficiency scale factor JetTagWeightB5, and pile-up related JES components: NP_Modelling1JES and PileRhoJES.

Parameter surviving pruning algorithm	1l	2l	3l	4l
Theory				
QCDscale_ttH		✓	✓	
QCDscale_ttW		✓	✓	
QCDscale_ttZ		✓	✓	✓
pdf_ttH		✓	✓	
pdf_ttW		✓	✓	
pdf_ttZ		✓	✓	✓
WZxsec		✓	✓	
Fake Estimates				
Fakes_syst_l1tau2	✓			
Fakes_syst_l2tau		✓		
Fakes_syst_l3			✓	
Theta_ee		✓		
Theta_mm		✓		
Experimental				
ElecIso		✓	✓	
MuonIso		✓	✓	
Eta_ModellingJES		✓		
FlavCompJES		✓	✓	
FlavRespJES		✓		
JetTagWeightB5		✓	✓	
NP_Modelling1JES		✓	✓	
PileRhoJES		✓		

11 Conclusions

References

[1] S. Dittmaier et al. Handbook of LHC Higgs Cross Sections: 1. Inclusive Observables. 2011.

[2] Performance of the ATLAS Electron and Photon Trigger in p-p Collisions at sqrts = 7 TeV in 2011. Technical Report ATLAS-CONF-2012-048, CERN, Geneva, May 2012.

[3] Performance of the ATLAS muon trigger in 2011. Technical Report ATLAS-CONF-2012-099, CERN, Geneva, Jul 2012.

[4] https://twiki.cern.ch/twiki/bin/view/AtlasProtected/EfficiencyMeasurements#Trigger.

[5] https://twiki.cern.ch/twiki/bin/viewauth/Atlas/MuonTriggerPhysicsTriggerRecommendations2

[6] G. Bevilacqua, M. Czakon, M.V. Garzelli, A. van Hameren, A. Kardos, C.G. Papadopoulos, R. Pittau, and M. Worek. HELAC-NLO. 184:986, 2013.

[7] Paolo Nason. A new method for combining NLO QCD with shower Monte Carlo algorithms. 11:040, 2004.

[8] S. Frixione, P. Nason, and C. Oleari. 11:070, 2007.

[9] S. Alioli, P. Nason, C. Oleari, and E. Re. 06:040, 2010.

[10] T. Sjöstrand, S. Mrenna, and P. Skands. A brief introduction to pythia 8.1.

[11] S Heinemeyer et al. Handbook of LHC Higgs Cross Sections: 3. Higgs Properties. 2013.

[12] S Guindon, E Shabalina, J Adelman, M Alhroob, S Amor dos Santos, A Basye, J Bouffard, M Casolino, I Connelly, A Cortes Gonzalez, V Dao, S D'Auria, A Doyle, P Ferrari, F Filthaut, R Goncalo, N de Groot, S Henkelmann, V Jain, A Juste, G Kirby, D Kar, A Knue, K Kroeninger, T Liss, E Le Menedeu, J Montejo Berlingen, M Moreno Llacer, O Nackenhorst, T Neep, A Onofre, M Owen, M Pinamonti, Y Qin, A Quadt, D Quilty, C Schwanenberger, L Serkin, R St Denis, J Thomas-Wilsker, and T Vazquez-Schroeder. Search for the Standard Model Higgs boson produced in association with top quarks and decaying to $b\bar{b}$ in pp collisions at $\sqrt{s}$= 8 TeV with the ATLAS detector at the LHC. Technical Report ATL-COM-PHYS-2013-1659, CERN, Geneva, Dec 2013. The note contains internal documentation of the ttH(bb) analysis approved as a preliminary result (ATLAS-CONF-2014-011).

[13] J. Alwall et al. Madgraph/madevent v4: the new web generation. 09:028, 2007.

[14] John M. Campbell and R. Keith Ellis. $t\bar{t}W^{+-}$ production and decay at NLO. *JHEP*, 1207:052, 2012.

[15] M.V. Garzelli, A. Kardos, C.G. Papadopoulos, and Z. Trocsanyi. t $\bar{t}$ W^{+-} and t $\bar{t}$ Z Hadroproduction at NLO accuracy in QCD with Parton Shower and Hadronization effects. *JHEP*, 1211:056, 2012.

[16] J. Alwall, R. Frederix, S. Frixione, V. Hirschi, F. Maltoni, et al. The automated computation of tree-level and next-to-leading order differential cross sections, and their matching to parton shower simulations. *JHEP*, 1407:079, 2014.

[17] A.D. Martin, W.J. Stirling, R.S. Thorne, and G. Watt. Parton distributions for the LHC. *Eur.Phys.J.*, C63:189–285, 2009.

[18] V Dao, S Henkelmann, S Guindon, K Kroeninger, A Quadt, E Shabalina, and T Vazquez-Schroeder. Measurement of the associated production of a vector boson (W, Z) and top quark pair in the opposite sign dilepton channel with pp collisions at $\sqrt{s} = 8$ TeV with the ATLAS detector at the LHC. Technical Report ATL-COM-PHYS-2014-399, CERN, Geneva, May 2014.

[19] S Biondi, D Boumediene, D Calvet, D DeMarco, E Dubreuil, S Gentile, M Kuna, C Lester, F Lasagni, J McFayden, S Monzani, P Onyisi, R Ospanov, D Parredes, M Pitt, G Salamanna, J Schaarschmidt, F Seifert, A Sidoti, A Sopczak, and S Valentinetti. Search for ttH in the multilepton final 1 state: backgrounds and their estimation. Technical Report ATL-COM-PHYS-2014-222, CERN, Geneva, Mar 2014.

[20] Glen Cowan, Kyle Cranmer, Eilam Gross, Ofer Vitells. Asymptotic formulae for likelihood-based tests of new physics. *Eur.Phys.J.C*, 71:1554, 2011.

A Experimental systematics uncertainity Tables

A.1 $t\bar{t}H$ systematic uncertainties

ttH	2ee4j		2ee5jincl		2em4j		2em5jincl	
	Down-Up Var. (%)		Down-Up Var. (%)		Down-Up Var. (%)		Down-Up Var. (%)	
lepTrigSFEventWeight	-0.15	0.15	-0.16	0.16	-0.33	0.33	-0.33	0.33
ElecResolution	-0.35	-0.70	0.32	-0.03	0.08	-0.15	0.03	-0.29
ElecScale	-0.03	0.27	0.00	0.19	-0.13	0.01	-0.12	-0.02
ElecId	-1.59	1.60	-1.56	1.57	-0.75	0.75	-0.76	0.76
ElecIso	-4.00	4.08	-4.06	4.15	-2.04	2.04	-2.04	2.04
ID	0.00	0.00	0.00	0.00	0.00	-0.07	0.07	0.15
MS	0.00	0.00	0.00	0.00	0.00	-0.20	0.11	0.06
SCALE	0.00	0.00	0.00	0.00	-0.07	0.15	-0.11	0.18
MuonReco	0.00	0.00	0.00	0.00	-0.13	0.13	-0.13	0.13
MuonIso	0.00	0.00	0.00	0.00	-1.97	1.97	-1.99	1.99
TauScale	0.17	0.00	0.70	-0.47	0.10	-0.25	0.21	-0.25
TauEVSF	0.00	0.00	0.00	0.00	0.00	0.00	0.00	0.00
TauIDSF	0.00	0.00	0.00	0.00	0.00	0.00	0.00	0.00

Table 30: Variation of the *ttH* expected events as a function of the experimental leptons and hadronic tau uncertainties for ee4jets, ee5morejets, em4jets and em5morejets channels.

ttH	2mm4j		2mm5jincl	
	Down-Up Var. (%)		Down-Up Var. (%)	
lepTrigSFEventWeight	-0.79	0.79	-0.75	0.75
ElecResolution	-0.17	-0.17	0.00	0.00
ElecScale	0.00	-0.17	0.00	0.00
ElecId	0.00	0.00	0.00	0.00
ElecIso	0.00	0.00	0.00	0.00
ID	0.00	0.00	-0.07	0.00
MS	0.00	-0.15	-0.07	-0.05
SCALE	0.00	0.00	-0.05	0.00
MuonReco	-0.25	0.25	-0.26	0.26
MuonIso	-3.88	3.95	-3.93	4.00
TauScale	0.19	-0.14	0.20	-0.13
TauEVSF	0.00	0.00	0.00	0.00
TauIDSF	0.00	0.00	0.00	0.00

Table 31: Variation of the *ttH* expected events as a function of the experimental leptons and hadronic tau uncertainties for mm4jets and mm5morejets channels.

ttH	1l2t		2lt		3l		4l	
	Down-Up Var. (%)		Down-Up Var. (%)		Down-Up Var. (%)		Down-Up Var. (%)	
lepTrigSFEventWeight	-1.28	1.28	-0.54	0.54	-0.20	0.20	-0.14	0.14
ElecResolution	0.00	0.00	-0.10	-0.40	-0.17	-0.05	0.07	0.37
ElecScale	0.00	0.00	-0.62	0.00	-0.29	0.14	-0.34	0.45
ElecId	-0.32	0.32	-0.87	0.88	-1.19	1.20	-1.79	1.81
ElecIso	-1.00	1.00	-1.92	1.94	-2.61	2.66	-3.52	3.61
ID	0.00	-0.14	0.00	0.24	0.00	-0.06	-0.12	-0.12
MS	0.00	0.00	0.00	0.00	0.00	0.01	0.13	-0.10
SCALE	-0.14	0.00	0.00	0.00	-0.21	0.03	0.12	0.00
MuonReco	-0.06	0.06	-0.13	0.13	-0.23	0.23	-0.31	0.32
MuonIso	-1.00	1.00	-2.07	2.09	-3.44	3.52	-4.68	4.85
TauScale	-3.57	4.09	-3.15	3.17	0.00	-0.00	0.00	0.00
TauEVSF	-0.05	0.05	-0.15	0.15	0.00	0.00	0.00	0.00
TauIDSF	-6.58	6.82	-2.74	2.74	0.00	0.00	0.00	0.00

Table 32: Variation of the *ttH* expected events as a function of the experimental leptons and hadronic tau uncertainties for 1lep+2tau, 2lep+tau, 3lep and 4lep channels.

ttH	2ee4j		2ee5jincl		2em4j		2em5jincl	
	Down-Up Var. (%)		Down-Up Var. (%)		Down-Up Var. (%)		Down-Up Var. (%)	
JER	—	1.22	—	-0.64	—	-0.48	—	0.92
JVF	-0.18	-0.81	0.24	-0.04	-0.73	0.08	0.79	-0.65
Eta ModellingJES	0.06	1.07	-1.47	0.75	-0.13	-0.72	-1.11	1.25
Eta StatAndMethodJES	1.63	0.47	-1.08	0.31	0.02	-0.32	-0.42	0.59
MuJES	0.51	0.10	-0.37	0.01	-0.22	-0.12	0.07	0.08
HighPtJES	0.00	0.00	0.00	0.00	0.00	0.00	0.00	0.00
NPVJES	1.06	0.90	-1.39	0.06	0.04	-0.66	-0.25	0.38
NP_Detector1JES	0.92	0.47	-1.02	0.32	0.24	-0.37	-0.50	0.61
NP_Detector2JES	0.24	0.00	-0.14	0.12	-0.15	0.03	-0.06	0.04
NP_Detector3JES	0.51	-0.28	-0.30	0.29	-0.15	0.19	-0.05	0.10
NP_Mixed1JES	0.00	-0.01	0.00	-0.00	-0.05	-0.01	-0.05	-0.01
NP_Mixed2JES	0.84	-0.04	-0.58	0.28	-0.27	-0.14	-0.09	0.30
NP_Modelling1JES	1.07	0.30	-3.76	2.34	0.63	-2.00	-2.47	3.08
NP_Modelling2JES	-0.08	0.76	0.32	-0.57	-0.06	-0.27	0.32	-0.09
NP_Modelling3JES	0.64	-0.27	-0.41	0.29	-0.25	0.11	-0.04	0.15
NP_Modelling4JES	0.01	-0.01	0.01	0.11	-0.05	0.00	-0.06	0.04
NP_Statistical1JES	0.91	0.21	-1.04	0.48	0.33	-0.37	-0.57	0.64
NP_Statistical2JES	-0.28	0.45	0.28	-0.30	0.19	-0.15	0.10	-0.05
NP_Statistical3JES	0.60	-0.29	-0.42	0.28	-0.16	-0.16	-0.05	0.30
FlavCompJES	0.58	0.01	-3.77	2.40	1.30	-2.44	-2.85	3.15
FlavRespJES	0.51	0.45	-2.19	1.13	-0.33	-1.21	-1.35	1.71
bJES	0.46	0.30	-0.68	0.50	0.19	-0.55	-0.22	0.65
PilePtJES	-0.00	-0.01	0.02	0.01	0.02	-0.00	0.01	-0.01
PileRhoJES	0.25	0.48	-2.21	1.43	-0.37	-1.31	-1.35	1.94
JetTagWeightLight0	0.00	-0.00	-0.01	0.01	-0.01	0.01	0.00	-0.00
JetTagWeightLight1	-0.00	0.00	-0.00	0.00	0.01	-0.01	-0.01	0.01
JetTagWeightLight2	-0.01	0.01	0.00	-0.00	-0.01	0.01	0.01	-0.01
JetTagWeightLight3	-0.00	0.00	-0.02	0.02	-0.01	0.01	0.00	-0.00
JetTagWeightLight4	-0.00	0.00	-0.03	0.03	0.00	-0.00	-0.01	0.01
JetTagWeightLight5	-0.00	0.00	-0.07	0.07	0.01	-0.01	-0.01	0.01
JetTagWeightLight6	-0.01	0.01	0.00	-0.00	-0.01	0.01	0.01	-0.01
JetTagWeightLight7	0.01	-0.01	-0.01	0.01	-0.01	0.01	0.01	-0.01
JetTagWeightLight8	-0.00	0.00	0.06	-0.06	-0.02	0.02	0.01	-0.01
JetTagWeightLight9	0.03	-0.03	0.02	-0.02	0.05	-0.05	-0.04	0.04
JetTagWeightLight10	-0.02	0.02	0.10	-0.10	0.04	-0.04	0.03	-0.03
JetTagWeightLight11	0.01	-0.01	-0.31	0.31	-0.03	0.03	-0.18	0.19
JetTagWeightT0	0.01	-0.01	0.01	-0.01	-0.01	0.01	-0.01	0.01
JetTagWeightT1	0.02	-0.02	0.01	-0.01	-0.01	0.01	0.01	-0.01
JetTagWeightT2	0.01	-0.01	-0.01	0.01	0.01	-0.01	-0.02	0.02
JetTagWeightT3	-0.02	0.02	-0.01	0.01	0.02	-0.02	0.01	-0.01
JetTagWeightC0	0.01	-0.01	0.08	-0.08	-0.02	0.02	0.05	-0.05
JetTagWeightC1	-0.17	0.17	-0.07	0.07	-0.02	0.02	-0.02	0.02
JetTagWeightC2	-0.10	0.09	-0.16	0.16	-0.01	0.01	-0.00	0.00
JetTagWeightC3	0.39	-0.39	0.13	-0.13	0.14	-0.14	-0.02	0.02
JetTagWeightB0	0.01	-0.01	0.03	-0.03	-0.01	0.01	-0.03	0.03
JetTagWeightB1	0.01	-0.01	0.03	-0.03	0.02	-0.02	0.02	-0.02
JetTagWeightB2	-0.11	0.11	-0.11	0.11	-0.26	0.26	-0.25	0.25
JetTagWeightB3	0.41	-0.42	0.45	-0.45	0.33	-0.33	0.34	-0.35
JetTagWeightB4	0.17	-0.17	0.31	-0.31	0.33	-0.34	0.28	-0.28
JetTagWeightB5	-1.22	1.16	-0.76	0.71	-0.95	0.88	-0.87	0.80
NonClosure AFIIJES	0.00	0.00	0.00	0.00	0.00	0.00	0.00	0.00

Table 33: Variation of the ttH expected events as a function of the experimental Jet uncertainties for ee4jets, ee5morejets, em4jets and em5morejets channels.

ttH	2mm4j		2mm5jincl	
	Down-Up Var. (%)		Down-Up Var. (%)	
JER	—	0.90	—	-0.08
JVF	-0.43	0.76	0.72	-1.21
Eta ModellingJES	0.93	-0.42	-1.63	1.26
Eta StatAndMethodJES	0.84	-0.09	-0.71	0.55
MuJES	0.50	0.41	-0.35	-0.03
HighPtJES	0.00	0.00	0.00	0.00
NPVJES	0.32	0.74	-0.02	0.04
NP_Detector1JES	0.56	0.10	-0.73	0.49
NP_Detector2JES	0.30	0.01	-0.16	0.20
NP_Detector3JES	0.39	0.01	-0.21	0.20
NP_Mixed1JES	0.00	0.03	0.00	0.00
NP_Mixed2JES	0.53	0.14	-0.40	0.30
NP_Modelling1JES	2.41	-1.68	-3.09	3.13
NP_Modelling2JES	0.11	0.39	0.30	-0.51
NP_Modelling3JES	0.59	0.04	-0.22	0.09
NP_Modelling4JES	0.30	0.03	-0.17	0.10
NP_Statistical1JES	0.58	-0.05	-0.75	0.58
NP_Statistical2JES	0.04	0.54	0.20	-0.29
NP_Statistical3JES	0.42	0.21	-0.33	0.19
FlavCompJES	3.85	-2.20	-3.36	2.74
FlavRespJES	3.30	-0.99	-2.30	1.44
bJES	-0.52	0.27	-0.41	0.92
PilePtJES	0.02	-0.00	0.08	-0.00
PileRhoJES	1.06	-0.63	-1.80	2.15
JetTagWeightLight0	-0.01	0.01	-0.00	0.00
JetTagWeightLight1	0.01	-0.01	0.01	-0.01
JetTagWeightLight2	-0.01	0.01	0.00	-0.00
JetTagWeightLight3	-0.00	0.00	-0.01	0.01
JetTagWeightLight4	-0.00	0.00	-0.01	0.01
JetTagWeightLight5	0.01	-0.01	-0.02	0.02
JetTagWeightLight6	-0.02	0.02	-0.01	0.01
JetTagWeightLight7	0.00	-0.00	0.01	-0.01
JetTagWeightLight8	-0.01	0.01	-0.01	0.01
JetTagWeightLight9	0.10	-0.10	0.08	-0.08
JetTagWeightLight10	0.06	-0.06	0.03	-0.03
JetTagWeightLight11	-0.04	0.04	-0.10	0.10
JetTagWeightT0	-0.00	0.00	0.01	-0.01
JetTagWeightT1	-0.01	0.01	-0.01	0.01
JetTagWeightT2	0.00	-0.00	0.00	-0.00
JetTagWeightT3	-0.01	0.01	-0.02	0.02
JetTagWeightC0	0.08	-0.08	-0.01	0.01
JetTagWeightC1	-0.13	0.13	-0.07	0.07
JetTagWeightC2	0.01	-0.01	0.01	-0.01
JetTagWeightC3	0.18	-0.18	-0.00	0.00
JetTagWeightB0	-0.01	0.01	-0.00	0.00
JetTagWeightB1	0.04	-0.04	0.02	-0.02
JetTagWeightB2	-0.36	0.35	-0.10	0.10
JetTagWeightB3	0.42	-0.43	0.25	-0.26
JetTagWeightB4	0.29	-0.29	0.18	-0.19
JetTagWeightB5	-1.02	0.96	-0.80	0.72
NonClosure AFIIJES	0.00	0.00	0.00	0.00

Table 34: Variation of the *ttH* expected events as a function of the experimental Jet uncertainties for mm4jets and mm5morejets channels.

ttH	1l2t		2lt		3l		4l	
	Down-Up Var. (%)		Down-Up Var. (%)		Down-Up Var. (%)		Down-Up Var. (%)	
JER	—	0.65	—	-0.42	—	-1.26	—	-1.67
JVF	0.36	-0.12	0.43	-0.58	0.31	-0.60	-0.00	-0.21
Eta ModellingJES	-0.19	0.31	-0.73	0.69	-0.66	0.76	-0.08	0.14
Eta StatAndMethodJES	-0.27	0.06	-0.41	0.07	-0.23	0.24	0.01	0.01
MuJES	-0.07	0.02	-0.60	0.11	-0.07	0.06	0.00	0.14
HighPtJES	0.00	0.00	0.00	0.00	0.00	0.00	0.00	0.00
NPVJES	-0.08	0.34	-0.58	0.03	-0.25	0.17	0.10	0.28
NP_Detector1JES	-0.13	0.11	-0.51	0.04	-0.32	0.27	0.02	-0.01
NP_Detector2JES	-0.09	0.00	-0.11	0.04	-0.03	0.03	-0.01	0.00
NP_Detector3JES	-0.10	0.05	-0.10	0.04	-0.04	0.07	0.00	0.01
NP_Mixed1JES	0.00	-0.00	0.00	-0.00	0.05	-0.00	0.00	-0.01
NP_Mixed2JES	-0.10	0.04	-0.33	0.07	-0.10	0.12	0.12	0.01
NP_Modelling1JES	-0.25	0.58	-1.69	1.75	-1.88	1.48	-0.04	0.36
NP_Modelling2JES	0.07	-0.10	0.06	-0.35	0.15	-0.11	0.02	0.10
NP_Modelling3JES	-0.06	0.01	-0.10	0.08	-0.08	0.08	0.00	0.01
NP_Modelling4JES	-0.10	0.01	-0.11	0.00	-0.03	0.01	0.00	-0.00
NP_Statistical1JES	-0.13	0.10	-0.47	0.06	-0.34	0.30	-0.24	0.02
NP_Statistical2JES	0.04	-0.10	0.07	-0.11	0.07	-0.08	0.01	-0.00
NP_Statistical3JES	-0.11	0.05	-0.32	0.08	-0.09	0.10	0.00	0.00
FlavCompJES	-0.37	0.35	-2.25	0.89	-1.51	1.33	0.09	-0.02
FlavRespJES	-0.11	0.11	-0.88	0.39	-0.65	0.68	0.01	-0.14
bJES	-0.07	0.23	-0.28	0.93	-0.46	0.41	-0.10	0.37
PilePtJES	-0.00	-0.02	0.00	-0.01	-0.00	-0.00	0.01	0.00
PileRhoJES	-0.27	0.38	-1.22	1.34	-0.86	0.94	-0.23	0.23
JetTagWeightLight0	0.00	-0.00	0.00	-0.00	-0.00	0.00	-0.00	0.00
JetTagWeightLight1	-0.00	0.00	0.00	-0.00	0.00	-0.00	-0.00	0.00
JetTagWeightLight2	0.00	-0.00	0.00	-0.00	0.00	-0.00	-0.00	0.00
JetTagWeightLight3	-0.01	0.01	-0.00	0.00	0.00	-0.00	0.00	-0.00
JetTagWeightLight4	-0.00	0.00	0.01	-0.01	-0.01	0.01	-0.00	0.00
JetTagWeightLight5	-0.02	0.02	-0.02	0.02	-0.01	0.01	0.02	-0.02
JetTagWeightLight6	-0.01	0.01	0.01	-0.01	-0.00	0.00	0.01	-0.01
JetTagWeightLight7	0.01	-0.01	-0.01	0.01	0.01	-0.01	0.00	-0.00
JetTagWeightLight8	-0.03	0.03	0.01	-0.01	0.01	-0.01	0.00	-0.00
JetTagWeightLight9	0.01	-0.02	-0.00	0.00	0.04	-0.04	-0.00	0.00
JetTagWeightLight10	0.03	-0.02	0.00	-0.00	0.05	-0.05	-0.02	0.02
JetTagWeightLight11	-0.22	0.23	0.13	-0.13	-0.11	0.11	-0.03	0.03
JetTagWeightT0	0.12	-0.12	0.00	-0.00	-0.00	0.00	-0.00	0.00
JetTagWeightT1	-0.28	0.29	-0.17	0.17	-0.02	0.02	0.00	-0.00
JetTagWeightT2	-0.06	0.06	-0.03	0.03	-0.01	0.01	-0.00	0.00
JetTagWeightT3	0.42	-0.42	0.35	-0.35	0.03	-0.03	-0.01	0.01
JetTagWeightC0	-0.02	0.02	-0.02	0.02	-0.02	0.02	-0.01	0.01
JetTagWeightC1	-0.08	0.08	-0.12	0.12	-0.09	0.09	-0.01	0.01
JetTagWeightC2	-0.07	0.07	-0.14	0.14	-0.03	0.03	-0.03	0.03
JetTagWeightC3	0.14	-0.14	0.23	-0.23	0.12	-0.12	0.05	-0.05
JetTagWeightB0	-0.08	0.08	0.02	-0.02	0.01	-0.01	0.01	-0.01
JetTagWeightB1	0.04	-0.04	0.02	-0.02	0.04	-0.04	0.04	-0.04
JetTagWeightB2	-0.36	0.36	-0.17	0.17	-0.40	0.40	-0.17	0.17
JetTagWeightB3	0.51	-0.52	0.34	-0.35	0.67	-0.67	0.41	-0.42
JetTagWeightB4	0.28	-0.28	0.29	-0.29	0.46	-0.47	0.28	-0.29
JetTagWeightB5	-1.12	1.08	-0.67	0.63	-1.71	1.68	-1.30	1.25
NonClosure AFIIJES	0.00	0.00	0.00	0.00	0.00	0.00	0.00	0.00

Table 35: Variation of the ttH expected events as a function of the experimental Jet uncertainties for 1lep+2tau, 2lep+tau, 3lep and 4lep channels.

A.2 $t\bar{t}W$ systematic uncertainties

ttW	2ee4j		2ee5jincl		2em4j		2em5jincl	
	Down-Up Var. (%)		Down-Up Var. (%)		Down-Up Var. (%)		Down-Up Var. (%)	
lepTrigSFEventWeight	-0.11	0.11	-0.12	0.12	-0.27	0.27	-0.29	0.29
ElecResolution	0.00	0.17	-0.20	-0.41	0.03	0.03	-0.02	0.18
ElecScale	-0.18	0.00	-0.20	0.29	-0.04	0.03	-0.23	0.17
ElecId	-1.50	1.51	-1.53	1.55	-0.74	0.74	-0.78	0.78
ElecIso	-4.29	4.38	-4.44	4.54	-2.16	2.16	-2.21	2.21
ID	0.00	0.00	0.00	0.00	0.00	0.00	0.00	0.00
MS	0.00	0.00	0.00	0.00	0.00	0.03	0.00	0.07
SCALE	0.00	0.00	0.00	0.00	-0.04	0.07	-0.11	0.12
MuonReco	0.00	0.00	0.00	0.00	-0.13	0.13	-0.13	0.13
MuonIso	0.00	0.00	0.00	0.00	-2.03	2.03	-2.05	2.05
TauScale	0.16	-0.00	0.00	-0.00	0.20	-0.19	0.27	-0.05
TauEVSF	0.00	0.00	0.00	0.00	0.00	0.00	0.00	0.00
TauIDSF	0.00	0.00	0.00	0.00	0.00	0.00	0.00	0.00

Table 36: Variation of the *ttW* expected events as a function of the experimental leptons and hadronic tau uncertainties for ee4jets, ee5morejets, em4jets and em5morejets channels.

ttW	2mm4j		2mm5jincl	
	Down-Up Var. (%)		Down-Up Var. (%)	
lepTrigSFEventWeight	-0.68	0.68	-0.69	0.69
ElecResolution	0.00	0.00	0.00	0.00
ElecScale	0.00	0.00	0.00	0.00
ElecId	0.00	0.00	0.00	0.00
ElecIso	0.00	0.00	0.00	0.00
ID	0.00	0.00	0.00	0.00
MS	0.00	0.00	0.00	0.13
SCALE	0.00	0.00	0.00	0.12
MuonReco	-0.25	0.25	-0.26	0.26
MuonIso	-4.04	4.12	-4.07	4.16
TauScale	0.00	-0.14	0.01	-0.17
TauEVSF	0.00	0.00	0.00	0.00
TauIDSF	0.00	0.00	0.00	0.00

Table 37: Variation of the *ttW* expected events as a function of the experimental leptons and hadronic tau uncertainties for mm4jets and mm5morejets channels.

ttW	1l2t		2lt		3l		4l	
	Down-Up Var. (%)		Down-Up Var. (%)		Down-Up Var. (%)		Down-Up Var. (%)	
lepTrigSFEventWeight	-1.28	1.28	-0.47	0.47	-0.13	0.13	0.00	0.00
ElecResolution	0.00	0.00	0.00	0.00	0.23	-0.18	0.00	0.00
ElecScale	0.00	0.00	-0.82	0.03	-0.02	0.20	0.00	0.00
ElecId	-0.35	0.35	-0.80	0.80	-1.22	1.23	0.00	0.00
ElecIso	-1.17	1.17	-1.95	1.97	-2.88	2.94	0.00	0.00
ID	0.00	0.00	0.00	0.87	0.05	-0.30	0.00	0.00
MS	0.00	0.00	0.00	0.87	0.05	-0.21	0.00	0.00
SCALE	0.00	0.00	0.00	0.87	-0.04	-0.17	0.00	0.00
MuonReco	-0.05	0.05	-0.14	0.14	-0.22	0.22	0.00	0.00
MuonIso	-0.93	0.93	-2.26	2.28	-3.44	3.52	0.00	0.00
TauScale	-5.04	8.60	-6.35	1.95	0.00	0.00	0.00	0.00
TauEVSF	0.00	0.00	0.00	0.00	0.00	0.00	0.00	0.00
TauIDSF	-4.10	4.18	-1.65	1.65	0.00	0.00	0.00	0.00

Table 38: Variation of the *ttW* expected events as a function of the experimental leptons and hadronic tau uncertainties for 1lep+2tau, 2lep+tau, 3lep and 4lep channels.

ttW	2ee4j		2ee5jincl		2em4j		2em5jincl	
	Down-Up Var. (%)		Down-Up Var. (%)		Down-Up Var. (%)		Down-Up Var. (%)	
JER	—	-0.93	—	4.39	—	1.83	—	0.81
JVF	0.72	-0.73	0.31	-1.37	0.50	0.38	0.46	-1.38
Eta ModellingJES	-2.31	-1.16	-1.57	2.67	0.75	0.56	-2.50	2.43
Eta StatAndMethodJES	-0.37	-0.85	-0.74	1.34	-0.25	0.95	-1.07	0.55
MuJES	-0.40	-0.66	0.41	0.71	0.35	-0.15	-0.52	0.59
HighPtJES	0.00	0.00	0.00	0.00	0.00	0.00	0.00	0.00
NPVJES	-0.66	-0.21	-1.97	1.63	0.07	1.48	-0.78	1.22
NP_Detector1JES	-1.21	-0.33	-0.27	1.33	-0.53	0.97	-0.98	0.65
NP_Detector2JES	-0.35	-0.48	-0.00	0.72	-0.13	0.06	-0.01	0.16
NP_Detector3JES	-0.30	-0.49	-0.05	0.72	-0.35	0.19	-0.10	0.28
NP_Mixed1JES	-0.02	-0.00	-0.01	-0.00	0.00	0.03	0.00	0.10
NP_Mixed2JES	-0.31	-0.54	-0.04	0.80	-0.40	0.36	-0.61	0.36
NP_Modelling1JES	-1.63	0.76	-4.00	4.57	0.20	2.68	-5.21	3.53
NP_Modelling2JES	-0.54	-0.29	0.78	-0.04	0.64	-0.32	0.35	-0.61
NP_Modelling3JES	-0.32	-0.48	-0.04	0.71	-0.51	0.13	-0.27	0.34
NP_Modelling4JES	-0.33	-0.18	0.00	0.25	-0.06	-0.02	-0.02	0.17
NP_Statistical1JES	-1.21	0.26	-0.25	1.34	-0.53	1.02	-1.06	0.71
NP_Statistical2JES	-0.49	-0.31	0.72	-0.04	0.12	-0.48	0.36	-0.18
NP_Statistical3JES	-0.30	-0.50	-0.06	0.72	-0.40	0.18	-0.62	0.35
FlavCompJES	-2.53	-1.46	-3.26	4.83	-0.08	2.08	-4.94	3.85
FlavRespJES	-1.01	-0.62	-2.44	2.05	0.51	1.43	-2.76	2.23
bJES	-0.51	1.68	-0.97	0.53	-0.17	0.79	-0.75	0.54
PilePtJES	-0.01	0.03	0.01	-0.02	0.01	0.10	0.01	-0.02
PileRhoJES	-1.85	0.09	-2.85	3.73	0.06	1.78	-2.85	2.68
JetTagWeightLight0	0.00	-0.00	0.00	-0.00	0.00	-0.00	-0.00	0.00
JetTagWeightLight1	-0.01	0.01	-0.01	0.01	0.00	-0.00	0.01	-0.01
JetTagWeightLight2	0.00	-0.00	0.01	-0.01	0.00	-0.00	0.00	-0.00
JetTagWeightLight3	0.01	-0.01	-0.00	0.00	0.00	-0.00	-0.00	0.00
JetTagWeightLight4	0.01	-0.01	-0.01	0.01	-0.01	0.01	0.00	-0.00
JetTagWeightLight5	0.02	-0.02	-0.06	0.06	0.02	-0.02	0.02	-0.02
JetTagWeightLight6	-0.00	0.00	-0.01	0.01	-0.00	0.00	0.01	-0.01
JetTagWeightLight7	-0.00	0.00	0.00	-0.00	0.02	-0.02	0.00	-0.00
JetTagWeightLight8	-0.02	0.02	0.01	-0.01	-0.01	0.01	-0.01	0.01
JetTagWeightLight9	-0.06	0.06	0.01	-0.01	0.04	-0.04	-0.01	0.01
JetTagWeightLight10	-0.08	0.08	-0.05	0.05	-0.00	0.00	-0.02	0.02
JetTagWeightLight11	0.16	-0.16	0.20	-0.19	-0.15	0.15	-0.03	0.03
JetTagWeightT0	-0.00	0.00	0.01	-0.01	0.00	-0.00	0.01	-0.01
JetTagWeightT1	0.01	-0.01	-0.00	0.00	-0.01	0.01	-0.00	0.00
JetTagWeightT2	-0.02	0.02	0.01	-0.01	0.00	-0.00	0.00	-0.00
JetTagWeightT3	-0.00	0.00	0.04	-0.04	0.01	-0.01	-0.00	0.00
JetTagWeightC0	0.04	-0.04	-0.04	0.04	0.03	-0.03	0.00	-0.00
JetTagWeightC1	-0.26	0.26	0.13	-0.13	-0.06	0.06	-0.06	0.06
JetTagWeightC2	-0.04	0.04	-0.00	0.01	-0.07	0.07	-0.02	0.02
JetTagWeightC3	0.28	-0.28	-0.12	0.12	0.16	-0.16	0.20	-0.21
JetTagWeightB0	-0.00	0.00	0.04	-0.04	0.06	-0.06	-0.04	0.04
JetTagWeightB1	0.01	-0.01	0.06	-0.06	0.00	-0.00	0.04	-0.04
JetTagWeightB2	-0.24	0.24	-0.27	0.27	-0.33	0.32	-0.25	0.25
JetTagWeightB3	0.75	-0.76	0.38	-0.39	0.46	-0.47	0.51	-0.51
JetTagWeightB4	0.32	-0.32	0.30	-0.29	0.24	-0.24	0.26	-0.26
JetTagWeightB5	-1.82	1.80	-1.64	1.62	-1.22	1.16	-1.66	1.61
NonClosure AFIIJES	0.00	0.00	0.00	0.00	0.00	0.00	0.00	0.00

Table 39: Variation of the *ttW* expected events as a function of the experimental Jet uncertainties for ee4jets, ee5morejets, em4jets and em5morejets channels.

ttW	2mm4j		2mm5jincl	
	Down-Up Var. (%)		Down-Up Var. (%)	
JER	—	-0.61	—	1.52
JVF	0.04	-0.88	0.85	-0.62
Eta ModellingJES	0.52	0.27	-1.81	1.98
Eta StatAndMethodJES	0.43	0.24	-1.06	0.63
MuJES	-0.05	0.45	-0.21	0.16
HighPtJES	0.00	0.00	0.00	0.00
NPVJES	0.43	-0.24	-1.49	1.26
NP_Detector1JES	0.97	0.28	-1.62	0.73
NP_Detector2JES	0.03	0.01	-0.06	0.01
NP_Detector3JES	0.18	-0.09	-0.23	0.14
NP_Mixed1JES	0.00	0.00	0.00	-0.00
NP_Mixed2JES	0.52	-0.27	-0.65	0.35
NP_Modelling1JES	0.26	1.35	-3.51	2.38
NP_Modelling2JES	0.01	0.25	0.37	-0.67
NP_Modelling3JES	0.21	-0.21	-0.28	0.30
NP_Modelling4JES	0.04	0.00	-0.05	-0.00
NP_Statistical1JES	0.95	0.11	-1.66	0.74
NP_Statistical2JES	-0.27	0.18	0.35	-0.24
NP_Statistical3JES	0.29	-0.33	-0.34	0.42
FlavCompJES	0.38	1.52	-3.74	2.22
FlavRespJES	0.53	0.52	-2.78	1.24
bJES	-0.28	0.08	-0.30	0.74
PilePtJES	0.19	-0.01	0.00	0.02
PileRhoJES	0.14	0.47	-2.80	2.11
JetTagWeightLight0	-0.00	0.00	-0.01	0.01
JetTagWeightLight1	0.01	-0.01	0.02	-0.02
JetTagWeightLight2	-0.00	0.00	-0.01	0.01
JetTagWeightLight3	-0.01	0.01	-0.01	0.01
JetTagWeightLight4	-0.01	0.01	0.00	-0.00
JetTagWeightLight5	-0.01	0.01	0.05	-0.05
JetTagWeightLight6	-0.01	0.01	0.01	-0.01
JetTagWeightLight7	-0.01	0.01	-0.01	0.01
JetTagWeightLight8	0.01	-0.01	-0.02	0.02
JetTagWeightLight9	0.03	-0.03	0.05	-0.05
JetTagWeightLight10	0.05	-0.05	-0.01	0.01
JetTagWeightLight11	-0.08	0.08	-0.14	0.14
JetTagWeightT0	-0.01	0.01	0.01	-0.01
JetTagWeightT1	-0.01	0.01	-0.00	0.00
JetTagWeightT2	-0.00	0.00	0.01	-0.01
JetTagWeightT3	0.01	-0.01	0.01	-0.01
JetTagWeightC0	0.09	-0.09	0.05	-0.05
JetTagWeightC1	-0.05	0.05	-0.12	0.12
JetTagWeightC2	-0.04	0.04	0.04	-0.04
JetTagWeightC3	0.09	-0.09	0.07	-0.07
JetTagWeightB0	0.04	-0.04	-0.02	0.02
JetTagWeightB1	0.05	-0.05	0.03	-0.03
JetTagWeightB2	-0.19	0.19	-0.19	0.18
JetTagWeightB3	0.47	-0.47	0.52	-0.52
JetTagWeightB4	0.23	-0.23	0.25	-0.25
JetTagWeightB5	-1.34	1.28	-1.20	1.12
NonClosure AFIIJES	0.00	0.00	0.00	0.00

Table 40: Variation of the *ttW* expected events as a function of the experimental Jet uncertainties for mm4jets and mm5morejets channels.

ttW	1l2t		2lt		3l		4l	
	Down-Up Var. (%)		Down-Up Var. (%)		Down-Up Var. (%)		Down-Up Var. (%)	
JER	—	1.41	—	0.44	—	1.37	—	0.00
JVF	0.00	0.00	1.00	0.00	0.56	-0.59	0.00	0.00
Eta ModellingJES	-1.76	0.07	0.22	1.07	-0.86	1.80	0.00	0.00
Eta StatAndMethodJES	-0.01	-0.02	-0.42	0.00	0.02	0.66	0.00	0.00
MuJES	-0.00	0.03	-0.09	0.01	-0.00	0.30	0.00	0.00
HighPtJES	0.00	0.00	0.00	0.00	0.00	0.00	0.00	0.00
NPVJES	-0.86	-0.04	0.19	3.24	0.26	0.73	0.00	0.00
NP_Detector1JES	0.06	-0.09	-0.49	0.88	-0.14	0.65	0.00	0.00
NP_Detector2JES	-0.06	0.05	-0.00	-0.01	-0.00	0.20	0.00	0.00
NP_Detector3JES	-0.00	-0.01	-0.00	0.01	0.00	0.19	0.00	0.00
NP_Mixed1JES	0.00	-0.00	0.00	-0.00	0.00	-0.00	0.00	0.00
NP_Mixed2JES	-0.00	0.05	-0.00	-0.00	0.00	0.32	0.00	0.00
NP_Modelling1JES	-3.91	-0.16	0.21	3.13	-1.63	3.43	0.00	0.00
NP_Modelling2JES	0.05	-0.13	-0.02	0.06	0.59	-0.00	0.00	0.00
NP_Modelling3JES	-0.03	0.04	0.01	0.05	0.00	0.32	0.00	0.00
NP_Modelling4JES	-0.01	-0.01	0.00	-0.01	0.00	0.19	0.00	0.00
NP_Statistical1JES	-0.01	0.03	-0.43	0.84	0.16	0.67	0.00	0.00
NP_Statistical2JES	0.05	-0.00	-0.01	-0.00	0.32	0.00	0.00	0.00
NP_Statistical3JES	-0.01	-0.02	0.05	0.00	0.01	0.33	0.00	0.00
FlavCompJES	-3.96	0.05	0.25	1.57	-1.75	2.50	0.00	0.00
FlavRespJES	-0.83	0.05	0.23	1.62	-0.47	1.51	0.00	0.00
bJES	0.05	-0.21	-0.07	1.58	-0.48	0.77	0.00	0.00
PilePtJES	-0.08	0.00	0.00	0.04	-0.00	0.02	0.00	0.00
PileRhoJES	-0.81	-0.02	0.25	2.90	-1.02	2.12	0.00	0.00
JetTagWeightLight0	0.00	-0.00	-0.00	0.00	0.00	-0.00	0.00	0.00
JetTagWeightLight1	-0.01	0.01	0.00	-0.00	-0.01	0.01	0.00	0.00
JetTagWeightLight2	0.01	-0.01	0.01	-0.01	0.01	-0.01	0.00	0.00
JetTagWeightLight3	0.01	-0.01	0.00	-0.00	0.00	-0.00	0.00	0.00
JetTagWeightLight4	-0.04	0.04	0.01	-0.01	-0.03	0.03	0.00	0.00
JetTagWeightLight5	-0.02	0.02	-0.05	0.05	-0.03	0.03	0.00	0.00
JetTagWeightLight6	-0.01	0.01	0.09	-0.09	-0.00	0.00	0.00	0.00
JetTagWeightLight7	0.03	-0.03	-0.02	0.02	0.02	-0.02	0.00	0.00
JetTagWeightLight8	0.01	-0.01	0.15	-0.15	0.01	-0.01	0.00	0.00
JetTagWeightLight9	-0.06	0.06	-0.07	0.07	0.02	-0.02	0.00	0.00
JetTagWeightLight10	-0.04	0.04	0.26	-0.26	-0.01	0.01	0.00	0.00
JetTagWeightLight11	-0.07	0.07	-0.33	0.33	-0.16	0.16	0.00	0.00
JetTagWeightT0	0.22	-0.22	-0.00	0.00	-0.00	0.00	0.00	0.00
JetTagWeightT1	-0.20	0.20	-0.05	0.05	-0.00	0.00	0.00	0.00
JetTagWeightT2	-0.03	0.03	0.02	-0.02	-0.00	0.00	0.00	0.00
JetTagWeightT3	0.20	-0.21	0.02	-0.02	0.00	-0.00	0.00	0.00
JetTagWeightC0	-0.12	0.12	-0.15	0.15	0.04	-0.04	0.00	0.00
JetTagWeightC1	-0.28	0.28	-0.41	0.42	-0.08	0.08	0.00	0.00
JetTagWeightC2	0.02	-0.02	0.09	-0.09	-0.07	0.07	0.00	0.00
JetTagWeightC3	0.40	-0.41	0.38	-0.37	0.09	-0.09	0.00	0.00
JetTagWeightB0	0.17	-0.17	0.06	-0.06	-0.04	0.04	0.00	0.00
JetTagWeightB1	0.13	-0.13	-0.03	0.03	0.04	-0.04	0.00	0.00
JetTagWeightB2	-0.39	0.38	-0.44	0.44	-0.57	0.57	0.00	0.00
JetTagWeightB3	0.59	-0.59	0.37	-0.38	0.94	-0.94	0.00	0.00
JetTagWeightB4	0.13	-0.14	0.07	-0.07	0.52	-0.52	0.00	0.00
JetTagWeightB5	-1.56	1.53	-0.99	0.95	-2.93	2.96	0.00	0.00
NonClosure AFIIJES	0.00	0.00	0.00	0.00	0.00	0.00	0.00	0.00

Table 41: Variation of the *ttW* expected events as a function of the experimental Jet uncertainties for 1lep+2tau, 2lep+tau, 3lep and 4lep channels.

A.3 $t\bar{t}Z$ systematic uncertainties

ttZ	2ee4j		2ee5jincl		2em4j		2em5jincl	
	Down-Up Var. (%)		Down-Up Var. (%)		Down-Up Var. (%)		Down-Up Var. (%)	
lepTrigSFEventWeight	-0.09	0.09	-0.11	0.11	-0.28	0.28	-0.29	0.29
ElecResolution	-0.41	-0.32	-0.69	-0.61	0.00	0.00	0.17	-0.35
ElecScale	-0.41	0.00	-0.33	0.00	0.18	-0.22	0.00	0.00
ElecId	-1.46	1.47	-1.57	1.58	-0.73	0.73	-0.77	0.77
ElecIso	-4.16	4.25	-4.46	4.56	-2.19	2.19	-2.25	2.25
ID	0.00	0.00	0.00	0.00	0.00	0.00	0.00	0.00
MS	0.00	0.00	0.00	0.00	0.00	0.21	0.00	0.00
SCALE	0.00	0.00	0.00	0.00	0.00	0.18	0.00	0.00
MuonReco	0.00	0.00	0.00	0.00	-0.14	0.14	-0.13	0.13
MuonIso	0.00	0.00	0.00	0.00	-2.04	2.04	-2.05	2.05
TauScale	0.00	-0.33	0.00	0.00	0.39	-0.22	0.13	0.00
TauEVSF	0.00	0.00	0.00	0.00	0.00	0.00	0.00	0.00
TauIDSF	0.00	0.00	0.00	0.00	0.00	0.00	0.00	0.00

Table 42: Variation of the *ttZ* expected events as a function of the experimental leptons and hadronic tau uncertainties for ee4jets, ee5morejets, em4jets and em5morejets channels.

ttZ	2mm4j		2mm5jincl	
	Down-Up Var. (%)		Down-Up Var. (%)	
lepTrigSFEventWeight	-0.69	0.69	-0.75	0.75
ElecResolution	0.00	0.00	0.00	0.00
ElecScale	0.00	0.00	0.00	0.00
ElecId	0.00	0.00	0.00	0.00
ElecIso	0.00	0.00	0.00	0.00
ID	0.00	-0.28	0.00	0.00
MS	0.00	-0.35	0.00	0.00
SCALE	-0.63	0.30	0.00	0.00
MuonReco	-0.26	0.26	-0.24	0.24
MuonIso	-4.01	4.09	-4.09	4.18
TauScale	0.41	-0.45	0.00	-0.58
TauEVSF	0.00	0.00	0.00	0.00
TauIDSF	0.00	0.00	0.00	0.00

Table 43: Variation of the *ttZ* expected events as a function of the experimental leptons and hadronic tau uncertainties for mm4jets and mm5morejets channels.

ttZ	1l2t		2lt		3l		4l	
	Down-Up Var. (%)		Down-Up Var. (%)		Down-Up Var. (%)		Down-Up Var. (%)	
lepTrigSFEventWeight	-1.27	1.27	-0.52	0.52	-0.17	0.17	-0.14	0.14
ElecResolution	0.00	0.00	-0.79	-0.79	0.13	0.52	0.25	-1.50
ElecScale	0.00	0.00	0.00	-0.20	0.02	0.33	-0.55	1.19
ElecId	-0.36	0.36	-0.89	0.90	-1.17	1.18	-1.83	1.86
ElecIso	-1.11	1.11	-1.96	1.98	-2.70	2.77	-3.78	3.90
ID	0.00	0.00	-0.73	0.00	-0.25	0.20	0.00	0.00
MS	0.00	0.00	0.00	-0.73	-0.00	0.88	0.00	-0.07
SCALE	0.00	0.00	0.00	-0.73	-0.05	0.29	0.00	-0.53
MuonReco	-0.06	0.06	-0.15	0.15	-0.23	0.23	-0.31	0.31
MuonIso	-0.98	0.98	-2.32	2.34	-3.61	3.71	-4.81	5.00
TauScale	-3.49	4.93	-0.69	2.32	0.00	0.00	0.00	0.00
TauEVSF	-0.12	0.12	-0.95	0.95	0.00	0.00	0.00	0.00
TauIDSF	-6.52	6.73	-2.22	2.22	0.00	0.00	0.00	0.00

Table 44: Variation of the *ttZ* expected events as a function of the experimental leptons and hadronic tau uncertainties for 1lep+2tau, 2lep+tau, 3lep and 4lep channels.

ttZ	2ee4j		2ee5jincl		2em4j		2em5jincl	
	Down-Up Var. (%)		Down-Up Var. (%)		Down-Up Var. (%)		Down-Up Var. (%)	
JER	—	1.53	—	1.68	—	3.55	—	-0.79
JVF	0.45	0.08	0.24	-0.70	0.06	-0.63	0.66	-0.62
Eta ModellingJES	-0.40	-0.82	-1.03	2.07	-0.15	0.69	-2.03	0.52
Eta StatAndMethodJES	-1.23	-2.82	-0.01	2.17	0.70	0.37	-1.54	0.30
MuJES	-1.40	-0.78	0.35	0.80	0.21	0.26	-0.58	-0.10
HighPtJES	0.00	0.00	0.00	0.00	0.00	0.00	0.00	0.00
NPVJES	-2.57	-2.27	0.43	1.74	0.50	0.55	-1.29	0.10
NP_Detector1JES	-1.42	-2.14	0.04	2.16	0.35	0.44	-1.42	0.36
NP_Detector2JES	-0.40	0.00	-0.00	-0.01	0.05	0.19	-0.15	0.01
NP_Detector3JES	-0.40	0.00	-0.01	-0.00	-0.06	0.21	-0.23	-0.00
NP_Mixed1JES	-0.39	-0.00	0.00	-0.00	-0.00	0.01	0.00	-0.00
NP_Mixed2JES	-0.85	-1.40	-0.00	1.07	0.09	0.80	-0.68	-0.00
NP_Modelling1JES	-1.73	-3.40	-1.47	4.65	-0.56	1.43	-4.32	2.39
NP_Modelling2JES	-1.78	-0.84	1.36	-0.01	0.78	0.15	-0.00	-0.84
NP_Modelling3JES	-0.40	-0.45	-0.01	0.34	-0.06	0.44	-0.24	0.01
NP_Modelling4JES	-0.40	-0.00	-0.01	-0.01	0.04	0.01	-0.14	-0.00
NP_Statistical1JES	-1.40	-2.18	-0.01	2.16	0.57	0.42	-1.43	0.40
NP_Statistical2JES	-0.44	-0.40	0.34	-0.00	0.45	-0.06	-0.00	-0.23
NP_Statistical3JES	-0.40	-0.47	-0.01	0.35	-0.06	0.61	-0.22	-0.01
FlavCompJES	-0.53	-3.85	-1.52	5.27	-1.92	1.51	-3.00	1.96
FlavRespJES	-0.37	-2.17	-1.28	2.73	-0.88	1.64	-2.06	0.86
bJES	-1.38	-0.74	0.05	0.84	0.98	-0.47	-1.51	0.78
PilePtJES	-0.41	-0.00	-0.01	-0.01	0.00	-0.03	-0.01	0.00
PileRhoJES	-1.86	-2.16	-1.19	3.04	0.36	1.50	-3.04	1.20
JetTagWeightLight0	-0.00	0.00	-0.01	0.01	0.01	-0.01	0.00	-0.00
JetTagWeightLight1	-0.00	0.00	0.02	-0.02	-0.01	0.01	-0.00	0.00
JetTagWeightLight2	-0.02	0.02	-0.00	0.00	0.00	-0.00	-0.01	0.01
JetTagWeightLight3	-0.01	0.01	-0.03	0.03	0.01	-0.01	-0.00	0.00
JetTagWeightLight4	-0.01	0.01	-0.06	0.06	0.01	-0.01	-0.02	0.02
JetTagWeightLight5	0.00	-0.00	-0.04	0.04	0.00	-0.00	-0.02	0.02
JetTagWeightLight6	-0.01	0.01	-0.03	0.03	-0.01	0.01	-0.03	0.03
JetTagWeightLight7	0.02	-0.02	-0.01	0.01	0.00	-0.00	0.02	-0.02
JetTagWeightLight8	0.01	-0.01	0.06	-0.06	-0.03	0.03	-0.01	0.01
JetTagWeightLight9	0.08	-0.08	0.14	-0.14	0.02	-0.02	0.02	-0.02
JetTagWeightLight10	0.02	-0.02	0.11	-0.11	-0.01	0.01	0.06	-0.06
JetTagWeightLight11	-0.17	0.17	-0.36	0.35	-0.01	0.01	-0.24	0.24
JetTagWeightT0	0.00	-0.00	0.02	-0.02	-0.01	0.01	-0.01	0.01
JetTagWeightT1	0.03	-0.03	0.00	-0.00	0.00	-0.00	0.01	-0.01
JetTagWeightT2	0.00	-0.00	-0.02	0.02	-0.00	0.00	-0.01	0.01
JetTagWeightT3	-0.04	0.04	0.01	-0.01	-0.02	0.02	0.00	-0.00
JetTagWeightC0	0.05	-0.05	0.10	-0.10	0.01	-0.01	-0.04	0.04
JetTagWeightC1	-0.10	0.10	-0.09	0.09	-0.09	0.09	0.05	-0.05
JetTagWeightC2	0.01	-0.01	0.07	-0.07	0.06	-0.06	0.02	-0.02
JetTagWeightC3	0.12	-0.12	0.10	-0.10	0.12	-0.12	-0.09	0.09
JetTagWeightB0	0.04	-0.04	-0.00	0.00	-0.02	0.02	-0.06	0.06
JetTagWeightB1	0.07	-0.07	0.15	-0.15	-0.04	0.04	0.01	-0.01
JetTagWeightB2	-0.26	0.26	-0.27	0.26	-0.37	0.37	-0.30	0.30
JetTagWeightB3	0.31	-0.32	0.17	-0.18	0.42	-0.43	0.26	-0.27
JetTagWeightB4	0.31	-0.32	0.12	-0.13	0.33	-0.33	0.32	-0.32
JetTagWeightB5	-1.64	1.62	-1.46	1.40	-0.98	0.94	-1.12	1.04
NonClosure AFIIJES	0.00	0.00	0.00	0.00	0.00	0.00	0.00	0.00

Table 45: Variation of the *ttZ* expected events as a function of the experimental Jet uncertainties for ee4jets, ee5morejets, em4jets and em5morejets channels.

ttZ	2mm4j		2mm5jincl	
	Down-Up Var. (%)		Down-Up Var. (%)	
JER	—	3.26	—	0.94
JVF	1.35	-2.08	0.92	0.00
Eta ModellingJES	1.28	1.36	-1.24	1.62
Eta StatAndMethodJES	0.05	0.93	-0.77	-0.03
MuJES	-0.27	1.08	-0.40	-0.01
HighPtJES	0.00	0.00	0.00	0.00
NPVJES	-1.59	2.20	-1.05	0.97
NP_Detector1JES	0.04	0.51	-0.76	0.31
NP_Detector2JES	-0.01	0.02	-0.00	0.01
NP_Detector3JES	-0.00	0.01	0.00	0.00
NP_Mixed1JES	0.00	-0.00	0.00	-0.00
NP_Mixed2JES	0.00	0.00	-0.49	-0.02
NP_Modelling1JES	1.40	3.22	-4.48	3.29
NP_Modelling2JES	0.41	0.35	-0.03	-0.76
NP_Modelling3JES	0.01	-0.00	-0.48	0.01
NP_Modelling4JES	-0.00	0.01	0.00	0.00
NP_Statistical1JES	0.06	0.67	-0.74	0.35
NP_Statistical2JES	0.01	0.00	0.00	-0.49
NP_Statistical3JES	0.01	0.01	-0.47	-0.00
FlavCompJES	2.89	3.94	-5.45	4.20
FlavRespJES	1.73	0.90	-3.19	2.32
bJES	-0.42	0.19	-0.01	0.21
PilePtJES	0.04	-0.01	0.01	-0.00
PileRhoJES	2.09	0.44	-2.83	2.54
JetTagWeightLight0	0.01	-0.01	0.00	-0.00
JetTagWeightLight1	-0.01	0.01	-0.01	0.01
JetTagWeightLight2	0.00	-0.00	0.01	-0.01
JetTagWeightLight3	0.00	-0.00	0.00	-0.00
JetTagWeightLight4	0.02	-0.02	-0.00	0.00
JetTagWeightLight5	-0.02	0.02	-0.02	0.02
JetTagWeightLight6	-0.02	0.02	-0.02	0.02
JetTagWeightLight7	0.00	-0.00	-0.01	0.01
JetTagWeightLight8	-0.04	0.04	-0.03	0.03
JetTagWeightLight9	0.02	-0.02	-0.09	0.09
JetTagWeightLight10	0.03	-0.03	-0.04	0.04
JetTagWeightLight11	-0.00	0.00	0.10	-0.10
JetTagWeightT0	-0.03	0.03	0.01	-0.01
JetTagWeightT1	-0.01	0.01	0.00	-0.00
JetTagWeightT2	-0.04	0.04	-0.00	0.00
JetTagWeightT3	0.04	-0.04	-0.03	0.03
JetTagWeightC0	0.03	-0.03	0.03	-0.03
JetTagWeightC1	0.18	-0.18	0.04	-0.04
JetTagWeightC2	-0.08	0.08	0.07	-0.07
JetTagWeightC3	-0.16	0.16	0.09	-0.10
JetTagWeightB0	-0.00	0.00	-0.04	0.04
JetTagWeightB1	-0.07	0.07	0.17	-0.17
JetTagWeightB2	-0.31	0.31	-0.32	0.32
JetTagWeightB3	0.51	-0.51	0.47	-0.48
JetTagWeightB4	0.44	-0.45	0.37	-0.37
JetTagWeightB5	-1.51	1.45	-1.55	1.52
NonClosure AFIIJES	0.00	0.00	0.00	0.00

Table 46: Variation of the *ttZ* expected events as a function of the experimental Jet uncertainties for mm4jets and mm5morejets channels.

ttZ	1l2t		2lt		3l		4l	
	Down-Up Var. (%)		Down-Up Var. (%)		Down-Up Var. (%)		Down-Up Var. (%)	
JER	—	-0.70	—	0.24	—	-0.84	—	-5.16
JVF	0.57	-0.00	0.00	-0.96	0.40	-0.62	0.00	0.00
Eta ModellingJES	-0.53	0.07	-0.82	1.22	-1.18	1.07	-1.00	-1.19
Eta StatAndMethodJES	0.02	0.60	-1.79	1.26	-0.26	0.41	-0.00	-0.01
MuJES	0.01	-0.01	-0.26	-0.00	-0.03	0.11	-0.33	-0.00
HighPtJES	0.00	0.00	0.00	0.00	0.00	0.00	0.00	0.00
NPVJES	-0.20	0.23	-0.29	0.43	-0.35	0.76	-0.32	-1.10
NP_Detector1JES	0.03	0.59	-1.79	1.77	-0.26	0.43	-0.31	0.04
NP_Detector2JES	-0.00	0.00	-0.00	0.48	-0.00	0.07	-0.00	-0.01
NP_Detector3JES	0.00	0.00	0.00	0.57	-0.00	0.11	-0.01	-0.00
NP_Mixed1JES	0.01	-0.00	-0.09	-0.00	0.00	-0.00	0.00	-0.00
NP_Mixed2JES	0.03	0.59	-0.86	1.26	-0.00	0.20	0.00	-0.00
NP_Modelling1JES	-1.36	1.65	-2.67	1.91	-1.76	2.51	-2.36	-1.65
NP_Modelling2JES	0.60	0.02	1.16	-1.71	0.29	-0.01	-0.02	-0.00
NP_Modelling3JES	0.00	-0.01	0.00	0.55	-0.01	0.11	-0.00	-0.02
NP_Modelling4JES	0.00	-0.00	-0.09	-0.00	-0.00	0.07	0.00	-0.00
NP_Statistical1JES	0.03	0.59	-1.69	1.83	-0.20	0.50	-0.33	-0.65
NP_Statistical2JES	0.00	-0.00	0.57	0.00	0.11	-0.00	-0.00	0.00
NP_Statistical3JES	0.01	0.60	-0.10	0.57	-0.00	0.19	-0.01	0.03
FlavCompJES	-1.42	1.12	-2.99	1.97	-1.59	2.00	-0.38	-2.33
FlavRespJES	-0.41	0.74	-0.87	1.83	-1.15	0.91	-0.85	-1.15
bJES	0.00	0.52	-0.87	-0.08	-0.62	0.73	-0.97	0.06
PilePtJES	0.01	-0.01	-0.01	-0.01	-0.00	0.00	0.02	0.03
PileRhoJES	0.03	1.02	-1.77	1.76	-1.27	1.32	-1.31	-1.09
JetTagWeightLight0	0.00	-0.00	-0.00	0.00	0.00	-0.00	0.00	-0.00
JetTagWeightLight1	-0.01	0.01	-0.02	0.02	0.00	-0.00	-0.00	0.00
JetTagWeightLight2	-0.00	0.00	0.01	-0.01	0.00	-0.00	0.01	-0.01
JetTagWeightLight3	0.01	-0.01	-0.01	0.01	0.00	-0.00	-0.02	0.02
JetTagWeightLight4	-0.02	0.02	-0.10	0.10	0.00	-0.00	0.01	-0.01
JetTagWeightLight5	0.01	-0.01	-0.10	0.10	-0.01	0.01	0.02	-0.02
JetTagWeightLight6	0.02	-0.02	-0.03	0.03	-0.01	0.01	0.02	-0.02
JetTagWeightLight7	0.01	-0.01	0.05	-0.05	0.01	-0.01	0.01	-0.01
JetTagWeightLight8	0.04	-0.04	0.07	-0.07	-0.01	0.01	-0.05	0.05
JetTagWeightLight9	-0.07	0.07	-0.04	0.04	0.06	-0.06	0.02	-0.02
JetTagWeightLight10	0.00	-0.00	0.00	-0.00	0.04	-0.04	-0.08	0.08
JetTagWeightLight11	-0.19	0.19	-0.54	0.53	0.01	-0.01	-0.03	0.03
JetTagWeightT0	-0.11	0.11	0.13	-0.13	0.01	-0.01	0.00	0.00
JetTagWeightT1	-0.08	0.08	-0.14	0.14	-0.01	0.01	0.00	0.00
JetTagWeightT2	-0.12	0.12	-0.12	0.12	-0.02	0.02	0.00	0.00
JetTagWeightT3	0.33	-0.32	0.26	-0.26	0.03	-0.03	0.00	0.00
JetTagWeightC0	-0.08	0.08	-0.17	0.17	0.01	-0.01	-0.01	0.01
JetTagWeightC1	-0.07	0.07	-0.04	0.04	-0.09	0.09	0.04	-0.04
JetTagWeightC2	-0.01	0.01	-0.22	0.22	-0.02	0.02	-0.11	0.11
JetTagWeightC3	-0.06	0.06	0.03	-0.03	0.14	-0.14	-0.00	0.00
JetTagWeightB0	-0.04	0.04	0.06	-0.06	-0.01	0.01	-0.02	0.02
JetTagWeightB1	0.02	-0.02	0.13	-0.13	0.01	-0.01	-0.02	0.02
JetTagWeightB2	-0.35	0.35	-0.16	0.15	-0.41	0.41	-0.31	0.31
JetTagWeightB3	0.40	-0.40	0.36	-0.36	0.63	-0.63	0.43	-0.44
JetTagWeightB4	0.48	-0.48	0.40	-0.40	0.39	-0.39	0.31	-0.31
JetTagWeightB5	-1.35	1.29	-1.24	1.12	-1.83	1.80	-1.62	1.58
NonClosure AFIIJES	0.00	0.00	0.00	0.00	0.00	0.00	0.00	0.00

Table 47: Variation of the *ttZ* expected events as a function of the experimental Jet uncertainties for 1lep+2tau, 2lep+tau, 3lep and 4lep channels.

B PileUp reweighting studies

The number of yields in the signal region has been calculated multiplying $< \mu >$ in simulations by 0.90 (the nominal value equivalent to divide by 1.11), 0.88, 0.80, 0.75, 0.94, 1.03. The values 0.94 and 0.88 correspond to shift $< \mu >$ scale factor up and down by about the uncertainty. Figure 40 shows the yields variations as a function of the $< \mu >$ scale value used in simulations. Table 40 contains the relative yields variation for $< \mu >$ scale 0.88 and 0.94. The largest variations (about 2%) are observed in the 2l_tau channel for $t\bar{t}Z$ and in 1l_2tau the for $t\bar{t}W$.

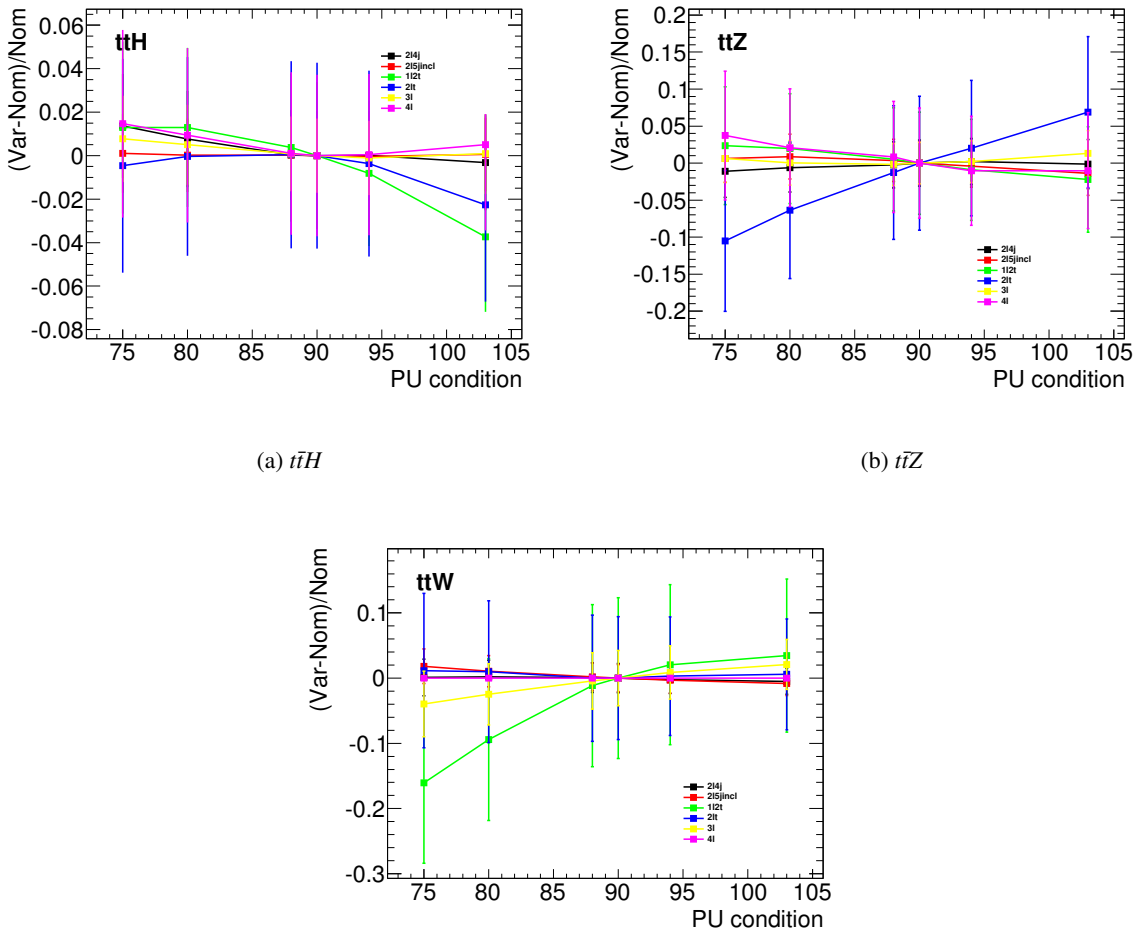

(a) $t\bar{t}H$

(b) $t\bar{t}Z$

(c) $t\bar{t}W$

Figure 40: Relative variation in number of expected $t\bar{t}H$ (a), $t\bar{t}Z$ (b) and $t\bar{t}W$ (c) events per channel as a function of pileup reweighting condition. The error bars show the relative statistical error for the specific point.

Table 48: Uncertainties (%) on $t\bar{t}H$, $t\bar{t}Z$, $t\bar{t}W$ acceptance in signal regions due to the $< \mu >$ scale factors uncertainty.

Sample	1l_2tau	2l 4j	2l 5j	2l_tau	3l	4l
$t\bar{t}H$	$^{+0.4}_{-0.8}$	$^{+0.0}_{-0.0}$	$^{+0.0}_{-0.0}$	$^{+0.0}_{-0.4}$	$^{+0.1}_{-0.1}$	$^{+0.1}_{-0.0}$
$t\bar{t}Z$	$^{+0.5}_{-0.9}$	$^{+0.2}_{-0.2}$	$^{+0.4}_{-0.4}$	$^{+2.0}_{-1.2}$	$^{+0.2}_{-0.2}$	$^{+0.8}_{-1.0}$
$t\bar{t}W$	$^{+2.1}_{-1.2}$	$^{+0.1}_{-0.2}$	$^{+0.2}_{-0.3}$	$^{+0.3}_{-0.0}$	$^{+0.9}_{-0.4}$	—

Process	Ref.	PDF(set)	$\sigma_{NLO}[fb]$	Nominal scale, μ_0	Scale Range	Scale Uncertainty [%]		PDF Uncertainty [%]	
$t\bar{t}+W^+$	[14]	MSTW2008nlo90cl	161	m_t	$[\mu_0/4, 4\mu_0]$	+12	-20	+7	-8
$t\bar{t}+W^-$	[14]	MSTW2008nlo90cl	71	m_t	$[\mu_0/4, 4\mu_0]$	+16	-21	+6	-8
$t\bar{t}+W^+$	[15]	CTEQ6.6	142.6	$m_t+m_W/2$	$[\mu_0/2, 2\mu_0]$	+10	-11	–	–
$t\bar{t}+W^-$	[15]	CTEQ6.6	60.5	$m_t+m_W/2$	$[\mu_0/2, 2\mu_0]$	+11	-12	–	–
$t\bar{t}+Z$	[15]	CTEQ6.6	205.7	$m_t+m_Z/2$	$[\mu_0/2, 2\mu_0]$	+9	-13	–	–

Table 49: Summary of NLO cross section and theoretical uncertainty calculations from [14, 15]. In all cases the renormalization scale, μ_R, and factorization scale, μ_F, are set equal to a common scale, $\mu = \mu_R = \mu_F$.

Process	Reference/ aMC@NLO	Nominal σ_{NLO} $[fb]$	Scale Uncertainty [%]		PDF Uncertainty [%]	
$t\bar{t}W^+$	[14]	161	+12	-20	+7	-8
	aMC@NLO	162.5	+11	-20	+7.7	-8.7
	[15]	142.6	+9	-10	–	–
	aMC@NLO	144.9	+9	-10	+8.7	-10
$t\bar{t}W^-$	[14]	71	+16	-21	+6	-8
	aMC@NLO	72.3	+14	-21	+6.3	-8.4
	[15]	60.5	+11	-11	–	–
	aMC@NLO	61.4	+10	-11	+7.5	-6.6
$t\bar{t}Z$	[14]	–	–	–	–	–
	aMC@NLO	234.5	+13	-22	+8.0	-9.2
	[15]	205.7	+9	-12	–	–
	aMC@NLO	205.6	+10	-12	+9.2	-8

Table 50: NLO cross section and theoretical uncertainty calculations from MadGraph5_aMC@NLO compared to those in Table 49.

C $t\bar{t}V$ Production Cross Section Calculations

C.1 Existing Theoretical Calculations

NLO cross section calculations have been performed for $t\bar{t}+W$ [14] and for both $t\bar{t}+W$ and $t\bar{t}+Z$ [15] at $\sqrt{s}$ = 8 TeV. These calculations include theoretical uncertainties on the cross section due to the choice of renormalisation and factorisation scale and in [14] the theoretical uncertainty due choice of PDF is also considered. These values and their respective uncertainties are summarised in Table 49.

It is difficult to directly compare these calculations as they differ in several aspects. Important differences are the choice of central scale ($\mu = m_t$ vs $\mu = m_t + m_V/2$), the definition of the scale uncertainty envelope ([μ/4,4μ] vs [μ/2,2μ]), the choice of PDF (MSTW2008nlo [17] vs CTEQ6.6 [**?**]), the inclusion (or not) of the PDF uncertainty calculation and there is of course only one prediction for $t\bar{t}Z$.

Process	σ_{NLO} [fb]	Scale Uncertainty [%]		PDF Uncertainty [%]		Total symmetrised uncertainty [%]
$t\bar{t}W^+$	144.9	+10	-11	+7.7	-8.7	13.3
$t\bar{t}W^-$	61.4	+11	-12	+6.3	-8.4	13.6
$t\bar{t}Z$	206.7	+9	-13	+8.0	-9.2	14.0

Table 51: NLO cross section and theoretical uncertainty calculations used for final values.

C.2 MadGraph5_aMC@NLO NLO Cross Section Calculations

As a result of the limitations of/differences between the two calculations, MadGraph5_aMC@NLO [16] is used to evaluate the cross sections and uncertainties with more optimal and consistent set of parameter choices. This was done using the internal scale and PDF reweighting that is available with MadGraph5_aMC@NLO.

To validate the MadGraph5_aMC@NLO setup we first attempt to reproduce the numbers from Refs. [14] and [15] (shown in Table 49) by matching the specific parameter choices made in each case. The result of this can be seen in Table 50 which shows that MadGraph5_aMC@NLO is able to accurately reproduce these values and hence serves as validation of the setup.

MadGraph5_aMC@NLO is then used to calculate the final NLO cross sections and uncertainties for both $t\bar{t}Z$ and $t\bar{t}W$ that enter in the analysis. The prescription for the scale envelope is taken from [15]: the central value $\mu = \mu_R = \mu_F = m_t + m_V/2$ and the uncertainty envelope is $[\mu_0/2, 2\mu_0]$. The PDF uncertainty prescription used is the recipe from [14]: calculate the PDF uncertaintly using the MSTW2008nlo PDF for the central value and then the final PDF uncertainty envelope is derived from three PDF error sets each with different α_S values (the central value and the upper and lower 90% CL values). The total uncertainty envelope is the combined envelope of all three error sets. The final NLO cross section central values and uncertainties are given in Table 51.